APPENDIX F
EROSION STUDIES

APPENDIX F
EROSION STUDIES

Changes in this Appendix Since the Revised Draft Environmental Impact Statement

The basic approach of using site-calibrated landscape evolution models used in the *Environmental Impact Statement for Decommissioning and/or Long-Term Stewardship at the West Valley Demonstration Project and Western New York Nuclear Service Center (Decommissioning and/or Long-Term Stewardship EIS) Revised Draft* has been retained for this Final EIS. The CHILD [Channel-Hillslope Integrated Landscape Development] erosion model was revised for this Final EIS to differentiate regolith, till and bedrock and then recalibrated using Monte Carlo (probabilistic) methods and more detailed calibration criteria. This approach identified five sets of calibration parameters that produced topography predictions that are close to current conditions.

These five sets of best-fit calibration parameters were used to develop topography predictions over 10,000 years for the unmitigated erosion scenario for both the Sitewide Close-In-Place and No Action Alternatives. The predictions considered both current climatology, and wetter climatology conditions to investigate the effects of potential climate change. Predictions in this Final EIS are based on a smaller grid scale around the areas containing waste or contamination than was used in the Revised Draft EIS. These predictions are generally similar to the predictions developed in the Revised Draft EIS analysis, but the use of multiple model calibrations increases the confidence in the predictions.

The material in this Appendix has been reorganized for clarity. The CHILD model calibration and subsequent model projections are now presented earlier in the Appendix and the previous measurements or studies that were useful in evaluating the reasonableness of the CHILD predictions were moved toward the back. A new section has been added about the potential for Buttermilk Creek capture of Franks Creek. Previous studies that were not useful in evaluating the reasonableness of the CHILD predictions were eliminated. Although the SIBERIA predictions from the Revised Draft EIS are generally comparable to predictions from the CHILD model in both the Revised Draft and Final EISs, the SIBERIA discussion and results were eliminated in the interest of simplifying this Appendix.

Erosional processes are actively changing the glacial till landscape at the Western New York Nuclear Service Center (WNYNSC), including the vicinity of the Project Premises and the New York State-Licensed Disposal Area (SDA). The North and South Plateaus are being modified through stream downcutting, slope movement, gully migration, and sheet and rill erosion. The rate at which the plateaus are eroding has been the subject of numerous studies at WNYNSC over the last 30 years (WVNS 1993a, 1993b).

The objective of this appendix is to describe current understanding of the erosion processes affecting WNYNSC and present a scientifically sound estimate of unmitigated erosion at the site (particularly in the areas of the North and South Plateaus) for both the No Action and Sitewide Close-In-Place Alternatives. The erosion predictions are estimated with the CHILD [Channel-Hillslope Integrated Landscape Development] landscape evolution model and verified with the limited amount of available site-specific data and short-term erosion analyses. Section F.1 presents an overview of the processes affecting erosion at WNYNSC and the geologic context in which those processes are acting. Section F.2 discusses observations of environmental conditions related to erosion and summarizes erosion rate estimates based solely on these observations. Section F.3 describes the CHILD landscape evolution modeling approach to predicting long-term erosional impacts on the site and determines the reasonableness of the predicted impacts through comparison to prior erosion rate estimates for both short and long periods of time. Section F.4 presents a summary of these studies.

F.1 Overview of Western New York Nuclear Service Center Erosional Processes and History

F.1.1 Overview of Erosional Processes

Erosion is the loosening and removal of soil by running water, moving ice, wind, or gravity. At WNYNSC, running water is the predominant mechanism that causes erosion. Development of the topography and stream drainage patterns currently observed at WNYNSC began with the glaciation and retreat process that ended approximately 17,000 years ago. Erosion processes have affected the WNYNSC topography due to gravitational forces and water flow within the Buttermilk Creek watershed. A portion of the watershed is represented schematically in the topographic map presented as **Figure F–1**. Buttermilk Creek flows in a northwesterly direction close to the central axis of WNYNSC at an elevation approximately 61 meters (200 feet) below the plateau on which most of the facilities are located. On the plateau, Erdman Brook divides the Project Premises and the SDA into two areas: the North Plateau, containing the industrial area, and the South Plateau, containing the disposal areas. The entire watershed is shown on **Figure F–2**. This figure shows the Project Premises and the SDA as a small area in the central portion of the watershed.

Major erosion processes affecting WNYNSC include stream channel downcutting, stream valley rim widening, gully advance, and, in disturbed areas, sheet and rill erosion. Each of these processes is discussed in the following paragraphs.

During precipitation events, surface water runoff can create sheet and rill flow, which can entrain and transport sediment particles. Sheet flow is a continuous film of water moving over smooth soil surfaces. Rill flow consists of a series of small rivulets connecting one water-filled hollow with another on the rougher terrain. Sheet and rill erosion occurs when the stress exerted by flow is sufficient to entrain and remove soil and sediment particles. This form of erosion is generally rare on well-vegetated surfaces, but can be significant when vegetation is sparse or absent.

The three small stream channels (Erdman Brook, Quarry Creek, and Franks Creek) that drain the Project Premises and the SDA are being eroded by the stream channel downcutting and valley rim–widening processes. The streams appear to be incising rapidly, as suggested by convex-upward longitudinal profiles, steep V-shaped valley-side profiles, and the paucity of floodplains over a major portion of their length. The streams within the plateau areas flow over glacial till material. As channel downcutting progresses, two specific mechanisms contribute to stream rim widening. Streambanks are undercut, causing localized slope failures (i.e., slumps and landslides). This process commonly occurs at the outside of the meander loops and produces a widening of the stream valley rim. Even in locations where there is no bank undercutting, downcutting of the stream will produce a steeper creek bank that is subject to slumping.

Gully advance is the third type of erosion process that results from local runoff and reflects soil characteristics. Gullies are most likely to form in areas along streambanks where slumps and deep fractures are present, seeps are flowing, and the toe of the slope intersects the outside of the meander loop. Gully growth is not a steady-state process; it occurs in response to episodic events, such as thaws and thunderstorms in areas where a concentrated stream of water flows over the side of a plateau, as well as in areas where groundwater pore pressure is high enough for seepage to promote grain-by-grain entrainment and removal of soil particles from the base of the gully scarp (a process sometimes known as “sapping”). Sapping causes small tunnels (or “pipes”) to form in the soil at the gully base, which can contribute to gully growth by undermining and weakening the scarp until it collapses. Surface-water runoff into the gully also contributes to gully growth by removing fallen debris at the scarp base, undercutting side walls, and scouring the base of a head scarp. Although human-induced changes to the surface-water drainage pattern can control the growth of some gullies, other natural processes that induce gully formation, such as the development of animal trails or tree falls, cannot be readily controlled.

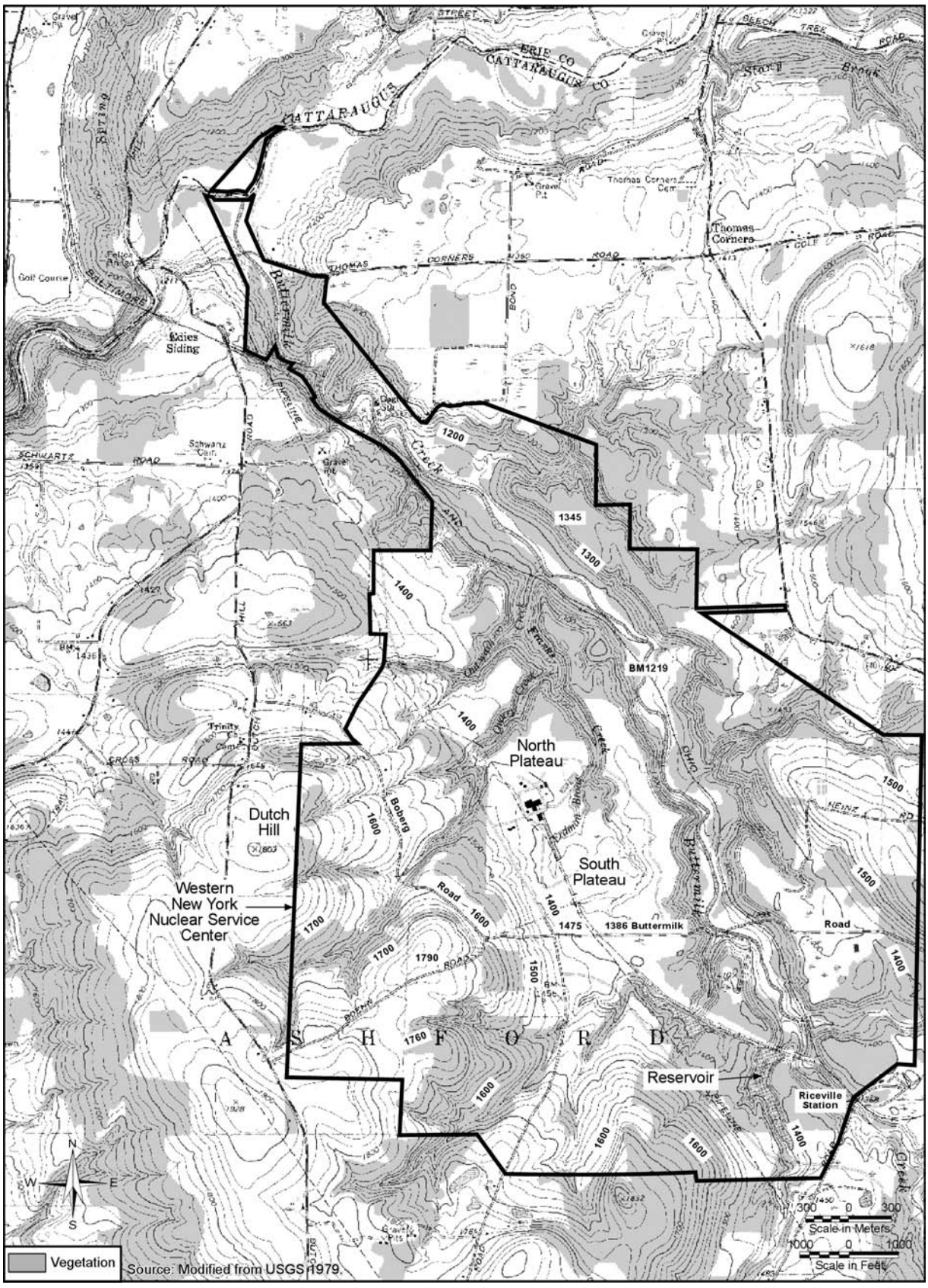

Figure F–1 Western New York Nuclear Service Center Topography

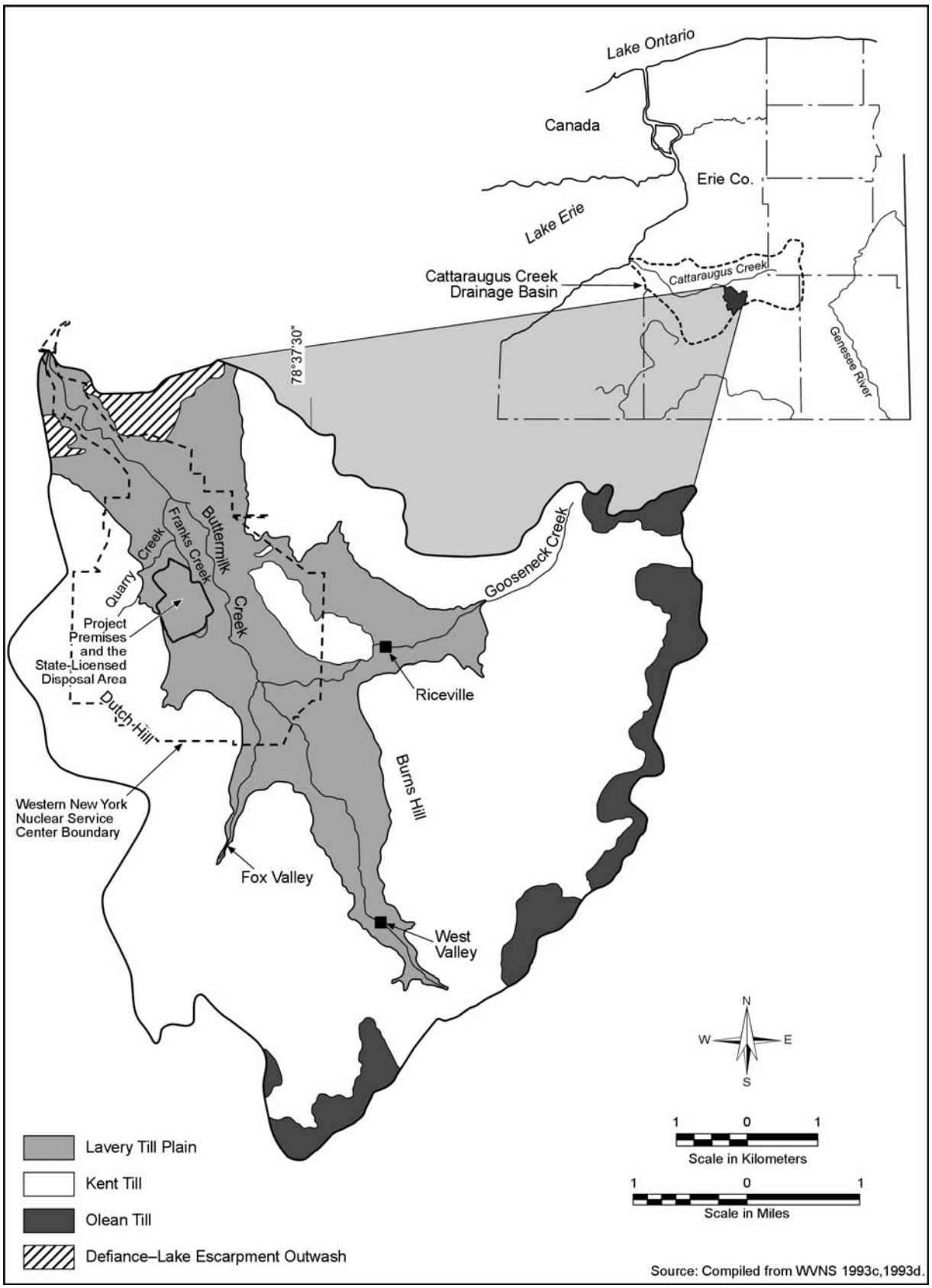

Figure F–2 Buttermilk Creek Drainage Basin

F.1.2 Overview of Geomorphic History

The postglacial geomorphic history of the site is relevant to calibrating long-term erosion models, so it is useful to briefly review what is known about that history. The Cattaraugus Creek drainage basin empties into Lake Erie. The bedrock geology consists of late–Paleozoic sedimentary rocks that dip 0.5 to 0.8 degrees to the south. Within the larger valleys, the bedrock is buried beneath a thick sequence of glacial, lacustrine, and alluvial deposits (LaFleur 1979; Boothroyd et al. 1979, 1982; Fakundiny 1985). These deposits, which are now partly dissected by stream incision, form an extensive set of low-relief, terrace-like surfaces inset into the bedrock topography. Thus, the catchment has three distinct topographic elements: rounded bedrock hills with peak altitudes on the order of 550 meters (1,805 feet), midlevel inset glacial terraces at an altitude of approximately 400 meters (1,312 feet), and modern valley floors etched several tens of meters below the glacial terraces (see **Figure F–3**). The glacial terraces that form the "second floor" in this landscape owe their existence to deposition during repeated advances of the Laurentide ice sheet. Glacial deposits within the Buttermilk Creek Valley are composed of a series of till units representing the Olean, Kent, and Lavery advances, together with interstadial deltaic, lacustrine, and alluvial facies (LaFleur 1979). At its maximum extent, the ice margin reached a position several kilometers south of the Cattaraugus basin (Millar 2005). The ice margin in this area is demarcated in part by the Kent moraine, which has been correlated with the maximum ice advance some time more recently than 24,000 years ago (Muller and Calkin 1993).

The best constraints on the timing of glacial recession in western New York State appear to come from stratigraphic studies in the Finger Lakes region. A seismic stratigraphic study by Mullins et al. (1996) showed that the Finger Lakes were last eroded by a surge of ice at approximately 14,500 radiocarbon (^{14}C) years before present (about 17,000 calendar years ago) that is correlated with Heinrich event H-1 (the most recent of the glacial North Atlantic large iceberg discharges). Radiocarbon-dated cores from Seneca Lake reveal that ice retreated rapidly from the northern end of the lake at about 14,000 ^{14}C years before present (approximately 16,600 calendar years before present) (Anderson and Mullins 1997, Ellis et al. 2004). (Note that the difference between measured ^{14}C years and actual calendar years represents a correction applied to compensate for natural variations through time in both the production rate and concentration of ^{14}C in the earth's atmosphere; see for example, Fairbanks et al. 2005 for details on calibration methods.)

Cattaraugus Creek and many of its tributaries are deeply incised into the complex of unconsolidated, glacially derived sediments that fill the bedrock valleys. The depth of incision varies but is typically on the order of 60 to 70 meters (197 to 230 feet). Near the outlet of Buttermilk Creek, for example, the modern channel lies about 60 meters (197 feet) below the adjacent glacial terrace. The incision is clearly postglacial because it cuts late–Wisconsin valley fills. Although some incision during one of the later interstadials (post–Erie) cannot definitely be ruled out, the geometry of the incised portion of drainage network makes this unlikely. Incision along Cattaraugus Creek extends downstream through the Zoar Valley, a narrow, deep (approximately 150 meters [492 feet]) bedrock canyon just east of Gowanda, New York. Downstream of the Zoar Valley, relief drops markedly as the creek enters a broad, tongue-shaped valley that appears to reflect the position of a former ice lobe. It is hypothesized that incision of the Zoar Valley and the valley fills upstream was triggered by baselevel lowering as the ice margin retreated north from the Gowanda area. Results from optically stimulated luminescence (OSL) dating in and near Buttermilk Creek, discussed in Section F.2.2, are consistent with this hypothesis, though additional dates from terraces along the Cattaraugus Valley upstream and downstream of the Zoar Valley would be necessary to confirm it.

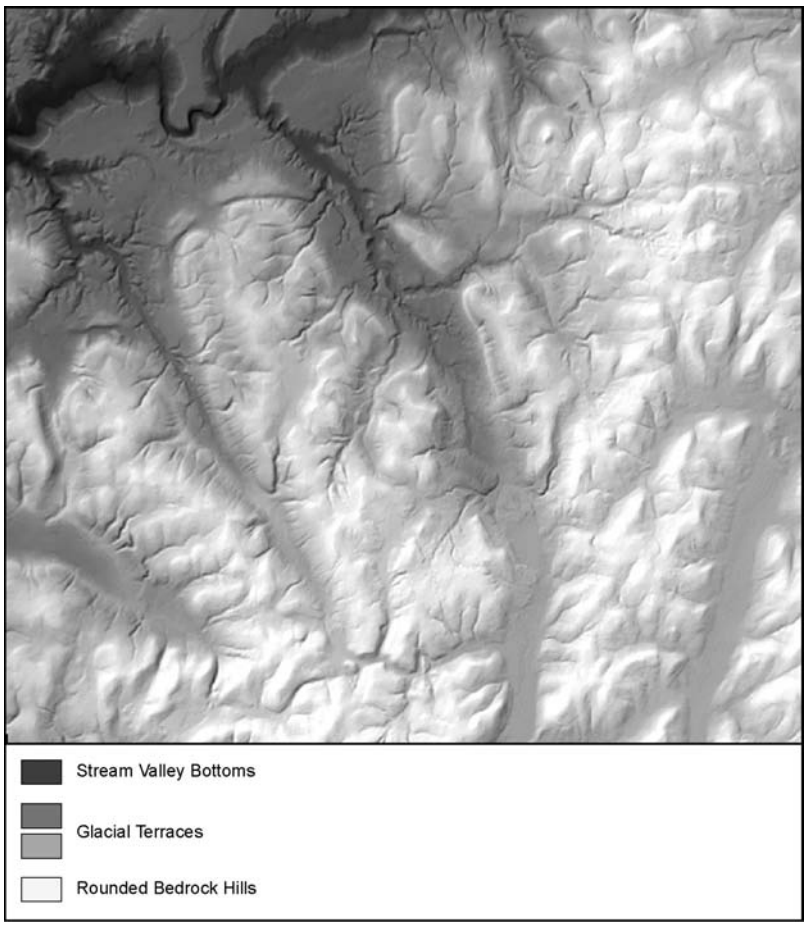

Figure F–3 Shaded Relief Image of Buttermilk Creek and Vicinity, Showing Rounded Bedrock Hills, Glacial Terraces, and Stream Valley Bottoms

F.2 Summary of Site Erosion Measurements

Site-specific historical erosion rates are important for testing the validity of any erosion predictions. Rates for the four dominant erosion processes (sheet and rill erosion, stream channel downcutting, stream valley rim widening, and gully advancement) for the Project Premises and the SDA have previously been estimated from measurements at the site. Sheet and rill erosion rates were directly measured using erosion frames at 23 locations along the stream valley banks adjacent to the Project Premises. Stream downcutting rates were determined from the age dating of terraces using ^{14}C and OSL methods and stream channel longitudinal profile measurements. The downcutting rates were translated into stream valley rim-widening rates using an estimate of the stable slope angle and geometric considerations. Gully migration rates were determined using aerial photographs and the Soil Conservation Service Technical Release 32 Method (USDA 1976). Observation of other geomorphic processes, including meandering and knickpoint advance, provides perspective but no additional quantitative information for erosion rate estimates.

These historical measurements provide perspective by which to judge the reasonableness of current erosion projections. All of these measurements, with the exception of OSL terrace dating, were collected before the current long-term erosion modeling effort was initiated and, therefore, were not designed as calibration measurements with quantifiable uncertainties. Thus, with the exception of the OSL age-dating data, specific measurements reported in this section were not directly used in the long-term modeling projections discussed in Section F.3.2.

F.2.1 Sheet and Rill Erosion Measurement

Field measurements of sheet and rill erosion on overland flow areas were taken at 23 locations along Erdman Brook, Franks Creek, and Quarry Creek using erosion frames (WVNS 1993a) (see **Figure F–4**). Each erosion frame was composed of a triangular steel structure designed to detect changes in surface height at the point of installation. Twenty-one frames were placed on hillslopes that are close to plant facilities and contain a variety of soil types and slope angles. Two frames (EF-5 and EF-9) were placed near the edges of stream valley walls to monitor the potential slumping of large soil blocks. The frames were installed in September 1990 and monitored monthly until 1993, at which point they were monitored at 6-month to 1-year intervals until September 2001. In September 1995, SDA construction activities necessitated removal of frames EF-3, EF-4, and EF-5 to allow for the construction of erosion controls in the SDA gully. Also, EF-12 was removed from the monitoring program in June 1998 because it had been displaced due to a gross slump (block) failure.

The sheet and rill erosion results are shown in **Table F–1**. These results show that soil buildup (aggradation) ranging from 0.003 to 0.16 meters (0.01 to 0.52 feet) was occurring at eight locations along Erdman Brook (EF-1, -2, -7, -8, -9, -21, -22, and -23), three locations along Franks Creek (EF-16, -19, and -20), and one location along Quarry Creek (EF-10) (WVNS 1993a). Soil depletion (degradation) ranging from -0.0003 to -0.015 meters (-0.001 to -0.05 feet) was observed at one location along Quarry Creek (EF-11) and five locations on Franks Creek (EF-6, -13, -15, -17, and -18). The Quarry Creek location (EF-11) is on the slope of the NP-1 gully (see **Figure F–5**), where a stormwater outfall (SO-4) is also located. The management practice of directing runoff to this location likely accelerated the gully development; however, none of the five locations on Franks Creek where degradation occurred are near stormwater outfall locations or appear to have been influenced by stormwater management practices. No soil aggradation or degradation was measured at the EF-14 location. The largest measured erosion rate over the 11-year period was 0.0014 meters (0.0046 feet) per year, which is equivalent to 1,400 millimeters (4.6 feet) per 1,000 years.

F.2.2 Stream Downcutting

Estimates of past rates of channel incision serve three purposes: they give an indication of potential future incision rates, they enable estimates of valley rim widening (using a geometric approach described in Section F.2.3), and they provide data for testing and calibrating long-term erosion models. Rates of stream incision were estimated using two complementary methods. The first method uses dated stream terraces to estimate average incision rates during the time period since terrace abandonment. The second relies on repeated surveys of channel cross sections to assess rates of channel lowering on annual to decadal time scales.

F.2.2.1 Radiocarbon and Luminescence Dating of Fluvial Deposits

LaFleur and Boothroyd calculated an average stream downcutting rate of approximately 6.0 meters (20 feet) per 1,000 years by means of the ^{14}C age dating of one wood fragment sample collected from the highest of 14 terrace levels on the western side of Buttermilk Creek (LaFleur 1979). The sample was extracted from a trench where wood fragments were buried 50 centimeters (20 inches) below the river gravel surface, and was determined to have an age of 9,920 ± 240 years before present (before present uncorrected carbon-14 years, dated by Richard Pardi, Queens College) (Boothroyd et al. 1979). Using the CalPal online radiocarbon calibration curve (http://www.calpal-online.de/), the corresponding calendar age is 11,502 ± 507 before present. This age was assumed to be close to the time of initial incision and downcutting of Buttermilk Creek. Because Buttermilk Creek has eroded to a depth of 55 meters (180 feet) at the Bond Road Bridge near the confluence with Cattaraugus Creek, Boothroyd et al. (1979) calculated a stream downcutting rate of 5.5 meters (18 feet) per 1,000 years as determined by dividing 55 meters by 10,000 years (the approximate uncalibrated age). The equivalent calculation using the calibrated age yields an average downcutting rate of 4.8 meters (15.7 feet) per 1,000 years.

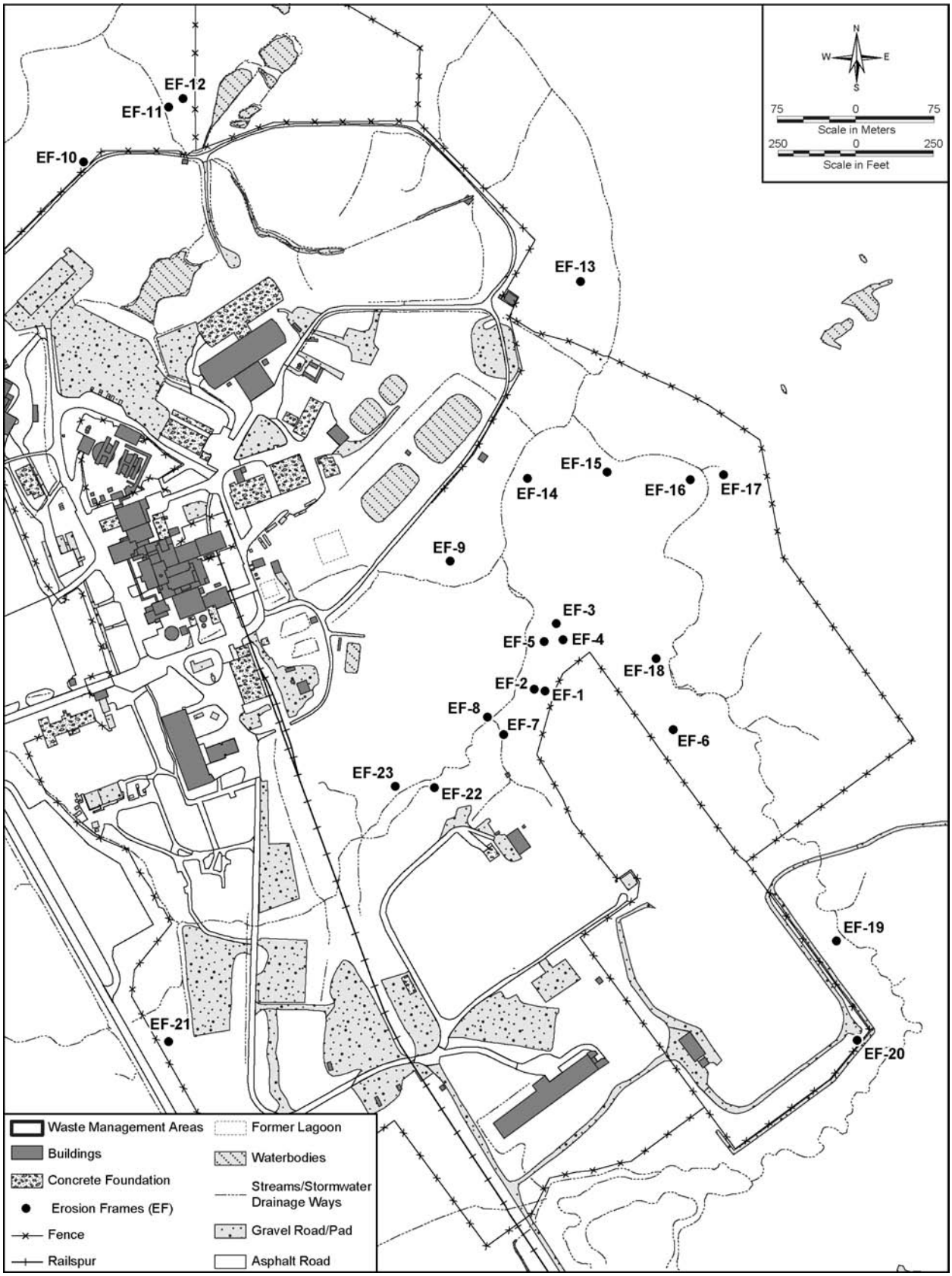

Figure F–4 Sheet and Rill Erosion Frame Measurement Locations

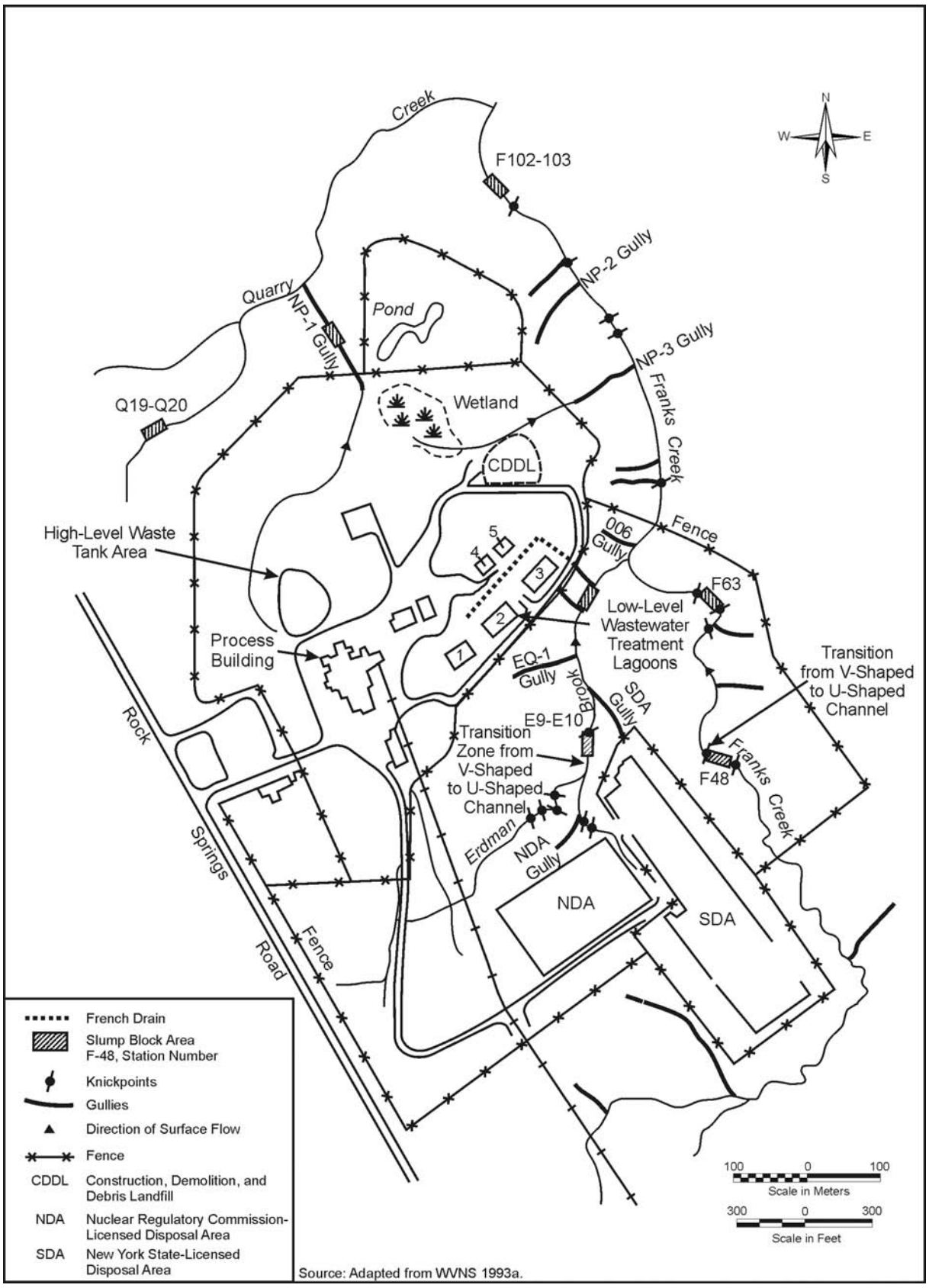

Figure F–5 North and South Plateau Gully Locations

Table F–1 Sheet and Rill Erosion Measurements

Frame Number	*Frame Location*	*Elevation Change between 1990 and 2001 (feet)*
EF-1	At northern end of SDA on slope to Erdman Brook	+0.39
EF-2	On slope to Erdman Brook downgradient of EF-1 location	+0.03
EF-3	Adjacent to gully located northeast of SDA	N/A
EF-4	In stream channel near northeastern corner of SDA	N/A
EF-5	On flat ground near northeastern corner of SDA	N/A
EF-6	At crest of a hillslope on the eastern slope of SDA	-0.02
EF-7	On ridge near northwestern corner of NDA	+0.11
EF-8	On ridge along Erdman Brook	+0.10
EF-9	On flat ground south of lagoon 2	+0.04
EF-10	On plateau at northern end of facilities near Quarry Creek	+0.01
EF-11	On western slope of the NP-1 gully	-0.04
EF-12	In gully NP-1 north of the security fence	N/A
EF-13	On western slope of lower Franks Creek	-0.001
EF-14	South of lagoon 3 on eastern slope of Erdman Brook	-0.000
EF-15	On south slope of Franks Creek	-0.04
EF-16	On western slope of Franks Creek	+0.07
EF-17	On eastern slope of Franks Creek	-0.05
EF-18	On western slope of Franks Creek	-0.004
EF-19	On slope outside the southeastern end of SDA	+0.52
EF-20	On slope outside the southern end of SDA	+0.13
EF-21	At southwestern end of site along Rock Springs Road	+0.06
EF-22	On southern bank of Erdman Brook north of NDA	+0.09
EF-23	On northern bank of Erdman Brook north of NDA	+0.24

+ = aggradation, - = degradation, SDA = State-Licensed Disposal Area, N/A = not applicable, frames removed due to construction activities in SDA and gross slump block failures, NDA = NRC [U.S. Nuclear Regulatory Commission]-Licensed Disposal Area.
Note: To convert feet to meters, multiply by 0.3048.

The single sample collected by Boothroyd et al. (1979) provided an indication of the time at which incision of Buttermilk Creek may have begun, but it provided no information about possible changes through time in the incision rate, or of possible variations at different positions in the watershed. It also provided no information about the elevation history near the outlet of Buttermilk Creek, which is important for constraining the catchment's baselevel history. In addition, it is often difficult to judge the reliability of a single sample because there are no other samples with which to compare it. It is generally best (though not always feasible) to collect multiple samples from a study area, so as to ensure that the ages make sense relative to one another given the geologic context. For example, when samples are collected at different levels from within a continuous stratigraphic sequence, the lower ones should be older than the higher ones.

The need for additional dating constraints motivated the collection of dating samples from 10 additional sites in and near the Buttermilk Creek drainage basin during November 2006. The objective of the field campaign was to search at each site for material that could be dated by either the ^{14}C method, the OSL method, or (ideally) both. These two methods are the most common and versatile dating methods for geologic deposits that are on the order of thousands to tens of thousands of years old (Walker 2005). Each method has strengths and weaknesses. An advantage of the ^{14}C method is that accelerator mass spectrometry can be used to obtain very precise dates. As one of the oldest methods in use for relatively young deposits, its application has become routine. However, no dating method is infallible. In the case of ^{14}C, one disadvantage is that it requires an assumption that the once-living material being dated (such as charcoal or bone) died shortly before burial. If the sample material undergoes a prolonged period of transport, or if it goes through multiple cycles of erosion

and re-deposition, it will be older than the deposit in which it is found. In addition, bioturbation (mixing of soils or sediments by plants or animals) can transport carbon-bearing material to higher or lower levels in the deposit, though potential presence of such mixing can often be judged on the basis of the sediment texture. As noted above, dates obtained from ^{14}C analysis must be calibrated to account for variations through time in the production rate of ^{14}C in the atmosphere. Finally, the age range for ^{14}C is generally limited to roughly the last 50,000 years.

Quartz-based OSL dating has become an increasingly popular method for dating deposits younger than roughly 100,000 years. In essence, it involves using mineral luminescence as a record of a quartz crystal's exposure to background ionizing radiation in the soil since the last time the crystal was exposed to sunlight (which resets the clock). Unlike the ^{14}C method, OSL dating involves direct dating of the sediments themselves. Because sand- and silt-sized quartz grains are common in sedimentary deposits, it is usually relatively easy to find datable material. One disadvantage of OSL is that grains may not be completely reset (or "bleached") during a deposition event; this may occur, for example, if a sample is deposited at night. (As discussed below, statistical methods have been developed to detect and correct for partial bleaching). The method also generally involves a larger analytical uncertainty than ^{14}C, and therefore is less precise. OSL analysis normally relies on the assumption that the soil radiation dose rate has been constant over the sample's lifetime. Finally, as with ^{14}C, bioturbation can mix together sediments of different ages.

Studies that compare results from the OSL method with independent dating techniques are becoming increasingly common. For example, a recent study by DeLong and Arnold (2007) showed good agreement among ^{14}C, OSL, and cosmogenic-exposure ages at alluvial fan sites in the western Transverse Ranges of California, while Magee and Miller (2004) showed very close agreement between radiocarbon, OSL, and uranium-series dates at a site in Australia. Other studies are reviewed by Rittenour (2008), who notes that "there is no evidence of systematic departure between OSL and independent ages over the last several hundred thousand years."

In November 2006, soil pits were hand-excavated at 10 locations along and near Buttermilk Creek. The sample sites are shown on **Figure F–6**, and their locations and characteristics are summarized in **Table F–2**. No material suitable for ^{14}C dating was identified at any of the locations, but each location yielded sand-bearing sediment suitable for OSL dating. OSL samples were collected in pairs where possible, to provide stored replicates for potential future analysis. Sample collection followed standard procedures for OSL sampling (http://crustal.usgs.gov/laboratories/luminescence_dating/prospective.html).

Three pairs of samples (OSL 4, 8, and 9) were collected from fluvial gravels deposited on or near the plateau surface. Two of the sites (8 and 9) were located near the axis of the Buttermilk Creek Valley, while the third (4) was located in alluvial-fan sediments on the east side of the valley. These sites were chosen to provide evidence of the onset of incision of Buttermilk Creek. One of the sites (location 9) proved particularly valuable, because it contained fluvial deposits overlying Lavery till "bedrock" in an abandoned meander cutoff high above the present valley floor, thus recording the earliest phase of incision along Buttermilk Creek.

Five pairs of samples (OSL 1, 2, 3, 5, and 6) were collected from fluvial terraces mapped by LaFleur (1979) and Boothroyd et al. (1982). These locations were chosen to provide constraints on the elevation history of Buttermilk Creek as it incised. An additional sample pair (OSL 7) was collected from a midlevel strath terrace in the Cattaraugus Valley near the Buttermilk Creek confluence. This location was chosen to provide information about the downcutting rate along Cattaraugus Creek in the vicinity of the Buttermilk Creek outlet, so as to establish Buttermilk Creek's baselevel history. The final sample pair (OSL 10), which is not shown on Figure F–6, was obtained from a high-level strath terrace in the adjacent Connoisarauley Creek Valley, which lies just to the southwest of the Buttermilk Creek watershed. This sample site was intended to provide a preliminary indication of whether the erosion history of Connoisarauley Creek is similar to that of Buttermilk Creek. All primary OSL samples were processed at the U.S. Geological Survey (USGS) Luminescence Laboratory (Mahan 2007), while the replicated samples were stored for potential future analysis.

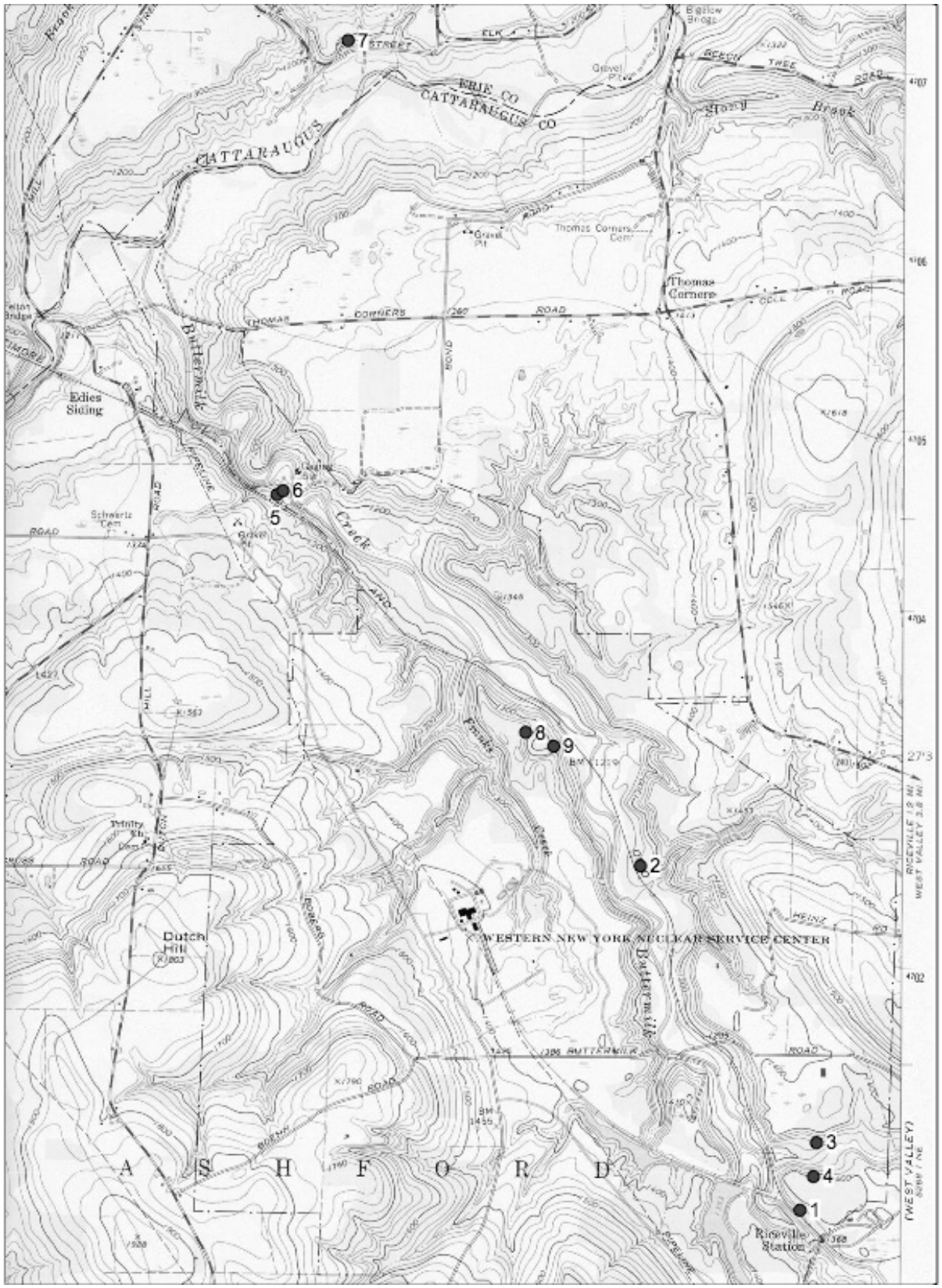

Figure F–6 Contour Map of Buttermilk Creek Showing Optically Stimulated Luminescence Sample Locations

Table F–2 Optically Stimulated Luminescence Sample Locations

Site Number	*Coordinates*	*Altitude (meters)*	*Location Notes*
WV-OSL-1	42.43542 N, 78.63179 W	414	Right-bank strath terrace, upper Buttermilk Creek Valley
WV-OSL-2	42.45270 N, 78.64275 W	382	Right-bank terrace, middle Buttermilk Creek Valley
WV-OSL-3	42.43885 N, 78.63079 W	410	Right-bank terrace in tributary valley
WV-OSL-4	42.43709 N, 78.63091 W	425	Gravel quarry on plateau surface, upper Buttermilk Creek Valley
WV-OSL-5	42.47130 N, 78.66745 W	379	Left-bank terrace, lower Buttermilk Creek Valley
WV-OSL-6	42.47155 N, 78.66703 W	367	Left-bank strath terrace, lower Buttermilk Creek Valley
WV-OSL-7	42.49426 N, 78.66277 W	365	Right-bank terrace, Cattaraugus Valley
WV-OSL-8	42.45938 N, 78.65047 W	408	Plateau-top terrace between Franks and Buttermilk Creeks
WV-OSL-9	42.45874 N, 78.64859 W	394	Fluvial gravel over till, south end of abandoned meander loop
WV-OSL-10	42.42475 N, 78.69410 W	440	Plateau sand/gravel over till, Connoisarauley Creek Valley

[a] Altitude represents terrace tread height rather than sample height.
Note: To convert meters to feet, multiply by 3.281.

F.2.2.2 Analysis and Interpretation of Dating Samples

The OSL sample results shown in **Table F–3** were obtained using a central-age model (CAM), which is most appropriate for well-bleached samples (i.e., those with a narrow equivalent-dose histogram). Three of the samples (OSL 1A, 5A, and 8A) show tight equivalent-dose histograms, indicating that the grains within them are likely to have been well bleached (Mahan 2007). In order to assess and, if necessary, correct for the possibility of partial bleaching, the sample aliquot data were also analyzed using an age-estimation procedure known as the three-parameter minimum-age model (MAM) (Arnold et al. 2009, Galbraith and Laslett 1993). This statistical age-model is designed to detect the presence of a broad tail in the age distribution among aliquots (sub-samples), which is thought to be indicative of partial bleaching, and correct for the resulting error by emphasizing the youngest aliquots. Results from applying the three-parameter MAM are shown in **Table F–4**.

Table F–3 Optically Stimulated Luminescence Sample Ages and Average Incision Rates using a Central-Age Model

Sample Number	*Central-Age Model Date (ky ± 1σ)*	*Depth Below Plateau (meters)*	*Height Above Valley Floor (meters)*	*Pre-terrace Incision Rate (meters per 1,000 years)*	*Post-terrace Incision Rate (meters per 1,000 years)*
1A	14.8 ± 1.33	14	18	6.5	1.2
2A	16.2 ± 1.31	42	9	52	0.56
3A	16.7 ± 0.88	20	10	66	0.60
4A	16.1 ± 2.01	5	25	5.3	1.6
5A	14.5 ± 1.08	32	28	13	1.9
6A	15.0 ± 2.04	44	16	22	1.1
7A	15.2 ± 1.82	40	25	22	1.6
8A	16.8 ± 1.53	7	45	N/A	2.7
9A	17.1 ± 1.39	21	31	N/A	1.8
10A	21.2 ± 1.17	N/A	N/A	N/A	N/A

1σ = one standard deviation, ky = 1,000 years, N/A = not applicable.
[a] Depth below plateau and height above valley floor estimated from contour map and/or digital elevation model.
[b] Pre-terrace incision rate based on assumed start time of incision of 17 thousand years before AD 1950.
Note: To convert meters to feet, multiply by 3.281.

Table F–4 Optically Stimulated Luminescence Sample Ages and Average Incision Rates using a Minimum-Age Model

Sample Number	*Minimum-Age Model (ky ± 1σ)*	*Depth Below Plateau (meters)*	*Height Above Valley Floor (meters)*	*Pre-terrace Incision Rate (meters per 1,000 years)*	*Post-terrace Incision Rate (meters per 1,000 years)*
1A	10.83 -1.26/+1.33	14	18	2.1	1.7
2A	15.10 -0.34/+0.36	42	9	22	0.60
3A	17.00 -1.36/+1.45	20	10	n/a	0.59
4A	7.91 -3.34/+3.76	5	25	0.55	3.2
5A	13.75 -1.76/+1.86	32	28	9.8	2.0
6A	10.86 -1.14/+1.21	44	16	7.2	1.5
7A	8.39 -1.34/+1.40	40	25	4.6	3.0
8A	17.35 -0.72/+0.75	7	45	N/A	2.6
9A	17.07 -1.07/+1.13	21	31	N/A	1.8
10A	18.92 -2.20/+2.30	N/A	N/A	N/A	N/A

1σ = one standard deviation, ky = 1,000 years, N/A = not applicable.
[a] Depth below plateau and height above valley floor estimated from contour map and/or digital elevation model.
[b] Pre-terrace incision rate based on assumed start time of incision of 17 thousand years before AD 1950.
Note: To convert meters to feet, multiply by 3.281.

Samples 8A and 9A originate at and near the top of the plateau, respectively, and are therefore considered to be particularly important because they establish the beginning of incision along Buttermilk Creek. Mahan (2007) noted that sample 8A is among 3 samples that show relatively tight histograms, suggesting that these 3 samples are likely to be the most reliable of the 10 collected. Results from applying the CAM and MAM to samples 8A and 9A overlap within 1-sigma uncertainty bounds. This means that while one can not completely rule out the possibility that these two samples are partially bleached, such partial bleaching is not apparent in the aliquot statistics. Using the 1-sigma uncertainty bounds as a guide, these two samples suggest that Buttermilk Creek began to incise some time between about 16,000 and 18,000 years ago.

The fact that one of the two samples (8A) comes from fluvial deposits atop the plateau, while the other comes from an abandoned meander cutoff incised into the Lavery till, suggests that these two deposits bracket the onset of incision. The overlapping age ranges of the two dates also suggest that early incision was relatively rapid. The implied 16,000 to 18,000-year age range for initial incision is also consistent with the estimate by Ellis et al. (2004) that the Laurentide ice sheet retreated from the Finger Lakes region some time around 16,600 years ago.

Of the Buttermilk Creek terrace samples, numbers 1A and 5A both show relatively narrow single-aliquot distributions, which are generally indicative of good bleaching. The MAM and CAM age estimates for sample 5A overlap within 1-sigma uncertainty, suggesting that the sample is indeed well bleached and can be considered reliable. The MAM age for sample 1A is lower than the CAM age, suggesting that the sample may have been incompletely bleached (despite the narrow range of individual aliquots). Both samples were obtained from terraces with treads lying roughly midway between the plateau surface and the modern valley floor. The age estimates for samples 1A and 5A, respectively, suggest that roughly half of the incision had occurred by 9,000 to 16,000 years before present, and that the remaining incision has occurred since that time. Thus, the incision rate along Buttermilk Creek may have slowed down over time. The post-terrace downcutting rates implied by these two samples are on the order of one to two meters per thousand years. Samples 2A and 3A suggest somewhat lower rates (see Tables F–3 and F–4), but the relatively broad distribution of single-aliquot ages in these samples suggest that they should be interpreted with caution. The MAM analysis of sample 4A, which comes from a coarse alluvial fan exposed in a quarry, shows a very broad dispersion of ages (the 1-sigma uncertainty bounds are greater than 3,000 years) and it is therefore not

considered to be a reliable age estimate. Mahan (2007) also noted that sample 4A exhibited a large variation in equivalent-dose measurements.

Sample 7A was collected from a soil pit on a midlevel terrace in the Cattaraugus Valley. The sample showed a large variation in equivalent-dose measurements among its aliquots, suggesting the potential for partial bleaching. The MAM age estimate is considerably younger (about 7,000 to 10,000 years) than the CAM estimate (about 13,000 to 17,000 years). The poor quality of this sample is unfortunate, because at present it provides the only quantitative constraint on the rate of baselevel lowering in the Cattaraugus Valley near the mouth of Buttermilk Creek. The MAM age implies a post-terrace incision rate on the order of a few meters per thousand years.

The origin of the discrepancy between the ^{14}C age and the OSL ages is not known. One possibility is that the radiocarbon was contaminated with younger carbon. Another possibility is that the OSL samples are biased toward older ages by incompletely bleached grains, though if this were the case it would have to apply to those samples for which the MAM analysis revealed no statistical evidence of partial bleaching. Another possibility is that the wood fragments were buried some time after incision had already begun. Resolution of the discrepancy would require additional data collection and/or analysis, such as collection of additional ^{14}C and/or OSL samples. Given the overall consistency among OSL dates, as well as their consistency with the deglacial chronology of the Finger Lakes region, their ages are considered more reliable than the single radiocarbon age reported by Boothroyd et al. (1979).

Collectively, the OSL dating samples obtained from fluvial deposits suggest that Buttermilk Creek has had an average incision rate on the order of one to a few millimeters per year over roughly the last 10,000 to 17,000 years.

F.2.2.3 Estimating Downcutting from Repeated Cross-Section Surveys

The second measurement for downcutting involves comparison of elevation changes in cross sections after 10 years. In 1980, a longitudinal profile survey was conducted by Dames and Moore (WVNS 1993a) on a section of Franks Creek starting at the Quarry Creek confluence and proceeding upstream to a point on the eastern side of the SDA. In 1990, a second survey was completed along the same section of Franks Creek, and a comparison of resulting data indicated a downcutting rate of approximately 0.6 meters (2 feet) per 10-year period, which is equivalent to 60 meters (200 feet) per 1,000 years. This downcutting rate is the result of direct measurement of the change in thalweg, the locus of the lowest points in a stream or valley depth over the 10-year period. Because this rate is based on a short (10-year) projection, it does not take into account the wider range of precipitation values that are likely to occur over the long term, and thus, is not considered to be representative of long-term conditions. The 10-year projection also relies heavily on the current status of land use in the watershed, which is industrial in the vicinity of the Project Premises. The larger percentage of impervious areas associated with the industrial complex results in higher surface-water runoff rates than are anticipated to occur following decommissioning.

F.2.3 Historical Stream Valley Rim Widening

Stream valley rim–widening rates were calculated using estimates of the stream channel downcutting rates and the stream valley stable slope angle. The estimate of stable slope angle was determined from measurements of slope movement rates on several stream valley slopes that are actively slumping. The average downcutting rate, as estimated from dated terraces and the longitudinal profile study, was translated into a rim-widening rate by dividing the downcutting rate by the tangent of the stable slope angle.

F.2.3.1 Rim-Widening Estimates Based on Stream Downcutting Measurements

Dames and Moore studied the angle of ravine slopes within the Buttermilk Creek drainage basin to estimate the angle of stable slopes. They measured 21 cross sections along Quarry Creek, Franks Creek, and Erdman Brook using the 0.61-meter (2-foot) contour interval on a topographic map compiled by stereo-photogrammetric methods from 1:6,000-scale aerial photographs taken on May 17, 1989, and compiled by Tallamy, Van Kuren, Gertis, and Associates of Orchard Park, New York (WVNS 1993a). The cross sections were taken in areas having rather stable stream valley walls (no evidence of active landsliding), and an average slope angle was calculated. The slope angle, approximately 21 degrees, is considered to be representative of an "at-rest" slope condition, meaning the valley walls have reached equilibrium. Slopes with angles greater than 21 degrees are viewed as potentially unstable.

A second method confirmed the estimate of a 21-degree stable-slope angle. In this second study, force balance analysis was applied to estimate the slope angles for eight areas along Erdman Brook and Franks Creek (WVNS 1993a). Five of the areas, with slope angles ranging from 18.4 to 24.9 degrees, were stable. One of the areas, with a slope angle of 27 degrees, was subject to creep. The remaining two areas, with slope angles of 26 and 38 degrees, were unstable.

Using the stable-slope estimate of 21 degrees and an average downcutting rate of 5,500 millimeters (18 feet) per 1,000 years computed from the uncalibrated ^{14}C age of the high-terrace sample, the average rim-widening rate for Buttermilk Creek is 0.0143 meters (0.05 feet) per year. The equivalent figure for the calibrated ^{14}C age is 0.0125 meters (0.04 feet) per year. The same calculation can be made using rates of downcutting estimated from OSL terrace ages. Dividing the height of mid-level Buttermilk Creek terraces (sample locations 1, 2, 3, 5, and 6) by their ages yields average downcutting rates ranging from 0.6 to 1.9 meters (2.0 to 6.2 feet) per 1,000 years (Table F–3). Of these, the most reliable figure is thought to come from the well-bleached sample 5A, with an estimated post-1,000 years ago downcutting rate of 2.0 meters (6.6 feet) per 1,000 years. The corresponding rim-widening rate is 5.8 meters (19.2 feet) per 1,000 years. Note, however, that downcutting estimates based on Buttermilk Creek would likely underestimate the current downcutting rate along Franks Creek, which has a partly convex-upward longitudinal profile that may indicate that it is still in a state of transient response to baselevel lowering in the Buttermilk Creek Valley, and therefore incising faster than Buttermilk Creek.

The rim-widening rate was also estimated using the measured short-term downcutting rate from the longitudinal profile study of approximately 0.6 meters (2 feet) per 10 years in conjunction with an assumed 21-degree stable slope. This approach results in a rim-widening rate of 0.156 meters (0.5 feet) per year for Franks Creek (see **Table F–5**).

Table F–5 Estimates of Stream Valley Rim Widening Based on Stream Downcutting

Location and Method	*Stream Downcutting Rate (meters per 1,000 years)*	*Stream Valley Rim–Widening Rate (meters per year)*
Buttermilk Creek (calibrated radiocarbon age dating of wood fragment)	4.8	0.014
Buttermilk Creek (optically stimulated luminescence dating of terrace alluvium, sample 5A)	2.0 (5A)	0.0058
Franks Creek (longitudinal profile survey)	60	0.175

Note: To convert meters to feet, multiply by 3.281.

F.2.3.2 Rim-Widening Estimates Based on Slope Movement Measurements

The slope movement rate was measured on active slump areas along Buttermilk Creek and Erdman Brook. A 1978 analysis examined movement of a slump block on the Buttermilk Creek ravine, referred to as the "BC-6" landslide, approximately 426 meters (1,400 feet) east of the Waste Management Area 2 lagoons (Boothroyd et al. 1979). Thirty-five steel posts were surveyed at locations on the slump block complex and adjoining slopes. Resurvey of the posts two years later yielded an estimated average downslope movement rate of 7.9 meters (26 feet) per year. This downslope movement rate corresponds to a stream valley rim–widening rate of 4.9 to 5.8 meters (16 to 19 feet) per year based on the angle of the slope (Boothroyd et al. 1982). This movement rate is believed to represent an upper estimate of the annual mass movement that has occurred on the slope because a moderately severe storm (recurrence interval: 10 to 20 years) was recorded during the measurement period and a sand layer 4.6 meters (15 feet) thick was identified near the top of the landslide. The cohesionless sand layer coupled with the moderately severe storm event likely induced rapid movement, potentially skewing results toward the high end. Also, the high rate is not sustainable over the long term because slope movement slows as the slope angle tends to stabilize and eventually stops as that angle attains equilibrium; movement may be rejuvenated, however, by stream incision at the base of the slope. Over the course of a 1,000-year period, many localized areas throughout the stream valley would develop unstable slopes, causing rapid movement over a short time before stabilizing.

Along the section of Erdman Brook referred to as the "North Slope of the SDA," the New York State Geological Survey installed and surveyed 30 posts in 1982 and resurveyed the post elevations in 1983 to assess slope movement. The downslope till movement rate for the first year (1982 to 1983) was reported to be 0.2 meters (0.66 feet) per year, equivalent to a stream valley rim–widening rate of approximately 0.15 meters (0.49 feet) per year (Albanese et al. 1984). The New York State Energy Research and Development Authority added 4 posts in 1991 and resumed yearly measurements in 1991 and reported a maximum decrease in surface elevation of 0.04 meters (0.12 feet) per year over the last 22 years (1982 to 2004) and a maximum of 0.02 meters (0.07 feet) per year over the last 13 years (1991 to 2004), indicating that the movement rate has slowed down over the last decade (WVNS 1993a). **Table F–6** summarizes these results.

Table F–6 Estimates of Stream Valley Rim Widening Based on Slope Movement

Location	*Slope Movement Rate (meters per year)*	*Stream Valley Rim–Widening Rate (meters per year)*
BC-6 landslide (on Buttermilk Creek 426 meters east of the lagoons)	7.9	4.9 to 5.8
North Slope of the SDA (on Erdman Brook) – first-year rate	0.2	0.15
North Slope of the SDA (on Erdman Brook) – 22-year rate	0.02 to 0.04	0.015 to 0.03

SDA = State-Licensed Disposal Area.
Note: To convert meters to feet, multiply by 3.281.

F.2.3.3 Measurement of Gully Advance Rates

Several existing gullies in the Buttermilk Creek drainage basin are migrating into the edge of the North and South Plateaus. If natural gully advancement proceeds without mitigation, the gully heads could cut into the areas in which residual radioactivity could be closed in place. To address this concern, studies have been initiated to determine the gully migration rate. As shown on Figure F–5, five gullies have been mapped on the North Plateau extending from Quarry Creek (NP-1), Erdman Brook (EQ-1), and Franks Creek (NP-2, NP-3, and 006) toward the industrial area, and two have been mapped on the South Plateau (the SDA and NRC [U.S. Nuclear Regulatory Commission]-Licensed Disposal Area [NDA]) extending from Erdman Brook toward the disposal facilities.

The headward advance rates of three active gullies (SDA, NP-3, and 006) were calculated (WVNS 1993a) using the Soil Conservation Service Technical Release 32 method (USDA 1976). Aerial photographs taken in 1955, 1961, 1968, 1977, 1978, 1980, 1984, and 1989 were reviewed in support of the calculation. As shown in **Table F–7**, this method indicated that the SDA gully was advancing toward SDA Disposal Trench 1 at a rate of 0.4 meters (1.2 feet) per year, implying that, without mitigation, the gully would reach the SDA fence in approximately 25 years and the trench in about 200 years. In 1995, as part of an effort to control infiltration and runoff at the SDA, the gully was filled to mitigate erosion. The NP-3 gully is advancing toward the Construction and Demolition Debris Landfill at a rate of 0.7 meters (2.2 feet) per year; without mitigation, this gully will encroach upon it in about 100 years. The 006 gully is migrating toward the area between the Construction and Demolition Debris Landfill and the wastewater treatment lagoons at a rate of 0.7 meters (2.3 feet) per year. Without mitigation, this gully is predicted to reach the area in approximately 150 years; however, given the present surface-water drainage course, the gully head is not likely to affect the two facilities. Other gullies on the Project Premises have not shown sufficient visible movement of the gully heads to allow for the calculation of migration rates by the Soil Conservation Service Technical Release 32 method.

Table F–7 Gully Advance Rate Measurements

Gully Name	*Gully Location*	*Gully Advance Rate (meters per year)*
SDA	On east bank of Erdman Brook north of SDA	0.4 [a]
NP-3	On west bank of lower Franks Creek, east of Construction and Demolition Debris Landfill	0.7
006	On west bank of Franks Creek, just north of confluence with Erdman Brook	0.7

SDA = State-Licensed Disposal Area.

[a] The SDA gully was reconstructed in 1995 and the 0.4 meters per year rate was measured before mitigation.

Note: To convert meters to feet, multiply by 3.281.

F.3 Erosion Rate Prediction Methods

Mathematical models are used to predict the nature and rates of erosion processes. A survey of the models shows that they fall into two broad categories. Models in the first category make short-term predictions (projections considered valid for decades). These short-term models are generally based on detailed simulation of one or two distinct erosional processes. Models in the second category use upper-level conservation equations representing the combined effect of multiple erosional processes to make long-term projections (thousands of years). The following paragraphs provide a discussion of the long-term erosion modeling study that was used to make the prediction of erosion at the site over the next 10,000-year period. It is followed by a discussion of the short-term modeling analyses that were completed over the last 30 years and are now being used to verify the reasonableness of the long-term modeling assessment.

F.3.1 Long-term Models

The geomorphic history of the site, together with observations of modern processes, dictates the type of model that is required to assess potential erosion rates and patterns over millennial time scales. As discussed earlier, geologic evidence indicates that the topography of the Buttermilk Creek drainage basin has changed substantially since the end of the last ice age. Dating samples imply that rates of stream downcutting have been on the order of 1 meter per 1,000 years or higher, which is relatively rapid for a moderate-relief landscape and suggests the potential for significant topographic change over the next 10,000 years. In addition, observations at and near the facilities indicate ongoing topographic change, in the form of mass movement on hillslopes, gully propagation, and measurable downcutting along creek valleys.

Because topography is expected to continue to evolve in the future, the applicability of standard "fixed terrain" erosion-prediction models, such as the Water Erosion Prediction Project (WEPP) and others like it, is limited. These standard "fixed terrain" models are derived from field-test plot data that was collected over a 20-year

period; thus, these models are not intended to be extrapolated for long periods into the future (i.e., thousands of years). Instead, they are useful for estimating erosion rates on an average annual basis or storm-by-storm basis over tens to hundreds of years. Ideally, a model of potential future erosion should be able to incorporate changing topography. Such a model should also be designed, to the extent possible given the state of the science, to represent the types of processes that are occurring today and likely to continue in the future, including sediment transport by streams, erosion of resistant (cohesive) material by streams, mass movement on hillslopes, and the formation of gullies. Thus, the logical tool of choice is a Landscape Evolution Model (LEM). The term, Landscape Evolution Model, is used here to refer to a computer program that calculates the evolution of a topographic surface over time by solving a set of equations and algorithms that represent the geomorphic processes acting on that surface. The development, testing, and refinement of LEMs is the subject of active ongoing research (for recent reviews, see Martin and Church 2004, Willgoose 2005, Codilean et al. 2006, Bishop 2007).

F.3.1.1 Review of Erosion Models

A survey of long-term erosion models was conducted to identify models that could be used for analysis of WNYNSC. Several criteria were used to help identify and evaluate models. These models must have the following capabilities and characteristics:

- Analysis of long-term erosion (thousands of years) with changing topography;
- Modeling of the dominant erosive processes of the site, including hillslope movement (soil creep and landsliding), stream channel downcutting, and gully formation;
- Calibration directly or indirectly using available models or measurements;
- Public availability; and
- Peer review and general verification based on ability to reproduce statistical characteristics of landforms.

Three specific models for predicting landscape evolution were identified. These models, SIBERIA, GOLEM [Geomorphic/Orogenic Landscape Evolution Model], and CHILD, are briefly described in the following paragraphs.

The SIBERIA model was initially developed in the late 1980s to predict landform changes over long periods of time (hundreds to millions of years). It is a physically based model that uses an effective-runoff approach over a specified timeframe and accounts for both fluvial and diffusive (hillslope) processes that move sediment through a drainage system. The fluvial processes include soil detachment and water transport (e.g., sheet and rill erosion, stream downcutting, gully advance), while the diffusional process represents soil creep and landsliding (e.g., slope movement). The central feature of SIBERIA is a sediment balance that is conducted over each rectangular grid element that forms part of the total grid representing the site. The change in sediment thickness within a grid is the basis for prediction of erosion or sedimentation within that grid. The model is one of the earliest of the current generation of landform evolution models. A continuing research program has been under way during the past 10 years to validate SIBERIA predictions against small-scale laboratory experimental and large-scale natural landscapes over a range of different landforms, geologies, and climates.

Studies in this program have demonstrated the following aspects of the SIBERIA model:

- It is able to simulate the statistical form of the Pokolbin catchment in the Hunter Valley in Australia (Willgoose 1994).
- It is able to simulate development of experimental model landscapes (Hancock and Willgoose 2001a).

- It can simulate natural landforms in a tectonically active region of New Zealand (Ibbitt et al. 1999).
- Using parameters derived from a short-term analogue site (i.e., an abandoned uranium mine at Scinto 6 in the South Alligator River Valley, Kakadu National Park, Australia), SIBERIA can accurately model gully development on a manmade postmining landscape over timespans of around 50 years (Hancock and Willgoose 2001b).
- Using parameters derived from a long-term analogue site (i.e., a natural, undisturbed site at Tin Camp Creek within the Myra Falls Inlier, Northern Territory, Australia), SIBERIA can accurately model the geomorphology and hydrology of a natural catchment over the long term (Hancock et al. 2002).

The second model that was identified was GOLEM. This model was developed in the early 1990s to simulate evolution of topography over geologic time scales. Like SIBERIA, it is a physically based model that uses average precipitation over a specified timeframe, accounts for both fluvial and diffusional processes, and conducts sediment balances over the grid elements that represent the site. Its structure is also similar to SIBERIA in that it uses a rectangular, finite-difference grid. It uses a somewhat different method for computing erosion and sedimentation by running water.

The CHILD model was developed in the late 1990s and is a descendant of the GOLEM and SIBERIA models. Like SIBERIA and GOLEM, it simulates the interaction of fluvial processes (slope wash and channel and rill erosion) and diffusive processes (weathering, soil creep, and other slope transport processes). However, this basic capability has been expanded with the addition of several features. It uses an irregular gridding method that makes it possible to represent different parts of the landscape at different spatial resolutions. Instead of using a single effective rainfall or runoff rate that represents a geomorphic average, it provides the option of stochastic rainfall input. Like the GOLEM model (and the related DELIM [Howard 1994]) it allows for detachment-limited, transport-limited, or mixed behavior in calculating runoff erosion. It computes hillslope sediment transport using either a linear or nonlinear diffusion model; the latter is designed to capture rapid mass movement on slopes close to the angle of repose. The ability of the CHILD model to reproduce observed ridge–valley topography and statistical properties such as the slope-area relationship has been demonstrated (Tucker et al. 2001b, Tucker 2004). A recent study (Attal et al. 2008) showed that the model is capable of simulating the topography of a drainage basin in central Italy that is undergoing a transient geomorphic response to accelerated tectonic uplift during the Pleistocene period. The model has also been used to simulate gully development (Istanbulluoglu et al. 2005, Flores-Cervantes et al. 2006), including gully cut-and-fill dynamics in response to stochastic rainfall variation (Tucker et al. 2001b, Arnold et al. 2009). Other published applications of the CHILD model include geomorphic impacts of glacial-interglacial climate variation (Bogaart et al. 2003), valley stratigraphy and geoarchaeology in a meandering river environment (Clevis et al. 2006), the role of vegetation in landscape evolution (Collins et al. 2004; Istanbulluoglu and Bras 2005), grain-size dynamics in drainage networks (Gasparini et al. 2007), karst landform development (Fleurant et al. 2008), and geomorphic effects of rainfall intensity and duration (Tucker and Bras 2000, Sólyom and Tucker 2004).

The CHILD model was selected as the primary analysis tool because (1) it uses a stochastic rainfall module that can be driven by rainfall intensity and duration statistics derived from onsite data, (2) it provides a multi-resolution capability that allows the site to be modeled at a higher resolution than the surrounding catchment, and (3) it allows for fluvial erosion to be limited by either sediment-transport capacity or material detachment capacity.

F.3.1.2 Overview of Approach to Erosion Modeling

Erosion modeling objectives at WNYNSC are to develop an understanding of local erosion processes and the manner in which those processes may develop over a long period of time, and to provide a basis for estimating potential health impacts related to erosion. Major analysis products include the development of future-erosion

scenarios at facilities on the North and South Plateaus, evaluation of gully and stream channel development, and assessment of the potential for alteration in drainage patterns.

Application of the CHILD model to the Buttermilk Creek drainage basin is designed to shed light on the nature and magnitude of potential long-term (10,000-year) geomorphic evolution of the area. Modeling over such long periods is based on a simple premise: *if a model, when given a plausible set of parameters and boundary conditions, can adequately reproduce the observed pattern of landscape evolution over the last 10,000 to 20,000 years, then there is increased confidence in the ability of that model to indicate potential erosion trends over a similar timeframe and under similar environmental conditions*. This approach takes advantage of the rather simple and well-constrained postglacial geomorphic history of Buttermilk Creek, which, as noted above, is interpreted to involve postglacial (circa 18,000 years ago) drainage network incision into glacial deposits due to baselevel lowering along Cattaraugus Creek.

In evaluating the output of landscape evolution models like CHILD, it is important to bear in mind that the details of computed drainage network patterns are known to be sensitive to initial conditions. For example, Ijjasz-Vasquez et al. (1992) showed that small perturbations of initial conditions led to notable differences in simulated drainage pathways, though the topography and network geometry were robust in a statistical sense. This instance of the "butterfly effect" means that these models are more useful for indicating general trends, patterns, and parameter sensitivities than for predicting the detailed erosional history at a particular spot in the landscape. The particular geometry of any simulated drainage network should be considered merely one of many possible realizations. Areas with initially very low relief are most prone to this effect. Initializing a model with a pre-existing drainage network (rather than a nearly flat surface) reduces the potential for sensitive dependence on initial conditions but cannot entirely eliminate it. A second consideration concerns the nature of the physical laws ("geomorphic transport laws" [Dietrich et al. 2003]) that go into landscape evolution models like CHILD. For the most part, these are semi-empirical statements about the relationship between sediment transport rates by a particular type of process (e.g., soil creep, channelized flow) and controlling variables such as gradient or fluid friction. For example, the linear and nonlinear soil creep laws rely on empirical rate coefficients that, at present, cannot be determined *a priori* from knowledge of soil type, biota, and climate alone. This means that, like most environmental models, landscape evolution models are provisional; they represent the current state of the science but are subject to continual improvement as the science evolves. In the context of evaluating erosion at WNYNSC, the best available test of these models' reliability is their ability to reproduce past landscape evolution. This is the basis for the testing and calibration strategy used in this study.

Determination of erosion processes and processes influencing erosion requires vastly different scales of space and time. Representative scales for the detachment of soil particles in rills are on the order of millimeters and seconds; those for river meandering or tectonic uplift, from one to thousands of kilometers and from centuries to thousands of years. Within this range of scales, different modeling approaches may be applicable. From the reductionist view, detailed specification of many processes is needed to understand all features of landscape evolution (Rodriguez-Iturbe and Rinaldo 1997). An opposing view holds that, for complex landform systems, a reductionist approach does not provide a self-consistent method (Werner 1999) and that large-scale structure is independent of detailed description of motion at small scales (Goldenfeld and Kadanoff 1999). The CHILD modeling approach is designed to use macroscopic-scale correlation of measured conditions projected over differing space and time scales. The following sections provide the rationale for the selection of the initial postglacial topography, the model boundary conditions, and the input parameters.

F.3.1.3 Overview of CHILD Model Calibration Strategy

Every mathematical-conceptual model has parameters that are the coefficients and exponents in the model equations. These parameters must be estimated for a given watershed and for each computational segment of the model. This requires determining the parameters' inherent relationships with physical characteristics or

tuning the parameters so that model response approximates observed response, a process known as calibration. In the calibration process, the modeling results are checked to determine whether they are reasonable for the area and time that was modeled, and for the conditions modeled. The calibration process can be quite complex and time consuming because of the limitations of the input and output data, imperfect knowledge of basin characteristics, the mathematical structure of the models, and limitations in the ability to quantitatively express preferences for how best to fit the models to the data.

Calibration of the CHILD model was accomplished through a forward modeling exercise, which starts with a postglacial (pre-incision) valley topography and attempts to reconstruct the modern topography. Within this framework, a number of different potential strategies, with varying degrees of complexity could be used. These range from Monte Carlo–based, multi-parameter optimization schemes to simple single-parameter tuning exercises. The advantage of complex, multi-parameter schemes such as Monte Carlo methods is that they can achieve the closest possible match to data and can also reveal the potential for model equifinality (multiple solutions providing equivalent matches to the data). They can also be used to place uncertainty bounds on the calibrated parameters. Their main disadvantage is the high cost and long times of computation. Simpler parameter-tuning methods have the advantage of computational efficiency, and are most effective where the majority of parameters can be estimated *a priori* using site-specific data.

The CHILD model was calibrated using a Monte Carlo approach that tested the ability of the model to reproduce the modern landscape, starting from a reconstruction of the ancient landscape. One thousand different runs were computed using randomly generated parameter sets. Parameter ranges, and the values of fixed parameters, were chosen on the basis of available data as described below. For each parameter that was varied at random, five unique values were identified. This "binning" of Monte Carlo parameters is sometimes known as the Latin Hypercube approach, and it has the effect of reducing the parameter space to a finite number of combinations and ensuring that parameter combinations are spread over the full range rather than clustering.

The results from each Monte Carlo run were tested against a set of metrics derived from the modern topography and from age-dating information. Based on these test metrics, a numerical score was assigned to each run. Criteria for an acceptable fit were determined, and those parameter sets fitting these criteria were identified. The overall best-fit run was identified as a "standard" case for developing forward-in-time simulations. Other parameter sets fitting the acceptance criteria were also identified for use in constructing alternative future erosion scenarios.

In calibrating a model in this manner, careful attention must be given to the initial and boundary conditions. The initial conditions for CHILD include the topography just prior to the onset of postglacial valley incision, and the distribution of lithologies within the basin. As noted previously and detailed further below, the postglacial topography was reconstructed on the basis of existing remnants of a once-continuous plateau surface. To represent the varying lithologies across the catchment, a choice must be made as to the degree of complexity in modeling the distribution of rock and sediment types. If strongly contrasting rock or sediment types are lumped together, there is a risk that the model will perform poorly because it fails to account for major differences in erosional resistance. On the other hand, if the landscape and its subsurface are divided into too many individual units, several problems can arise. First and most important, including multiple lithologic categories increases the number of poorly constrained parameters that must be calibrated. Second, the more loosely constrained parameters that are included in a model, the harder it is for an analyst to understand and interpret the model's behavior. Third, information about the spatial distribution of lithologies, particularly in the subsurface, may be (and usually is) limited or incomplete. To paraphrase Albert Einstein, it is generally best to make a model as simple as possible, but no simpler. In keeping with this philosophy, the approach used in the erosion analysis has been to err on the side of simplicity wherever possible. Thus, the representation of lithologic variability in the CHILD calibration and forward runs has been limited to the three

primary and most strongly contrasting lithology classes observed at WNYNSC: (1) Paleozoic bedrock, (2) thick but unlithified glacial sediments, and (3) shallow surface soils/sediments. The choice of parameters to represent these three units, as well as their spatial distribution, is discussed further below.

The boundary conditions for the simulation include the elevation history of the Cattaraugus Valley at the outlet of Buttermilk Creek, which provides the baselevel, and the climate history over time. The elevation history of the Cattaraugus Valley reflects changing baselevels as the Laurentide ice retreated. From the perspective of Buttermilk Creek, what matters is the elevation history of the valley floor in the vicinity of the Buttermilk-Cattaraugus junction, because it is that point that provides the baselevel for Buttermilk Creek. Scenarios for this baselevel history are developed on the basis of topographic features and OSL dating, as described below.

The climate history since ice retreat represents the most difficult set of parameters to constrain. While there are numerous published studies that provide indirect information about the postglacial climate based on proxies such as lake levels and pollen, at present there is no simple method for deriving rainfall or runoff statistics from these proxies. For example, changes in the level of a lake can occur for many different reasons, including changes in rainfall amount or frequency, changes in seasonal temperatures, changes in catchment runoff ratios due to land-cover change, or even changes in atmospheric humidity and wind speed. Thus, interpretation of proxy data in terms of quantitative hydrologic variables such as average storm frequency or intensity would be problematic. In view of this, the logical choice is to err on the side of simplicity and treat the climate as having been essentially constant during the calibration period. This choice inevitably introduces uncertainty into the calibration process. This uncertainty is considered to be no less than the uncertainty that would be introduced by using proxy records to develop educated guesses about the variation in rainfall statistics over the past 17,000 years, while the constant-climate approach has the advantage of parsimony. In addition, as described below, climate uncertainty is addressed to some extent by including among the forward-model scenarios a group of runs that are based on a future doubling of mean rainfall intensity coupled with a very low value for soil infiltration capacity.

F.3.1.4 Parameter Selection for CHILD Model

This section discusses the selection of parameter and parameter-range values for CHILD, as shown in **Table F–8**. A detailed description of the model can be found in Tucker et al. (2001a) and Tucker (2008), while some of the basic data structures and algorithms are presented in Tucker et al. (2001b). Applications of the model to various research problems can be found in a variety of publications (Tucker and Bras 2000, Sloan et al. 2001, Bogaart et al. 2003, Lancaster et al. 2003, Collins et al. 2004, Sólyom and Tucker 2004, Tucker 2004, Istanbulluoglu and Bras 2005, Istanbulluoglu et al. 2005, Clevis et al. 2006, Flores-Cervantes et al. 2006, Crosby et al. 2007, Gasparini et al. 2007, Fleurant et al. 2008).

F.3.1.4.1 Reconstructed Postglacial Topography of Buttermilk Creek

The starting condition for the model was a Digital Elevation Model (DEM), which represented the topography of Buttermilk Creek as it would have existed following the initial retreat of the ice sheet. The last glacial retreat from the area left behind thick accumulations of glacial deposits within the main valleys, including the valleys of the modern Cattaraugus Creek and its tributaries. In the Buttermilk Creek watershed, these glacial deposits, together with a thin mantle created by postglacial fan deposits, formed a low-relief surface sloping gently downward to the north-northwest. Since deglaciation, Cattaraugus Creek and its tributaries have incised these glacial deposits (Fakundiny 1985). Extensive remnants of the incised postglacial valley surface remain throughout the Buttermilk Creek basin, forming a dissected, semicontinuous, low-relief surface with an altitude that ranges roughly from 400 to 430 meters (1,300 to 1,400 feet) within the Buttermilk Creek basin. These remnants appear to be only thinly mantled by postglacial deposits (see, for example, Quaternary geologic map and generalized cross section in LaFleur [1979]), so it is logical to assume that they provide a reasonably accurate representation of the valley topography shortly before stream incision began.

Table F–8 Values of CHILD Input Parameters Selected for Calibration Runs

Parameter	*Symbol*	*Value*
Mean rainfall intensity	$\bar{P}$	1.45 millimeters per hour
Rainfall duration parameter	F_p	0.08
Global time-step length	T_g	0.1 years
Infiltration capacity	I_c	[3.82, 8.29, 16.8, 19.4, 68.7] meters per year
Sediment transport efficiency factor	k_f	[20, 100, 500, 2500, 12500] square meters per year per pascal $^{3/2}$
Sediment transport capacity discharge exponent	m_f	0.667
Sediment transport capacity slope exponent	n_f	0.667
Excess shear stress exponent	p_f	1.5
Bedrock erodibility coefficient (till)	K_{bt}	[1, 10, 100, 1000, 10000] meters per year per pascal
Bedrock erodibility coefficient (bedrock)	K_{br}	[0.001, 0.01, 0.1, 1, 10] meters per year per pascal
Regolith erodibility coefficient	K_r	10,000 meters per year per pascal
Shear stress coefficient (=$\rho\, g^{2/3}\, C_f^{1/3}$; see page F-34)	K_t	[1000, 1250, 1500, 1750, 2000] pascals per (square meter per second) $^{2/3}$
Bedrock erodibility specific discharge exponent	m_b	0.667
Bedrock erodibility slope exponent	n_b	0.667
Exponent on excess erosion capacity	p_b	1
Critical shear stress for bedrock	τ_{cb}	[1, 4, 16, 80, 400] kilograms per meter per second squared
Critical shear stress for regolith	τ_{cr}	[4, 10, 23, 54, 124] kilograms per meter per second squared
Hillslope creep coefficient	k_d or κ	[0.0003, 0.001, 0.003, 0.01, 0.036] square meters per year
Critical slope	S_c	0.3839 meter per meter
Initial regolith thickness	H_{r0}	1.5 meters
Run duration (start of base level lowering)	-	[18.3, 17.5, 16.7, 16.0, 15.24] thousand years
Time at which baselevel reaches terrace 7A	-	[17.04, 14.5, 12.0, 9.5, 7.05] thousand years
At-a-station channel width-discharge exponent	ω_s	½
Downstream channel width exponent	ω_b	½
Channel width coefficient	k_w	4.46 meters per (cubic meters per second) ^{½}

Note: Values in square brackets represent alternative values used in Monte Carlo simulations.

The pre-incision valley topography was reconstructed using the valley slope projection method. This method uses the slope of the existing topographic remnant features within the Cattaraugus Valley. The slope of the initial, pre-incision valley was estimated by projecting the modern-day slopes of the remnant surfaces down the valley toward the outlet of Buttermilk Creek. The resulting pre-incision valley gradient lies between 0.003 and 0.004. Total postglacial incision depth at the Buttermilk Creek outlet was obtained from the difference between the modern creek elevation and the elevation of the surrounding terrace remnants, ranging between 60 and 80 meters (200 and 260 feet) of incision depending on which nearby plateau fragment is selected. The plateau heights in the confluence area appear to reflect the presence of a fill or strath terrace about 20 meters (60 feet) below the original valley surface; this feature is suggested by a gentle east-west-trending scarp that separates two low-relief surfaces above the left bank of lower Buttermilk Creek, in the vicinity of Edies Siding. For purposes of model calibration, we have adopted intermediate values of 0.0035 for the paleo-valley gradient and 405 meters (1,329 feet) for the initial outlet elevation, which implies a total postglacial incision depth of 69 meters (226 feet). The topography of the pre-incision valley was reconstructed by combining two DEMs: one representing the modern topography of the catchment and one representing the postglacial valley-surface topography. The postglacial valley-surface DEM was built using the following algorithm:

- Assignment of a pre-incision elevation (in this case 405 meters [1,329 feet]) to the outlet point.
- Setting the elevation of each remaining DEM cell in the DEM to $z(x,y) = z_0 + L\ S_v$, where z_0 is the outlet elevation, L is the Euclidian distance from the outlet ($= \sqrt{x^2 + y^2}$), S_v is the projected valley slope (in this case 0.0035), and x and y are the east-west and north-south distances, respectively, from the outlet point.

The initial topography DEM was then constructed by assigning to each cell the value of the corresponding cell in either the modern topography DEM or the valley-surface DEM, whichever was greater. This method yielded a smooth, gently sloping central valley whose height corresponds approximately to the present-day height of the plateau remnants, as shown on **Figure F–7**. Finally, the present-day drainage network was lightly etched into the reconstructed plateau surface by reducing by a small amount (2 meters) the elevation of cells containing the mainstem Buttermilk or its larger tributaries. This etching procedure, which has been used in other landscape modeling studies (Anderson 1994), does not substantially alter the marcroscopic erosion patterns (which are dictated by the generalized topography and the process parameters), but it does help reduce the number of "false negative" solutions in which the computed erosion depths and spatial patterns are comparable to the present day but the main streams are shifted to one side or the other in the main valley due to small discrepancies between the actual and modeled initial conditions.

No attempt was made to reconstruct subtle variations in the initial valley topography that may reflect features such as recessional moraines or proglacial lake shorelines. Such features demonstrably exist, but for the most part they are below the resolution of the best available topographic maps, and are therefore subject to considerable uncertainty. Likewise, no attempt was made to correct for postglacial erosion or aggradation within the small tributaries above the valley remnants (in the bedrock region), such as upper Quarry Creek, because there appears to be no data set available at present on which to base such corrections. In the future, acquisition of high-resolution, vegetation-corrected airborne laser-swath maps could allow for greater precision in reconstructions of pre-incision topography because such data would allow for improved Quaternary geologic mapping and feature identification, mapping of smaller terrace features, and quantification of historic rates of land surface change.

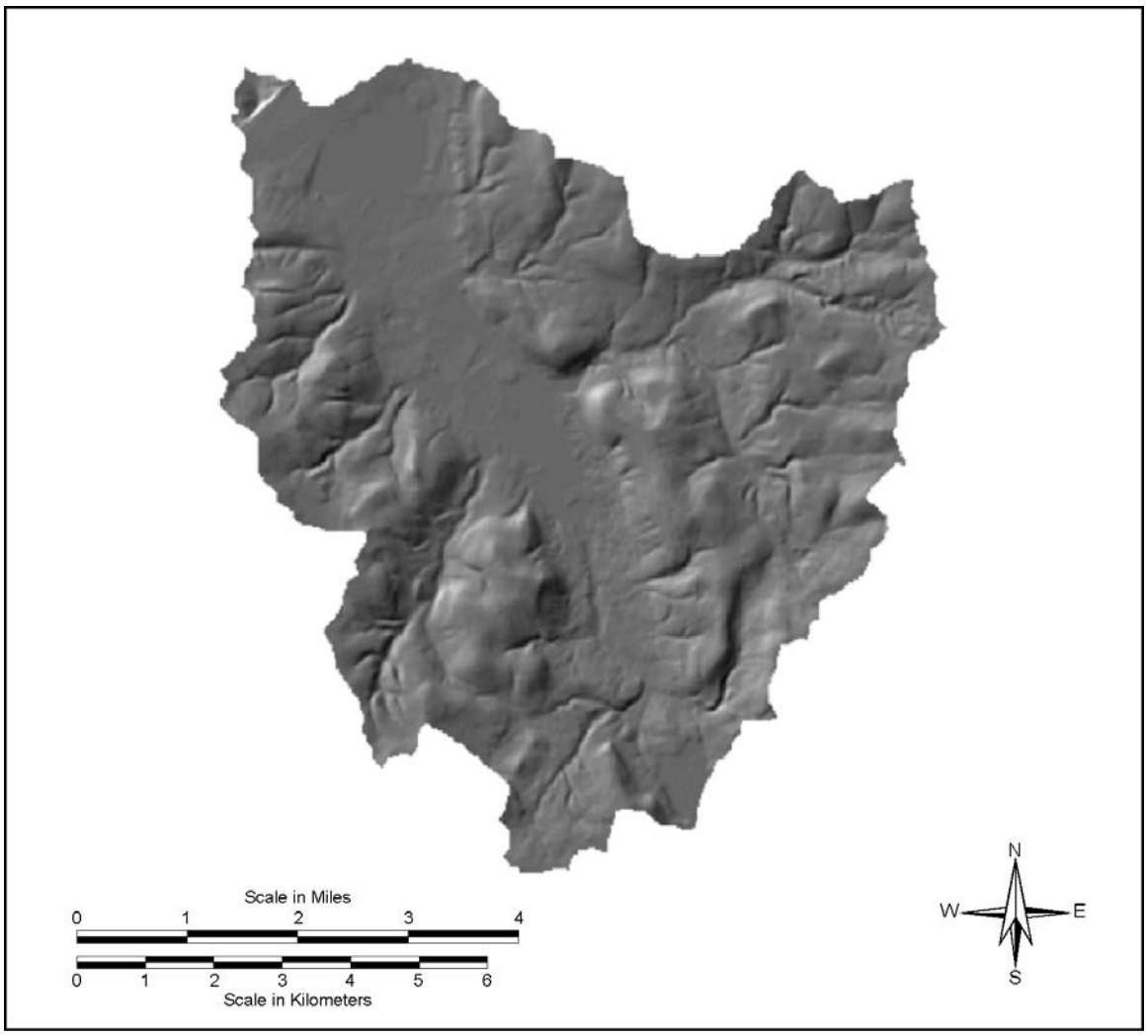

Figure F–7 Topography of the Pre-Incision Buttermilk Creek Valley that was used to Calibrate the Landscape Evolution Models

F.3.1.4.2 Boundary Conditions: Baselevel History

Glacial recession from the Lake Erie basin appears to be the ultimate cause of stream incision within the Cattaraugus Valley and its tributaries. For purposes of erosion evaluation, however, the key boundary condition is the elevation history in the reach of Cattaraugus Creek, for it provides the baselevel for the Buttermilk Creek catchment. In order to estimate this baselevel history, it was necessary to answer the following questions: When did incision begin here? How fast did Cattaraugus Creek incise here? Has this rate varied through time, and if so, how?

In order to constrain the timing of base level lowering, and also provide information on the history of incision within the Buttermilk Creek Valley itself, 10 samples for OSL dating were collected from various points in and around the Buttermilk Creek catchment, as described in Section F.2.2. The samples were analyzed in the USGS Luminescence Dating Laboratory (Mahan 2007). A well-bleached sample obtained from fluvial sediments near the top of the plateau implies that Buttermilk Creek began incision about 17,000 years ago (i.e., 16,800 ±1,530 [1 sigma] from OSL sample 8A [see Table F–3]). This timing agrees, within uncertainty, with the timing of glacial retreat from the Finger Lakes to the east (e.g., at Seneca Lake, final retreat is estimated to have occurred approximately 16,600 calendar years before present [Anderson and Mullins 1997, Ellis et al. 2004]). Note that the common practice in the literature of reporting uncalibrated ^{14}C ages can sometimes cause confusion; for example, 14,000 uncalibrated ^{14}C years corresponds to approximately 16,600 calendar years according to current calibration curves.

A set of alternative baselevel histories was developed by estimating the times at which the Cattaraugus-Buttermilk confluence lay at three different elevations: the starting (postglacial) elevation of the plateau before incision, the elevation of the terrace from which OSL sample 7A was collected, and the elevation of the modern confluence. At the onset of incision, the confluence is assumed to have been at an elevation of 405 meters above modern sea level, as discussed previously. Samples 8A and 9A are believed to bracket the onset of incision. Sample 8A, the higher of the two, is therefore used as the basis for the onset of baselevel lowering. As discussed in Section F.2.2.2, Sample 8A appears to be well bleached, based on its unusually tight equivalent-dose histogram and on the overlap between the CAM and MAM ages. Its CAM 1-sigma age range is 15,240 to 18,300 years. Thus, the five alternative parameter values for the start of baselevel lowering are: [18,300, 17,500, 16,700, 16,000, 15,240] years.

The next parameter to estimate is the time at which the confluence reached the elevation of the terrace from which Sample 7A was collected. As noted earlier, the CAM and MAM age estimates for Sample 7A differ considerably: the former (with 1-sigma uncertainty bounds) is 13,400 to 17,000 years while the latter is 7,000 to 9,800 years. The parameter range explored in the calibration covers this full age range: 7,050, 9,500, 12,000, 14,500, 17,040. In deriving incision rates from this midlevel terrace, it is assumed that the terrace is a strath (bedrock-cut platform mantled by alluvium) rather than a thick fill terrace. Without deeper (backhoe) sampling at this site, this assumption cannot be confirmed, but it is supported by similar ages from two confirmed strath terraces at similar levels in the Buttermilk Creek Valley (samples 1A and 6A).

Uncertainty in the derived baselevel history reflects uncertainty in the dating. Reducing this uncertainty would require additional identification and dating of strath terraces in the vicinity of the Buttermilk–Cattaraugus confluence. This would produce a larger sample size, yield a greater likelihood of identifying well-bleached (and therefore more-reliable) samples and/or material datable by ^{14}C analysis, and (if additional terrace levels could be identified) increase the time resolution in the baselevel reconstruction.

F.3.1.4.3 Boundary Conditions: Glacio-Isostatic Uplift

Removal of the load of the ice sheets leads to isostatic rebound of the lithosphere. From the point of view of a drainage basin subjected to such glacio-isostatic uplift, there are three potential effects. First, if a catchment drains to a body of water such as a lake or ocean that has a fixed altitude, glacio-isostatic uplift (or subsidence) will change the elevation difference between the catchment and its baselevel. It may also alter the length of the catchment by, for example, exposing part of a coastal shelf (or drowning the lower part of a catchment, in the case of subsidence). Isostatic uplift along a shoreline can lead to either increased or decreased erosion and transport rates, depending on the slope of the uplifted shelf relative to the stream slope near the coastline (Summerfield 1986, Snyder et al. 2002). Regional postglacial isostatic uplift in the Lake Erie basin has been well documented, as have fluctuations in lake levels through time (Holcombe et al. 2003). From the point of view of Buttermilk Creek, the net effect of these processes has been to change the baselevel at its junction with Cattaraugus Creek, as discussed previously. In other words, the influence of postglacial isostatic uplift on local baselevel is incorporated in the model by specifying the baselevel history at the Buttermilk–Cattaraugus confluence.

A second potential effect of postglacial isostatic uplift relates to climatology. A substantial increase in the absolute elevation of a catchment can indirectly influence rates of weathering and erosion by altering the catchment's mean temperature (due to the environmental lapse rate) and precipitation (due to orographic effects). However, in this case the magnitude of absolute uplift is sufficiently small (likely less than a few hundred meters [several hundred feet]) that any associated changes in temperature or precipitation fall well within the existing uncertainties regarding postglacial climate variation.

The third potential effect of isostatic adjustment is tilting of the surface due to spatial variations in uplift rate. Spatial variations in glacio-isostatic uplift rates are well documented in eastern North America. For the Lake Erie basin, Holcombe et al. (2003) used bathymetry data to map submerged paleo-shorelines. Based on a tilted 13,400-year-old shoreline, their data suggest about 52 meters (170 feet) of differential uplift over a distance of approximately 130 kilometers (80 miles), which implies a down-to-the-west tilt of about 4×10^{-4}. By comparison, the gradient of the modern Buttermilk Creek Valley in its lower-middle reaches is about 8×10^{-3}, while the gradient of the plateau is approximately 3.5×10^{-3}, as discussed above (see also the generalized Buttermilk Creek Valley profile of LaFleur [1979]; Figure 3 shows an average creek gradient from Riceville Station to the outlet of approximately 0.0085, and a plateau gradient of approximately 0.003). Thus, assuming that Buttermilk Creek experienced postglacial tilting of a similar magnitude to that observed in Lake Erie, even if that tilt were aligned directly along the valley axis, it would alter the initial valley gradient by only about 10 percent. Therefore, the postglacial tilting likely had only a second-order effect on stream gradients. Because the likely magnitude of tilt is comparable to the uncertainty in the estimates of paleo-valley gradient, it is not incorporated in the model calibration.

F.3.1.4.4 Parameters Related to Climate

CHILD uses a stochastic representation of rainfall and runoff in which a sequence of storm and interstorm events is drawn at random from exponential frequency distributions (Eagleson 1978; Tucker and Bras 2000). The rainfall model requires three parameters: the average storm intensity, P, the average fraction of time (between zero and one) that precipitation occurs at the site F_p, and the size of a global model time step T_g, which represents the average duration of a storm and interstorm sequence.

The mean rainfall intensity parameter was derived from 9.8 years of 5-minute resolution precipitation data collected at the WNYNSC weather station. Individual storms were identified using an approach (Eagleson 1978) in which a storm is defined as any period of precipitation that is both preceded and followed by dry periods of 2 hours' duration or longer. The depth and duration were computed for each storm, and the means of each computed for the entire length of record. The mean annual precipitation for the 9.8 years of

high-resolution data is 1.02 meters (3.35 feet) per year. The average storm duration for this period of record is 2.57 hours, while the mean depth is 3.73 millimeters (0.15 inches). The estimated mean storm intensity derived from these values is 1.45 millimeters (0.06 inches) per hour; this value falls within the range of monthly values obtained by Hawk and Eagleson (1992) (0.43 to 2.1 millimeters [0.02 to 0.08 inches] per hour) from hourly precipitation data at the Buffalo-Niagara International Airport, New York. The value of the precipitation-duration parameter F_p can be derived from mean annual precipitation P_a via the relation $F_p = P_a / P$, which yields a value of 0.08 (in other words, precipitation occurs on average for 8 percent of any given year).

The model is relatively insensitive to T_g as long as its value is sufficiently small. To determine a reasonable value for T_g, a series of 1,000-year sensitivity tests were conducted using the modern topography of Buttermilk Creek as an initial condition. Results showed that values of T_g of approximately 1 year or smaller produce very similar results (average root-mean-square differences in model-cell height of less than 30 centimeters (11.81 inches) after 1,000 years of erosion). A value of 0.1 years was used in calibration and forward runs.

F.3.1.4.5 Soil Infiltration Capacity

The current version of CHILD provides four alternative means of computing runoff. Of these, the simplest and most commonly used is a single-parameter infiltration capacity model in which any rainfall in excess of a specified infiltration rate contributes to runoff. In general, the use of such a model in a humid temperate setting would be questionable because rainfall intensity rarely exceeds soil infiltration capacity under normal circumstances. In such settings, most runoff tends to be generated in localized areas where soils readily become saturated due to topographic convergence and/or low gradient (Dunne and Black 1970). However, the study area is somewhat unusual in having a high proportion of soils derived from clay-rich and fairly impermeable glacial sediments; therefore, widespread hillslope runoff generation during heavy rains will be more common than in many humid-temperate environments. This is supported by the results of hydrologic monitoring discussed in the Surface Water Environmental Information Document (WVNS 1993c). In the South Plateau disposal area, nearly 80 percent of the gauged flow resulted from runoff, implying that the effective infiltration capacity of soils formed from the clay-rich glacial sediments is rather low (not surprisingly, the study also found a higher effective permeability in the alluvial fan–derived soils of the North Plateau). For purposes of this study, a simple one-parameter infiltration-capacity runoff model is adopted, with the recognition that future studies of hydrologic response may point toward a different choice. The parameter is the effective infiltration capacity I_c (with dimensions of length per time, or L/T). The effective infiltration capacity represents the maximum rate at which rainfall can be absorbed by the soil before generating runoff. When the rainfall rate exceeds the effective infiltration capacity, runoff is generated at a rate equal to the difference between rainfall intensity and infiltration capacity.

Several different methods were used to estimate a range of plausible values for I_c. The first method is based on water-balance models that were developed for the sand and gravel unit on the North Plateau. The method involves combining the derived rainfall intensity parameter with these recharge estimates. The effective infiltration capacity can be related to the storm-intensity parameter P, the mean annual precipitation P_a, and the annual total infiltration I_a as follows:

$$I_c = -P \ln(1 - I_a / P_a)$$

The annual total infiltration I_a represents precipitation that does not generate runoff (though it may contribute to baseflow in streams), and it includes both aquifer recharge and evapotranspiration. Because P_a is known (1.02 meters [3.35 feet] per year) and a value for P has been estimated (1.45 millimeters [0.06 inches] per hour or 12.74 meters (41.80 feet) per year), one can estimate I_c if I_a is known.

Appendix E of the *2008 Revised Draft Environmental Impact Statement for Decommissioning and/or Long-Term Stewardship at the West Valley Demonstration Project and Western New York Nuclear Service Center* reviews two water-balance models for the fan sand and gravel unit on the North Plateau. This study cites a figure of 50 centimeters (19.69 inches) per year recharge from precipitation based on Kappel and Harding's data (Kappel and Harding 1987), and notes that Yager (1987) estimates 46 centimeters (18.11 inches) per year. These water-balance calculations give us only a minimum value of I_a, because the aquifer recharge does not include water that initially infiltrates to the unsaturated zone or is intercepted, and later is returned to the atmosphere via evapotranspiration.

Using the formula derived above for I_c, with P = 12.74 meters (41.80 feet) per year, P_a = 1.02 meters (3.35 feet) per year, and I_a = 0.5 meters (1.64 feet) per year, the minimum infiltration capacity on the North Plateau is 8.58 meters (28.15 feet) per year, which is equivalent to 0.979 millimeters (0.04 inches) per hour. With the alternative estimate (Yagers') of I_a = 0.46 meters (1.51 feet) per year, the corresponding minimum I_c = 7.64 meters (25.10 feet) per year, which is equivalent to 0.872 millimeters (0.03 inches) per hour. However, as noted above, these are minima. To get a rough upper bound on I_a, it is reasonable to suppose that runoff is unlikely to be smaller than 10 percent of mean annual precipitation. Taking recharge plus evapotranspiration as 90 percent of the mean annual rainfall of 102 centimeters (40.16 inches), the corresponding maximum I_c = 29.33 meters (96.23 feet) per year, which is equivalent to 3.35 millimeters (0.13 inches) per hour. Because this water balance was developed for the North Plateau, it applies only to that location, but it does provide a range of estimates to work with.

There seems to be some disagreement concerning recharge and runoff on the North Plateau. WVNS (1993c) estimated total infiltration (evapotranspiration plus recharge) at 74.7 centimeters (29.29 inches) per year, with runoff at 25.5 centimeters (10.04 inches) per year and a mean annual precipitation of 100.1 centimeters (39.41 inches). Using these figures, the corresponding I_c = 22.47 meters (73.72 feet) per year, which is equivalent to 2.56 millimeters (0.10 inches) per hour. Other analyses discussed in Appendix E of this environmental impact statement, put recharge as low as 5 to 12 centimeters (1.97 to 4.72 inches) per year. In sum, the North Plateau water-balance estimates, combined with the derived mean precipitation intensity parameter, suggest an effective I_c value somewhere in the range of 1 to 4 millimeters (0.04 to 0.16 inches) per hour.

This range is lower than the estimates of K_{sat} for the North Plateau thick-bedded unit. As discussed in Appendix E, K_{sat} for this unit ranges from 1.25×10^{-4} to 3.78×10^{-2} centimeter (0.00005 to 0.01 inches) per second, which is equivalent to 1,360 millimeters (53.54 inches) per hour. The reason for the difference between these estimates is not known, but one possibility is that a higher clay content in the surface soil layer renders it less permeable than the underlying deposits.

For the weathered Lavery till on the South Plateau, seven measurements record widely varying hydraulic conductivity values, for which the mean is 12 millimeters (0.47 inches) per hour, the median is 6.2 millimeters (0.24 inches) per hour, and the geometric mean is 1.78 millimeters (0.07 inches) per hour (see Appendix E), which is similar to the effective infiltration capacity estimated from the North Plateau water balance. For weathered bedrock, Prudic (1986) estimates a value of 1×10^{-5} centimeters (3.94×10^{-5} inches) per second or 0.36 millimeters (0.01 inches) per hour.

An alternative method for estimating I_c relies on streamflow measurements. The method involves the following steps: (1) estimate the fraction of flow in the stream that arises from runoff (storm flow); (2) convert the storm-flow discharge into a runoff rate by dividing by the area of the basin; and (3) given a mean storm intensity and duration factor, calculate the I_c that would be required to generate an equivalent average-annual runoff. This approach was applied to streamflow measurements obtained from four gauging stations: Buttermilk Creek (October 1961 to September 1968), Franks Creek (December 1975 to September 1979), Cattaraugus Creek near Gowanda (November 1939 to February 2009), and Cattaraugus Creek near Versailles

(October 1915 to September 1923). Baseflow was estimated from these records using the BFLOW program (Arnold et al. 1995) as shown in **Table F–9**. The mean annual basin runoff rate R was calculated by dividing the difference between total flow, Q, and baseflow, Q_{bf}, by the area of the basin. The corresponding effective infiltration capacity, I_c, was then calculated using the formula:

$$I_c = -P \ln(R / P_a)$$

The resulting estimates of I_c range over about a factor of 3, from 0.82 to 2.43 millimeters (0.03 to 0.10 inches) per hour, which is equivalent to 7.2 to 21.3 meters (23.62 to 69.88 feet) per year (see Table F–9). The estimates from Buttermilk Creek and Cattaraugus Creek data are similar to one another, while that for Franks Creek is substantially lower. To test whether the short period of record for Franks Creek was unusually wet, climate data for Buffalo, New York for the 1975–1979 period were compiled. The mean annual precipitation at Buffalo for that time period was 1.11 meters (43.73 inches). Assuming that this figure is representative of precipitation at the site during that period, the corresponding I_c is 0.939 millimeters (0.04 inches) per hour, which is equivalent to 8.29 meters (27.20 feet) per year. Thus, while it does appear that the short period of record may have been wetter than normal, this does not explain the lower effective permeability of soils in the Franks Creek basin relative to the average value of the larger Buttermilk and Cattaraugus watersheds. It is possible that the difference reflects a larger fraction of clay-rich, till-derived soils in the Franks Creek basin.

Collectively, using the corrected value for Franks Creek, the I_c estimates derived from streamflow range from 8.29 to 21.3 meters (27.20 to 69.88 feet) per year, which is equivalent to 0.946 to 2.43 millimeters (0.04 to 0.10 inches) per hour, while the minimum I_c estimates from the North Plateau water balance range from 7.64 to 29.33 meters (25.07 to 96.23 feet) per year, which is equivalent to 0.872 to 3.35 millimeters (0.03 to 0.13 inches) per hour. To choose a range of I_c values for Monte Carlo calibration, a logical approach is to pick three values that are reasonably well supported by data, plus two extreme bracketing values. The three preferred central values are: (1) the Franks Creek stormflow estimate of 8.29 meters (27.20 feet) per year (because it is the most geographically appropriate); (2) the Cattaraugus Creek record of 19.4 meters (63.65 feet) per year at Gowanda, New York, (because it is the longest); and (3) the North Plateau infiltration estimate of 16.8 meters (55.12 feet) per year (because it is also geographically relevant, and comes from a different source). The lowest value, 3.82 meters (12.53 feet) per year, is equal to half of the lowest water-balance estimate (7.64 meters year). The highest value, 68.66 meters (225.26 feet) per year, is somewhat more than twice the highest water-balance estimate. Thus, the five I_c values used in Monte Carlo calibration are: I_c = [3.82, 8.29, 16.8, 19.4, 68.7] meters per year.

Table F–9 Drainage Area, Storm Discharge, and Runoff at Gauging Stations

Gauging Station Location	*Basin area (square miles)*	*Q-Q_{bf} (cubic meters per second)*	*R (meters per year)*	*I_c (meters per year)*
Buttermilk Creek	30.0	0.580	0.236	18.7
Franks Creek	0.28	0.0133	0.579	7.21
Cattaraugus Creek near Gowanda	436	7.99	0.223	19.4
Cattaraugus Creek near Versailles	466	7.35	0.192	21.3

I_c = infiltration capacity, Q = total flow, Q_{bf} = baseflow, R = runoff rate.
Note: To convert square miles to square kilometers, multiply by 2.59; cubic meters to cubic feet, multiply by 2118.9; meters to feet, multiply by 3.281.

F.3.1.4.6 Channel Width Parameters

The channel width, *W*, at any given node is calculated using an empirical relationship between width and discharge, *Q*:

where:

$$W_b = k_w Q_b^{\gamma}$$

and:

$$\frac{W}{W_b} = \left(\frac{Q}{Q_b}\right)^{\omega}$$

where the subscript *b* denotes quantities at the bank-full stage. There are four parameters required: the coefficient k_w, the runoff rate R_b that corresponds to bank-full discharge Q_b, and the exponents γ and ω. There do not appear to be any data available on variations in channel width downstream or at a particular point through time in the Buttermilk Creek watershed. Therefore, parameter values were estimated on the basis of a USGS study of channel hydraulic geometry in New York Hydrologic Region 6, which covers WNYNSC (Mulvihill et al. 2005). The study concluded that the bank-full discharge, Q_b, and bank-full width, W_b, of streams in Region 6 are related to basin area *A* according to:

$$Q_b = 48.0\ A^{0.842}$$

$$W_b = 16.9\ A^{0.419}$$

where *A* is in square miles, Q_b is in cubic feet per second, and W_b is in feet. Using a little algebra, one can combine these to convert the Mulvihill et al. (2005) coefficients and exponents into the parameters k_w and γ:

$$W_b = (d/b^{e/c})\ Q^{e/c}$$

where $d = 16.9$, $b = 48.0$, $e = 0.419$, and $c = 0.842$. Thus, $k_w = (d/b^{e/c})$, while the bank-full width-discharge exponent $\gamma = e/c = 0.419/0.842 = 0.498$ (approximately 0.5). When the coefficient k_w is converted into units of meters and seconds, its value is 4.49.

The remaining parameters are ω and R_b, which describe the changes in channel width at a particular point on the river channel (as opposed to upstream and downstream) as *Q* rises and falls over time. Unfortunately, data to constrain these parameters for either the onsite streams or the New York Region 6 in general are not available. Data from other rivers suggest that ω is often similar to γ (Leopold et al. 1964). Given the lack of data, the most parsimonious approach is to set ω equal to γ, in which case the value of R_b plays no role. Errors resulting from this assumption are considered to be small relative to other sources of uncertainty.

F.3.1.4.7 Parameters Related to Water Erosion and Sediment Transport

The erosion and transport laws should be appropriate to the processes occurring at the site. Based on reports and field observations, fluvial processes in the Buttermilk Creek watershed include: (1) transport of gravel through the stream network (Boothroyd et al. 1979, 1982), and (2) stream incision into cohesive clay-rich till (as well as other units, e.g., fan gravels, proglacial lake sediments). The presence of coarse bed sediment in Buttermilk Creek suggests that the stream system cannot be realistically treated solely with a detachment-limited model (Howard et al. 1994). One method would be to use a transport-limited fluvial model, which

effectively treats the channel bed as loose sediment. However, the active incision of till and bedrock by Franks Creek and other tributaries suggest that a transport-limited model may not correctly capture incision of Lavery till. Therefore, it is reasonable to use a hybrid model that accounts for both bed-load transport of gravel and detachment of the till (or other bedrock) substrate. CHILD's standard water erosion algorithm computes bed lowering as the lesser of (1) bedrock detachment capacity and (2) excess sediment transport capacity per unit surface area.

This approach requires a choice of transport-capacity law and a choice of detachment-capacity law. Because the substance being detached is mostly clay till, it is appropriate to choose a detachment-rate formula that is applicable to cohesive, clay-rich substrates. Howard and Kerby (1983) found that the detachment (lowering) rate of cohesive clay sediments in a badland area was roughly proportional to the cross-section average bed shear stress. Correlations between detachment rate and boundary shear stress have also been found in field tests of soil erosion (Elliot et al. 1989) and in studies of hydrodynamic erosion of cohesive riverbanks (Julian and Torres 2006). This motivates the use of the widely used du Boys formula for computing the detachment capacity of cohesive material:

$$D_c = K_b(\tau - \tau_{cb})_+$$

where D_c is the detachment capacity (with dimensions of length per time); τ is boundary shear stress; τ_{cb} is a threshold shear stress below which detachment is negligible; and K_b is a lumped dimensional coefficient that depends on bulk density, effective particle size, and the strength of cohesive bonds between particles. The + subscript indicates that the relationship only applies when $\tau > \tau_{cb}$; otherwise, the detachment capacity is zero.

As noted previously, the Buttermilk Creek basin is underlain by two strongly contrasting types of "bedrock": Paleozoic sedimentary rock, and thick till and related glacio-fluvial units that were deposited in the main valley during the last glacial maximum. This contrast is modeled by using a different set of K_b values for these two lithology classes. The spatial distribution of the two lithology classes is based on the map shown on Figure F–2; those units mapped as Lavery Till Plain and Defiance Lake Escarpment Outwash are considered to be underlain by thick, till-rich material. In contrast, while geologic maps indicate that Olean and Kent tills mantles the uplands, this cover amounts to only a thin (roughly 5 foot) veneer over Paleozoic bedrock. Therefore, those areas mapped as Olean or Kent till are assigned to the "Paleozoic bedrock" category. The initial condition for calibration runs accounts for the thin till cover by placing a 1.5-meter (5-foot) layer of alluvium atop the surface at all nodes.

To the best of our knowledge, no studies have tested the detachment capacity of West Valley glacial sediments or bedrock in response to applied fluid shear stress. Thus, in order to estimate a plausible range of values for the parameters K_b and τ_{cb}, it is necessary to rely on independent data. One data source is a set of field experiments on soil detachment conducted in conjunction with development of the U.S. Department of Agriculture WEPP model (Elliott et al. 1989). Most relevant to the site are test soils with a relatively high clay content. The WEPP experimental data include six test soils with >30 percent clay content: Sharpsburg, Heiden, Los Banos, Pierre, Gaston, and Opequon. The detachment-rate parameters (the K_r parameter) for these six soils are 4.6×10^{-3}, 8.0×10^{-3}, 1.1×10^{-3}, 1.0×10^{-2}, 4.2×10^{-3}, and 3.4×10^{-3} seconds per meter, respectively. The corresponding values of critical shear stress, τ_{cb}, are 3.1, 2.9, 2.9, 4.8, 5.3, and 6.2 pascals, respectively.

Converting the K_b values from the WEPP experiments into CHILD's required unit of meters per year per pascal of excess stress, one obtains a range from 35 to 320. This range should be considered subject to significant uncertainty, because the data come from very different geographical areas and surface conditions and because they were derived from relatively short experimental time scales. Thus, it is appropriate to consider a wide range of potential parameter values in the calibration process. Here, a conservative approach was used in which the central value of 100 meters (328.08 feet) per year per pascal is chosen to reflect the

range of values in the WEPP experiments, while the range covers two orders of magnitude on either side of this. The resulting parameters for areas of the Buttermilk basin underlain by thick till are designated by the K_{bt} symbol. The K_{bt} range = [1, 10, 100, 1,000, 10,000] meters per year per pascal.

The detachment coefficient for the Paleozoic bedrock of the uplands is even more difficult to constrain. Bedrock channel erosion is an area of very active research in the geomorphology community, and there is considerable debate over the mechanisms responsible and the resulting rates. The choice of parameters to represent bedrock detachment capacity must therefore be considered speculative. It is assumed that cemented bedrock is, in general, considerably more resistant to detachment than clay till; how much so is unknown. A broad range of values, overlapping somewhat with, but generally much smaller than K_{bt}, is therefore adopted for the rock-detachment coefficient designated with the K_{br} symbol. The K_{bt} range = [0.001, 0.01, 0.1, 1, 10] meters per year per pascal. The primary role of the K_{br} parameter is to control the degree of gullying and sediment production in the bedrock uplands.

The critical shear stress τ_{cb} represents the level of stress below which detachment is negligible. Data from the WEPP test soils show a relatively narrow range of 3 to 6 pascals. Experiments on soils by Dunn (1959) showed a range of values from 2 to over 20 pascals, with a strong dependence on silt-clay percentage. Vegetation tends to enhance the effective value of τ_{cb}. Julian and Torres (2006) report vegetation coefficients—multipliers of t_c that depend on vegetation amount and characteristics—ranging from unity to approximately 20. Thus, according to these data, one could in theory have an effective τ_{cb} as high as 400 (20 pascals times a vegetation coefficient of 20). On the other hand, riverbank erosion data of Julian and Torres (2006) suggested τ_{cb} values as low as approximately 1 pascal. These maximum and minimum values were adopted as bounding parameters values, leading to a range of τ_{cb} values of τ_{cb} = [1, 4, 16, 80, 400].

CHILD offers several alternative formulations for calculating the sediment transport capacity of channelized flow. The coarser fraction of sediment, which tends to move as bed load, is considered to be the limiting factor for erosion of detached sediment. Therefore, a transport formula designed for bed load is considered appropriate. For practical reasons of simplicity and computational efficiency, a single effective grain size, rather than multiple grain-size fractions, is used for this study. The general form is:

$$Q_c = WK_f\left(\tau^p - \tau_{cr}{}^p\right)_+$$

where Q_c is the volumetric sediment transport capacity, W is the width of the channel, τ_{cr} is the critical shear stress for entraining loose sediment ("r" for regolith), and K_{f} is a transport efficiency factor that incorporates fluid and sediment density and gravitational acceleration. A number of laboratory and field studies show a strong correlation between transport rate and excess shear stress raised to the 3/2 power, which is consistent with the hypothesis that transport rate depends on unit stream power (which represents the rate of energy expenditure per unit bed area and is equal to the product of shear stress and flow velocity). This motivates a choice of p = 3/2. The transport efficiency factor, K_f, is treated as a calibration parameter. Simons and Sentürk (1992) determined an experimental dimensionless coefficient of 8, and this leads to a dimensional value of K_f in metric units (kilograms, meters, seconds) of about 1.5×10^{-5}. The equivalent converted to time units of years, which CHILD requires as an input parameter, is approximately 500. This should not be considered a highly precise value, for two reasons: (1) experimental data on sediment transport show a high degree of variation depending on experimental conditions, and (2) the transport rate can vary depending on a wide number of factors, including the grain-size mixture on a channel bed and the geometry of bars and other bedforms. Thus, a wide range of values of this parameter is allowed in the Monte Carlo calibration: K_f = [20, 100, 500, 2,500, 12,500].

The critical threshold parameter, τ_{cr}, represents the level of applied fluid shear stress below which the entrainment of loose sediment grains is negligible. Although it obviously plays the same mathematical role as

the "bedrock" detachment threshold, it differs in the sense that it represents loose, noncohesive material (such as riverbed sediment) rather than cohesive or indurated material (such as dense clay till or bedrock). Thus, its value may differ from τ_{cb}. The standard method for calculating τ_{cr} is to use the Shields curve (Julien 1995). For the fully turbulent conditions that apply to nearly all natural channelized flows of water, experimental data indicate that initiation of motion of noncohesive sediment occurs when the dimensionless shear stress exceeds a threshold value between 0.03 and 0.06 (Buffington and Montgomery 1997). The corresponding dimensional value depends on the median sediment diameter and the sediment density. Standard practice is to assume sediment density equivalent to quartz (2,650 kilograms per cubic meter). According to grain-size measurements along Buttermilk Creek (Boothroyd et al. 1979), the median grain diameter is approximately 32 millimeters (1.26 inches). However, bed grain size can vary from one reach of a river to another as well as through time. A reasonably broad but still plausible range of median grain-size values considers values a factor of four lower (8 millimeters [0.31 inches]) than the central value estimated from Boothroyd's data, and a factor of four higher (128 millimeters [5.04 inches]). Uncertainty in the value of reference dimensionless shear stress is about a factor of two (Buffington and Montgomery 1997). Combining these ranges, a reasonable spread of possible τ_{cr} values is τ_{cr} = [4, 10, 23, 54, 124].

Note that there is no single generally accepted transport formula for bed-load flux. Rather, there are a number of competing approaches that involve somewhat different scaling of the key variables (Howard 1980, Martin 2003) and have varying degrees of explanatory power depending on which data sets are examined. The choice of the above equation is based on the fact that its scaling is common to a number of frequently used and reasonably successful transport formulas. One limitation is that CHILD presently has no way to handle suspended or wash load: thus, for example, when a cubic meter of clay is eroded, it becomes "sediment" of a specified size. A more-realistic approach would be to specify a percentage of fines for the eroded substrate, and have these directly removed (Kirkby and Bull 2000), but this would require additional model development and testing, and it is considered unlikely to have a significant effect on the behavior of the model in this setting.

The cross-section averaged bed shear stress exerted by running water is based on a force balance between gravity and friction for steady, uniform, fully turbulent flow in a wide channel:

$$\tau = \rho g^{2/3} C_f^{\ 1/3} \left(\frac{Q}{W} \right)^{2/3} S^{2/3}$$

where Q is water discharge, S is channel gradient, ρ is water density (1,000 kilograms [1.1 tons] per cubic meter), g is gravitational acceleration at earth's surface, and C_f is a dimensionless friction factor that depends weakly on relative roughness (flow depth relative to roughness height). The leading factors are collected into a single parameter, K_t that depends weakly on roughness:

$$K_t = \rho g^{2/3} C_f^{\ 1/3}$$

Roughness is often quantified using the Manning n factor, which is related to C_f by:

$$C_f^{\ 1/3} = \frac{g n^2}{H^{1/3}}$$

where H is flow depth. Based on the criteria of Chow (1959), appropriate values of n for Buttermilk Creek range from about 0.033 to 0.06. Flow depth obviously varies from place to place, but C_f is not especially sensitive to it (one takes the cube root). Using a reference depth of 1 foot, the corresponding range of K_t values is 1,150 to 1,750. Rounding up and down, we adopt the following five alternative values of K_t to be explored in Monte Carlo calibration runs: K_t = [1,000, 1,250, 1,500, 1,750, 2,000].

F.3.1.4.8 Parameters Related to Sediment Transport by Soil Creep and Landsliding

For this application, CHILD uses a nonlinear soil creep transport law that was introduced by Howard et al. (1994) and tested in the field and laboratory by Roering et al. (1999, 2003):

$$q_{sc} = -\frac{K_d \nabla z}{1 - \phi^2}$$

$$\phi = \begin{cases} |\nabla z| / S_c & \text{if } |\nabla z| \le 0.999 S_c \\ 0.999 & \text{otherwise.} \end{cases}$$

where z is land-surface height, K_d is a transport coefficient (L2/T), and S_c is a threshold slope gradient.

At low slope angles, CHILD uses an equation for hillslope mass transport that is equivalent to the well-known slope-linear soil creep law, in which the volumetric rate of downslope sediment transport per unit slope width is equal to the product of slope gradient times a transport coefficient, K_d; (in other words, this is how the above formula behaves when the right-hand term in the denominator is small, reflecting gentle slopes). Values of K_d have been estimated in many parts of the world, often for purposes of morphologic dating of landforms such as earthquake fault scarps. In general, the inferred creep coefficients range over two orders of magnitude, from approximately 10^{-4} to approximately 10^{-2} square meters (0.01 to 1.08 square feet) per year (Hanks 2000). There is some evidence that creep rates vary according to climate, with colder and/or wetter environments generally experiencing higher rates of creep. For example, in the compilation by Hanks (2000), the highest creep coefficients come from Michigan and coastal California, while the lowest are found in desert regions in Israel and the arid U.S. Basin and Range province (Nevada and Utah). Oehm and Hallet (2005) compared modern creep rates across a broad range of climates, and found a strong increase in the effective creep coefficient with latitude north of 50 degrees north.

For purposes of this study, published estimates of K_d were compiled. Among these, the study sites that match most closely in climate include sites in Michigan, Ohio, northern Europe, Montana (Yellowstone National Park), and Japan (**Table F–10**). In a study of fault-scarp degradation in the Rhine River Valley near Basel, Switzerland, Niviere et al. (1998) calibrated a creep coefficient using observed degradation of an approximately 100-year-old railway embankment, arriving at an estimate of 0.0015 square meters (0.016 square feet) per year. A study by Nash (1984) of a single degraded terrace scarp in the subhumid climate of northwestern Montana yielded an estimate of 0.002 square meters (0.021 square feet) per year. In a compilation of modern creep rates and profiles by Oehm and Hallet (2005), data from Japan (latitude 35 degrees north) suggest creep coefficients ranging from 0.0036 to 0.014 square meters (0.039 to 0.151 square feet) per year. The degradation of an 1,800-year-old embankment and trench in south-central Ohio provided Putkonen and O'Neal (2006) an opportunity to estimate a creep coefficient of 0.0005 square meters (0.0054 square feet) per year through forward modeling. Nash (1980) analyzed modern and abandoned cliffs carved in glacial till along the Lake Michigan shoreline, and derived a best-fit estimate of 0.012 square meters (0.129 square feet) per year.

In summary, estimates of K_d obtained in humid to subhumid climates range over more than an order of magnitude, from 5×10^{-4} square meters (0.0054 square feet) per year to a little over 10^{-2} square meters (0.108 square feet) per year. In terms of climate, soil texture, and time scale, the closest match to WNYNSC is that presented in the study of Nash (1980). The regional climate is humid temperate with cold winters; temperatures drop below zero degrees Celsius on 150 or more days per year on average, promoting transport by frost heave. Like WNYNSC, the environment is predominantly forest covered, and both sites are underlain by glacial sediments. Unlike some of the other studies, the time scale for Nash's (1980) estimate spans a large fraction of the postglacial period (10,500 and 4,000 years, respectively, for two different scarp populations),

and the data come from a population of scarp profiles rather than a single profile (as used for example by Nash [1984], Putkonen and O'Neal [2006], and Niviere and Marquis [2000]). However, among the other humid-temperate and/or clay-rich sites, there are values that are much smaller than this (0.0003 square meters [0.003 square feet] per year for the lowest Swiss estimate) and somewhat higher than this (0.036 square meters [3.88 square feet] per year from McKean et al. [1993]). These are used as bounding values for a range of five alternative calibration values: K_d = [0.0003, 0.001, 0.003, 0.01, 0.036].

The critical-slope parameter S_c represents the angle above which a hillslope is totally unstable. A commonly accepted threshold angle at the site is 21 degrees, and that value is adopted here for S_c.

Table F–10 Published Values of the Coefficient K_d

Location	*Reference K_d (square meters per year)*	*Source*
Emmet County, Michigan	0.012	Nash 1980a, ESPL 5:331–345
West Yellowstone, Montana	0.002	Nash 1984, GSA Bulletin 95(12):1413–1424
Upper Rhine Graben, Central Europe	0.0014	Nivière B 2000, Geophysical JI 141(3):577
Near Basel, Switzerland	0.0015	Nivière B. 1998, Geophy Res Letters 25(13):2325
Chillicothe, Ohio	0.0005	Putkonen and O'Neal 2006
Switzerland	0.0021	Oehm 2005, Zeithschrift fur Geomorph 49(3):353
Switzerland	0.0031	Oehm 2005, Zeithschrift fur Geomorph 49(3):353
Switzerland	0.0047	Oehm 2005, Zeithschrift fur Geomorph 49(3):353
Switzerland	0.0003	Oehm 2005, Zeithschrift fur Geomorph 49(3):353
Japan	0.0036	Oehm 2005, Zeithschrift fur Geomorph 49(3):353
Japan	0.0093	Oehm 2005, Zeithschrift fur Geomorph 49(3):353
Japan	0.0135	Oehm 2005, Zeithschrift fur Geomorph 49(3):353
Japan	0.0059	Oehm 2005, Zeithschrift fur Geomorph 49(3):353

Note: To convert meters to feet, multiply by 3.281.

F.3.1.4.9 Model-Data Comparison Metrics

There are a number of different metrics that one could use in comparing observed and modeled topography. Studies of stream and hillslope profile evolution using one-dimensional models typically use metrics based on the differences between observed and modeled surface height at a series of points along the profile (Rosenbloom and Anderson 1994, Stock and Montgomery 1999, Whipple et al. 2000, van der Beek and Bishop 2003, Tomkin et al. 2003). Comparing two-dimensional models of drainage basin evolution with observed topography is less straightforward. Point-by-point comparison of observed and simulated topography suffers from the problem that small differences in drainage pathways can lead to large apparent errors, even though the modeled topography may be statistically very similar to the real landscape. Thus, most tests of drainage basin evolution models have been based on statistical measures of terrain such as the catchment-wide slope–area relationship, the hypsometric curve, and the drainage-area distribution function (Hancock et al. 2002).

The ideal set of metrics should provide a strong filter against "false positive" solutions (in other words, getting the right answer for the wrong reasons). They should also include tests of multiple aspects of predicted topography (for example, elevation properties as well as drainage-network geometry). If possible, they should include information on intermediate states during the course of landscape evolution, rather than just the present-day topography. Given these considerations, the following six model-data comparison metrics were selected: the long profile of Buttermilk Creek, catchment hypsometric curve, log-binned slope–area diagram, width function, cumulative area function, and the time-elevation position of two dated strath terraces. These metrics are described below:

1. **Buttermilk Creek's longitudinal profile** – Stream profiles (the elevation of the stream bed as a function of distance downstream) are closely linked to three-dimensional topography (Tucker and Whipple 2002) and are of critical importance to future erosion at the WNYNSC, because they set the baselevel for surrounding hillslopes. One complication that can arise in comparing observed and predicted topography is that, as noted above, modeled stream profiles may differ slightly from their target landscapes in length, sinuosity, or direction. For example, Buttermilk Creek has a series of entrenched meanders along its lower reach. These meanders will not appear in the simulations because meandering has been omitted (although CHILD has a meandering submodel, it is considered too experimental for this study in terms of additional poorly constrained parameters). Thus, it is expected that the length and exact pathway of the observed and modeled Buttermilk Creek will differ slightly. The solution adopted here is to project the long profiles onto a north–south axis. The comparison procedure applies the following steps to both the 10-meter resolution DEM of the Buttermilk Creek watershed and the simulated CHILD grid: (1) starting at a common headwater point (Universal Transverse Mercator 697,536 meters east, 4,696,570 meters north), extract points along the profile in upstream-to-downstream order until reaching the outlet; (2) remove any small loops using linear interpolation; (3) interpolate the profile to a set of 101 equally spaced points between the head and the outlet; and (4) compute the sum-of-squares difference between observed and modeled profiles.

2. **Hypsometric curve** – The hypsometric curve is a plot of the cumulative area of land (in this case, within the Buttermilk Creek catchment) that lies below a given altitude. It is a widely used indicator of landscape morphology, and it is one of four metrics suggested by Hancock et al. (2002) for testing landscape evolution models. Its role is to provide a statistical comparison of altitudes across the catchment. Modeled and observed hypsometric curves are compared by interpolating each curve to 101 equally spaced altitude intervals (ranging from 300 to 700 meters above sea level), and computing the sum-of-squares difference.

3. **Slope–area diagram** – A slope–area diagram compares the gradients of a set of points on the landscape with their upstream contributing areas. The shape of the slope–area relationship is closely linked to the physics of erosional processes as well as to landscape history, and therefore it represents a valuable statistic for testing landscape evolution theory (Willgoose et al. 1991, Dietrich et al. 1993, Willgoose 1994, Ijjasz-Vasquez and Bras 1995, Snyder et al. 2000, Hancock et al. 2002, Tucker and Whipple 2002). One advantage is that it encompasses both hillslope processes (whose relative strength is reflected in location of the peak of the curve) and fluvial processes (whose behavior is reflected by the graph slope and intercept). Here, the modeled and observed slope–area patterns are compared by computing the average slope in a series of logarithmic bin increments between drainage areas of 10^2 and 10^9 square meters (bin increments are 10^2, $10^{2.2}$, $10^{2.4}$, …10^9). The sum-of-squares differences between observed and modeled average gradients are computed.

4. **Width function** – The catchment width function is a frequency distribution of flow-path length within the catchment, and it reflects drainage network structure and catchment shape. Observed and modeled width functions are compared by interpolating each to a set of 101 equally spaced length intervals between zero and 20 kilometers and calculating the sum-of-squares differences. The width function was among the metrics used by Hancock et al. (2002).

5. **Cumulative area distribution** – Another of the four metrics used by Hancock et al. (2002) for model-data comparison, the cumulative area distribution measures the rate of flow aggregation within a drainage network. It is computed by first calculating the contributing drainage area at each cell in a DEM, then plotting (usually on a log-log graph) the cumulative distribution of drainage areas. The observed and modeled area distributions are compared using the following steps: (1) divide the y-axis (proportion of cells) into 0.1 log increments, ranging from the fractional area of one cell to unity;

(2) interpolate to find the corresponding value of drainage area at each interval; and (3) compute the sum-of-squares difference.

6. **Strath terrace positions** – A strath terrace is a fluvially eroded surface that represents the position of a stream channel at some point in the past. As discussed in Section F.2.2, dating of strath terraces can reveal average rates of downcutting. The existence of dated straths at the site provides a valuable constraint on the model's evolutionary history: a correct model must place Buttermilk Creek at the right altitude at the right time. Two Buttermilk Creek straths are used to test this. The first is located at OSL Sample site 1A, and it is used here because it provides a constraint on elevation history of the upper portion of the main Buttermilk Creek Valley. Its potential age range, based on the 1-sigma bounds for both the CAM and MAM estimates, falls between 9,120 and 16,080 years ago. The second terrace is located at OSL Sample site 5. It is chosen because the OSL sample appears to be of high quality, with no evidence of significant partial bleaching, and because it provides a constraint along the lower reach of Buttermilk Creek Valley. Its age range is 11,990 to 15,610 years. In order to assign altitude ranges to these terraces, several factors must be considered. The 10-meter (32.81-foot) USGS digital elevation model, from which the sample altitudes were estimated, is subject to uncertainty; the USGS website quotes an expected root-mean-square elevation uncertainty of 7 meters (23 feet) for National Elevation Data products. In addition, the altitude of a stream is somewhat fuzzy because the water depth varies from place to place in association with features such as pools and riffles. For a stream the size of Buttermilk Creek, the associated uncertainty is likely to be on the order of a meter. There will also be a difference between the height of a terrace surface and the height of the former bedrock bed because the latter is mantled by a variable amount of sediment (based on our site observations, this is typically on the order of a few meters). Finally, there is uncertainty on the order of 10 meters (32.81 feet) associated with the horizontal sample location, though given the low gradient of the terrace surfaces, the comparable vertical uncertainty is likely to be below 1 meter (3.28 feet). Given these considerations, a conservative estimate of terrace uncertainty is judged to be +/-10 meters (32.81 feet), most of which reflects DEM uncertainty. Simulations that fail to place the channel within the correct altitude range (404 to 424 meters [1,325 to 1,391 feet] for terrace 1 and 369 to 389 meters [1,211 to 1,276 feet] for terrace 5) at the right geographical location within the right time range, are judged to be failures, and are given a score of zero on this metric. Those that do correctly capture the terrace heights are assigned a terrace score of unity.

The scores associated with each of the first five metrics are normalized, so that the minimum possible score is zero and the maximum is close to one. This normalization provides a way to weight the metrics equally; otherwise, metrics yielding large numbers would dominate those yielding small numbers. Ideally, one would like to normalize metrics according to some independent measure of the uncertainty in the data. For example, one might consider that any model whose uncertainty score is less than the intrinsic uncertainty in the measured data might be said to be as close a match to the data as can be feasibly measured. However, we have only one landscape, and only one DEM. Although the root-mean-square uncertainty for the DEM is documented, without having multiple, independently generated DEMs, there is no way to know how the DEM's elevation root-mean-square uncertainty translates into uncertainty in the metrics that are derived from it. Thus, independent estimates of metric uncertainty are not available. In addition to this intrinsic uncertainty, there is also uncertainty involved in comparing a model at one resolution (nominally 90 meters [295.28 feet]) with data at another resolution (10 meters [32.81 feet]). This latter uncertainty, which is hereafter called "resolution uncertainty," can be calculated by computing sum-of-square differences between metrics derived from 10-meter (32.81-foot) data and those derived from the modern topography represented at the calibration resolution of 90 meters (295.28 feet). As a pragmatic choice, then, the metrics are normalized as follows. For each metric, the top scoring 1 percent of calibration runs (10 runs) are identified, and their average sum-of-squares uncertainty is calculated as a "minimum model uncertainty." If the resolution uncertainty is larger than the model uncertainty, then the resolution uncertainty is used to normalize the metrics; otherwise, the minimum model uncertainty is used.

Scores for the first five metrics are averaged to create a composite score, while the sixth metric provides a binary pass/fail criterion.

F.3.1.5 Testing and Calibration Results

A model calibration run is considered to represent an acceptable fit to the modern topography if it meets the following criteria (the numbers in parentheses indicate the number of calibration runs satisfying each criterion):

1. Total average score >0.5 (36 of 1,000 runs),
2. Longitudinal profile score >0.7 (12 of 1,000 runs),
3. Correct elevations at terrace locations 1 and 5 in the correct time span (215 of 1,000 runs), and
4. Qualitative visual agreement between modeled and observed topography, including preservation of extensive remnants of the initial glacial plateau and minimal erosion of the bedrock uplands.

Six runs out of the calibration set of 1,000 met all of the first 3 criteria, and 5 of these were judged to pass the visual-match criterion. The parameters associated with these runs are listed in **Table F–11**. Among the 5, the parameter set with the highest overall score (0.680) is used as a standard case in the forward modeling discussed below. The remaining 4 are considered to be alternative and equally viable parameter sets, and they are also used in forward projections.

Table F–11 Parameters Associated with the Top Scoring Calibration Runs

Parameter	*Run 298 (0.680)* [a]	*Run 321 (0.677)*	*Run 622 (0.643)*	*Run 891 (0.617)*	*Run 972 (0.669)*
Start of incision (years before present)	17,500	18,300	17,500	17,500	15,200
Time outlet reaches terrace 7 height (years before present)	14,500	14,500	12,000	12,000	14,500
Soil infiltration capacity (meters per year)	19.4	3.82	16.8	19.4	16.8
K_f [b]	2,500	2,500	500	2,500	100
K_t [b]	1,750	1,500	1,000	1,000	1,250
τ_{cb} (pascals)	1	80	1	80	80
τ_{cr} (pascals)	124	124	54	23	54
K_d (square meters per year)	0.001	0.0003	0.0003	0.003	0.003
K_{bt} [b]	10,000	100	10,000	100	10
K_{br} [b]	1	0.1	0.001	0.01	0.001

[a] Five-metric average score.
[b] See Table F–8 for units.
Note: To convert meters to feet, multiply by 3.281; square meters to square feet, multiply by 10.764.

Figures F–8a and F–8b compare the best-fit calibration run with the observed topography. As expected, there are differences in detail. However, the run succeeds in capturing the overall pattern and extent of valley incision, while preserving the uplands. The simulated present-day topography preserves remnants of the till plateau flanking the incised valley, and it predicts about the right depth of incision along the main trunk stream. The simulated drainage patterns in the Franks Creek area are similar to the observed patterns (Figures F–8a and 8b**)**. The modeled valleys are generally narrower, which is to be expected because the model runs did not incorporate the lateral channel migration process (i.e., the lateral shifting in channel position due to natural instabilities in the flow that lead to bank erosion and gradual horizontal migration in the channel position). **Figures F–9** to **F–13** compare the best-fit model with the data for each metric.

Note that the match shown on Figures F–8a and F–8b is by no means inevitable. **Figure F–8c** gives an example of a run that predicts too little erosion, while **Figure F–8d** shows an example of a run that predicts far too much erosion (as well as extreme rearrangement of drainage patterns). Of the 1,000 calibration runs, about 130 failed with numerical errors before running to completion. The numerical instability that leads to such

failures arises under extreme erosion scenarios (even more erosive than the clearly unrealistic example on Figure F–8d), and therefore, these cases are assumed to represent unrealistically erosive parameter combinations.

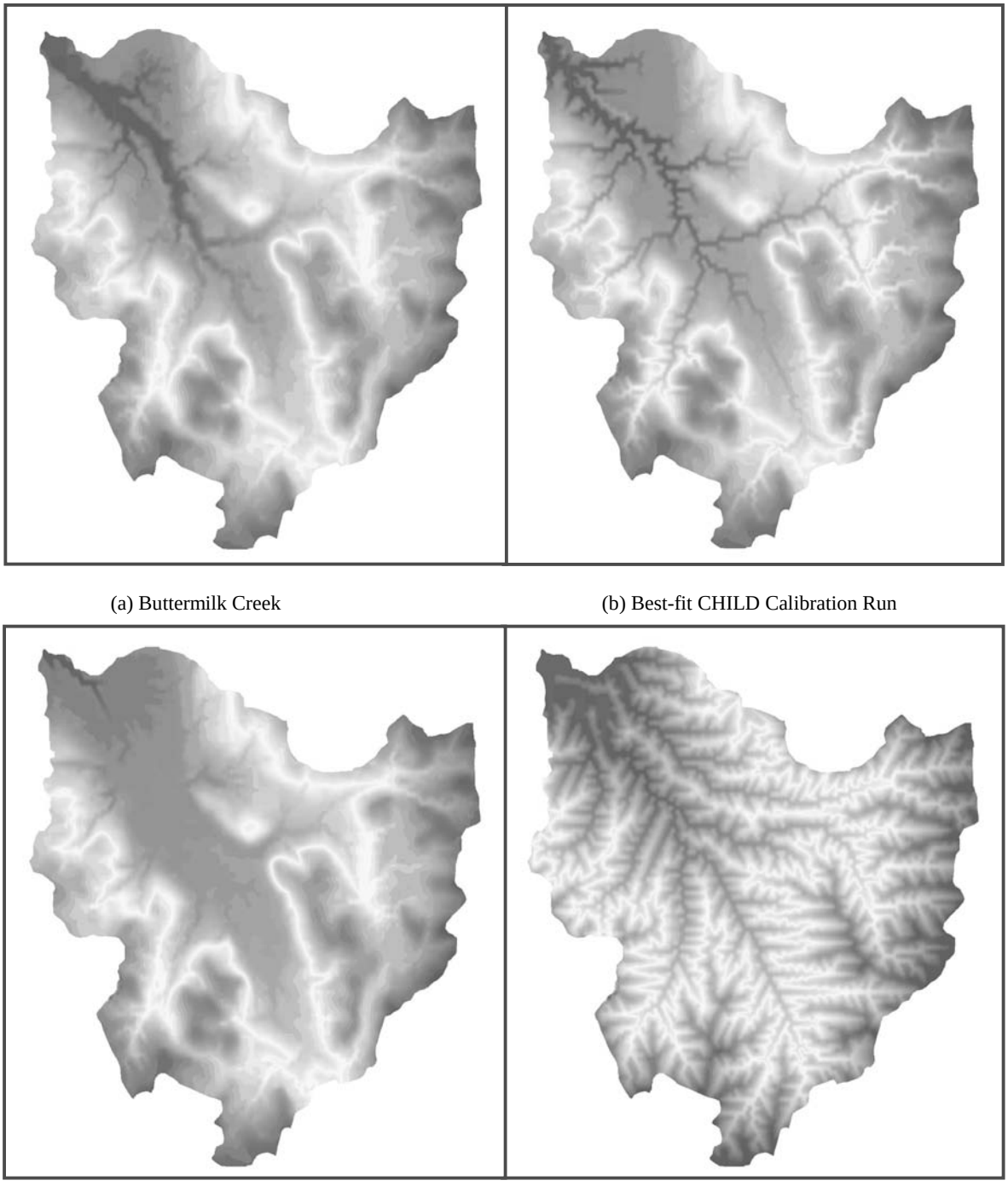

(a) Buttermilk Creek

(b) Best-fit CHILD Calibration Run

(c) CHILD Run with Too Little Erosion

(d) CHILD Run with Too Much Erosion

Figure F–8 Plan-view Images of Buttermilk Creek and Best-fit CHILD Calibration Run and Two Examples of Poor Fit CHILD Calibration Runs (lower left and lower right)

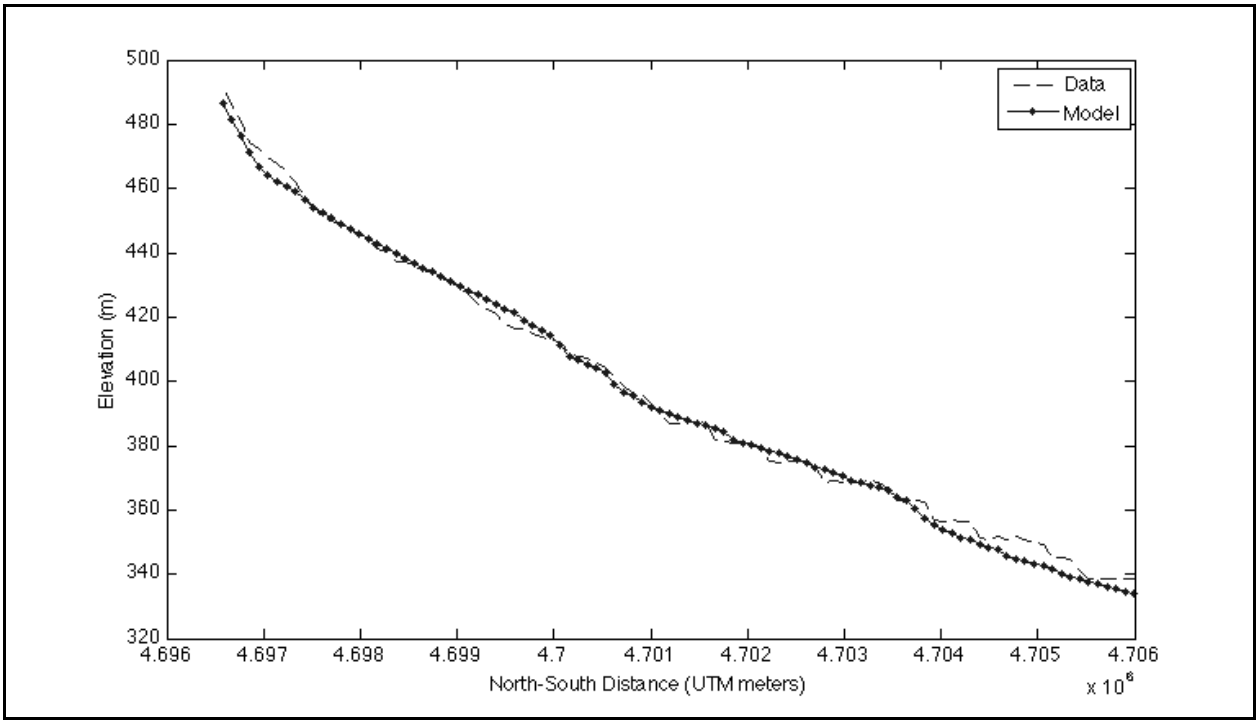

Figure F–9 Comparison of Observed and Best-fit Longitudinal Profile, Projected to North–South Axis

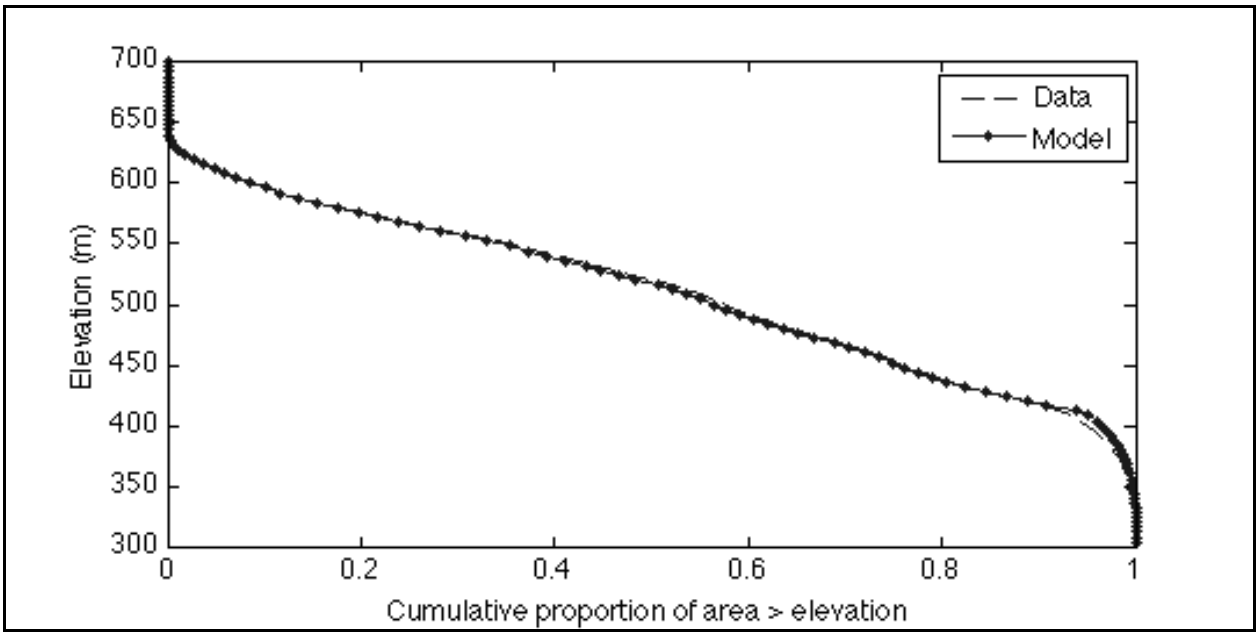

Figure F–10 Comparison Between Observed and Predicted Hypsometric Curve

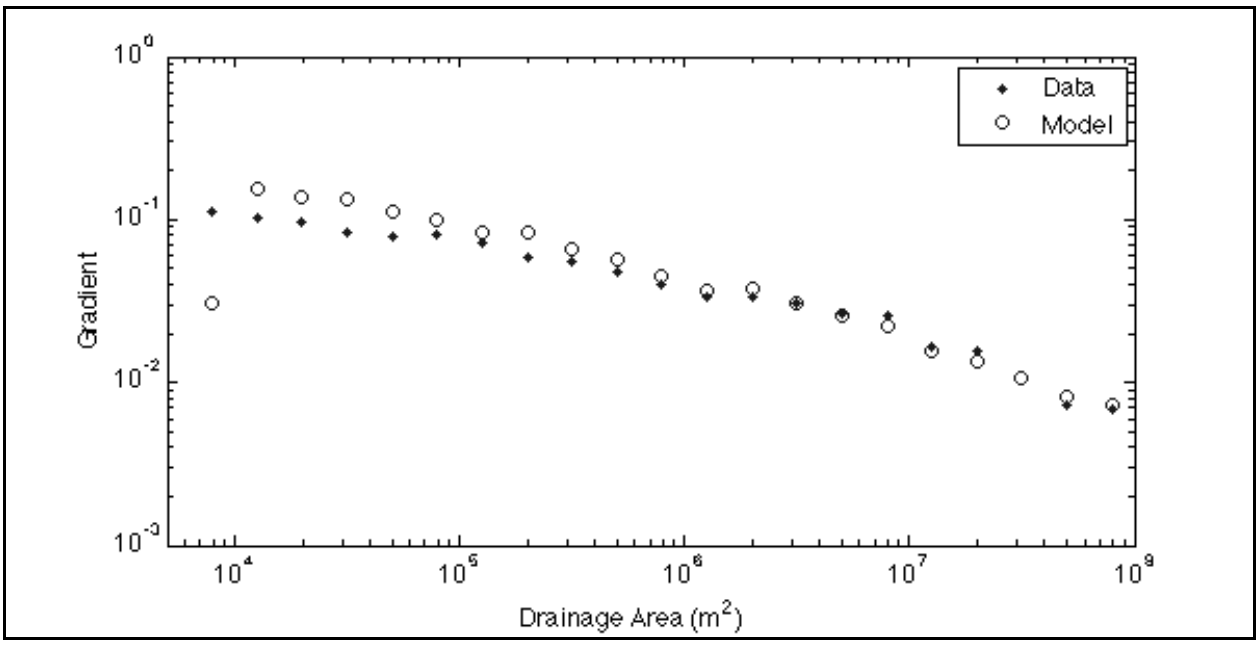

Figure F–11 Observed and Predicted Slope–Area Distribution

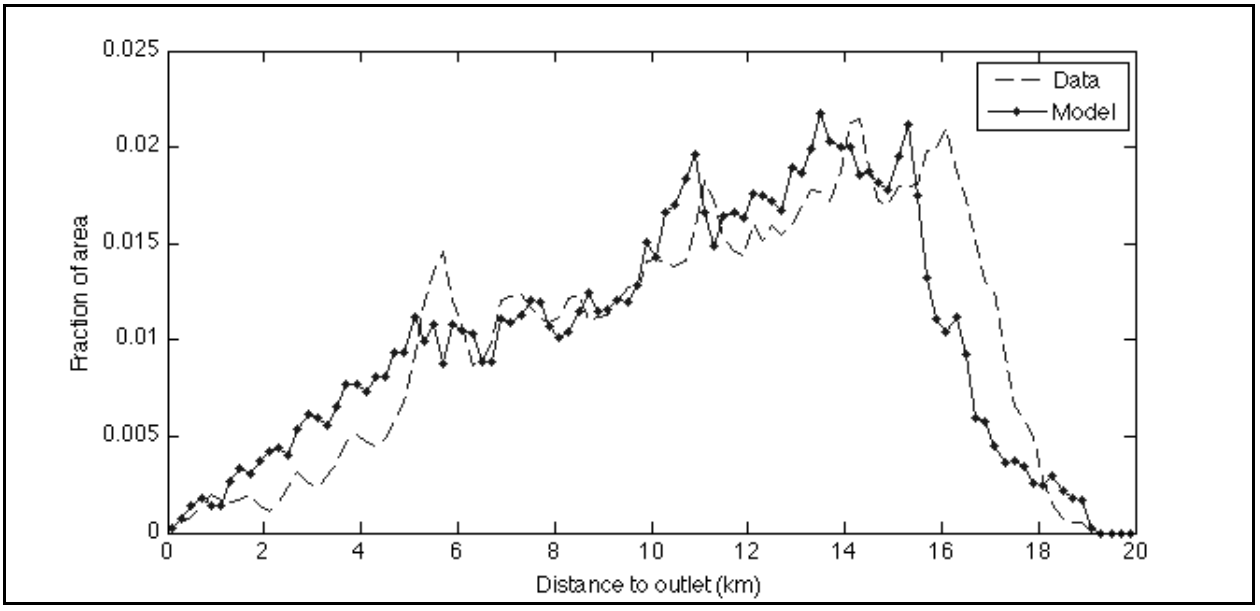

Figure F–12 Observed Versus Best-fit Modeled Width Function

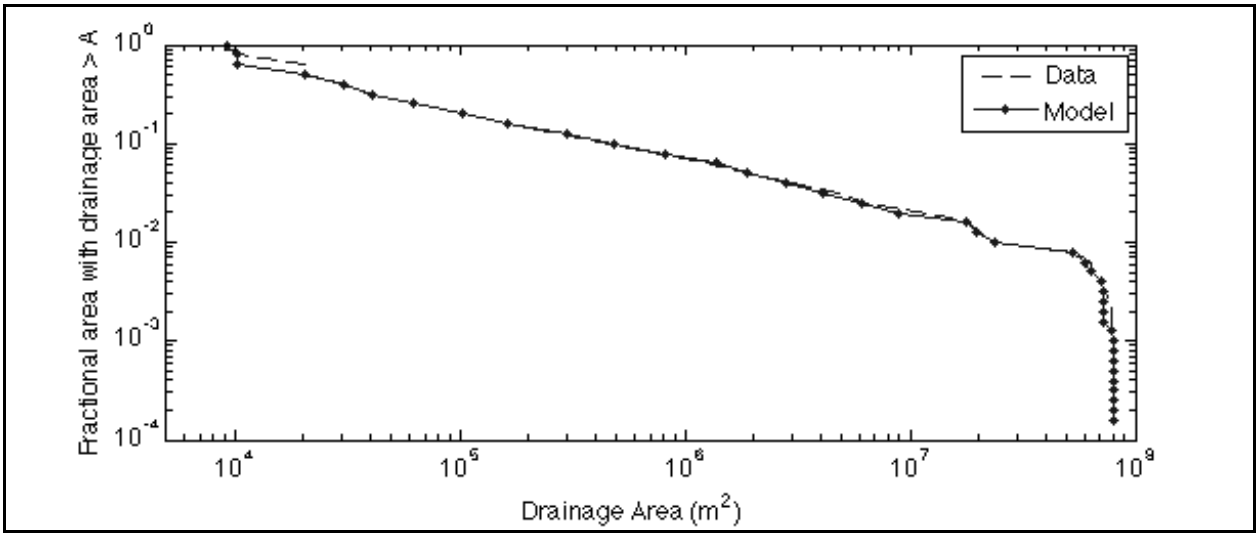

Figure F–13 Observed Versus Best-fit Modeled Cumulative-area Index

F.3.1.6 Forward Modeling of Erosion Patterns

A series of erosion projections were made that take no credit for the effect of active erosion control measures.

F.3.1.6.1 General Approach

The model was run forward in time for a period of 10,000 years using the five calibration parameter sets shown in Table F–11. A sixth parameter set, discussed below, represents a case in which the climate becomes wetter and the soils less permeable. The scenarios represented by the six parameter sets are referred to henceforth as Standard, Alternate 1, Alternate 2, Alternate 3, Alternate 4, and Wet, respectively. In one set of runs, the initial topography was derived from the modern topography of the Buttermilk Creek watershed as shown in **Figure F–14**. In a second set of runs, the initial topography incorporated two burial mounds on the North and South Plateaus that were proposed as part of the Close-In-Place Alternative as shown in **Figure F–15**. To create the initial simulation mesh, the 10-meter (32.81-foot) USGS DEM was interpolated to the model mesh resolution (with the addition of DEMs representing the burial mounds for runs representing the Close-In-Place Alternative). In all cases, the base-level lowering rate applied at the outlet was equal to the final base-level lowering rate in the corresponding calibration run.

F.3.1.6.2 Model Resolution

As discussed in Section F.1.1, gullying is an important mode of erosion at WNYNSC. In order to be able to simulate the potential growth of relatively small gullies, the model resolution must be relatively fine. On the other hand, the resolution must be sufficiently coarse to ensure reasonable model integration times. A series of tests were conducted to determine the highest feasible model resolution. The results indicated that a nominal point spacing of 2.8 meters (9.19 feet) was operationally feasible provided that the area represented at this resolution was relatively small. The tests showed that representing both the North and South Plateaus at this resolution simultaneously would be impractical. Therefore, two different model meshes were generated: one in which only the North Plateau is represented at a 2.8-meter (9.19-foot) resolution while the remainder of the Buttermilk Creek basin is modeled at the calibration resolution of 90 meters (295.28 feet), and another in which only the South Plateau is represented at a 2.8-meter (9.19-foot) resolution. The two mesh configurations are shown on **Figure F–16**.

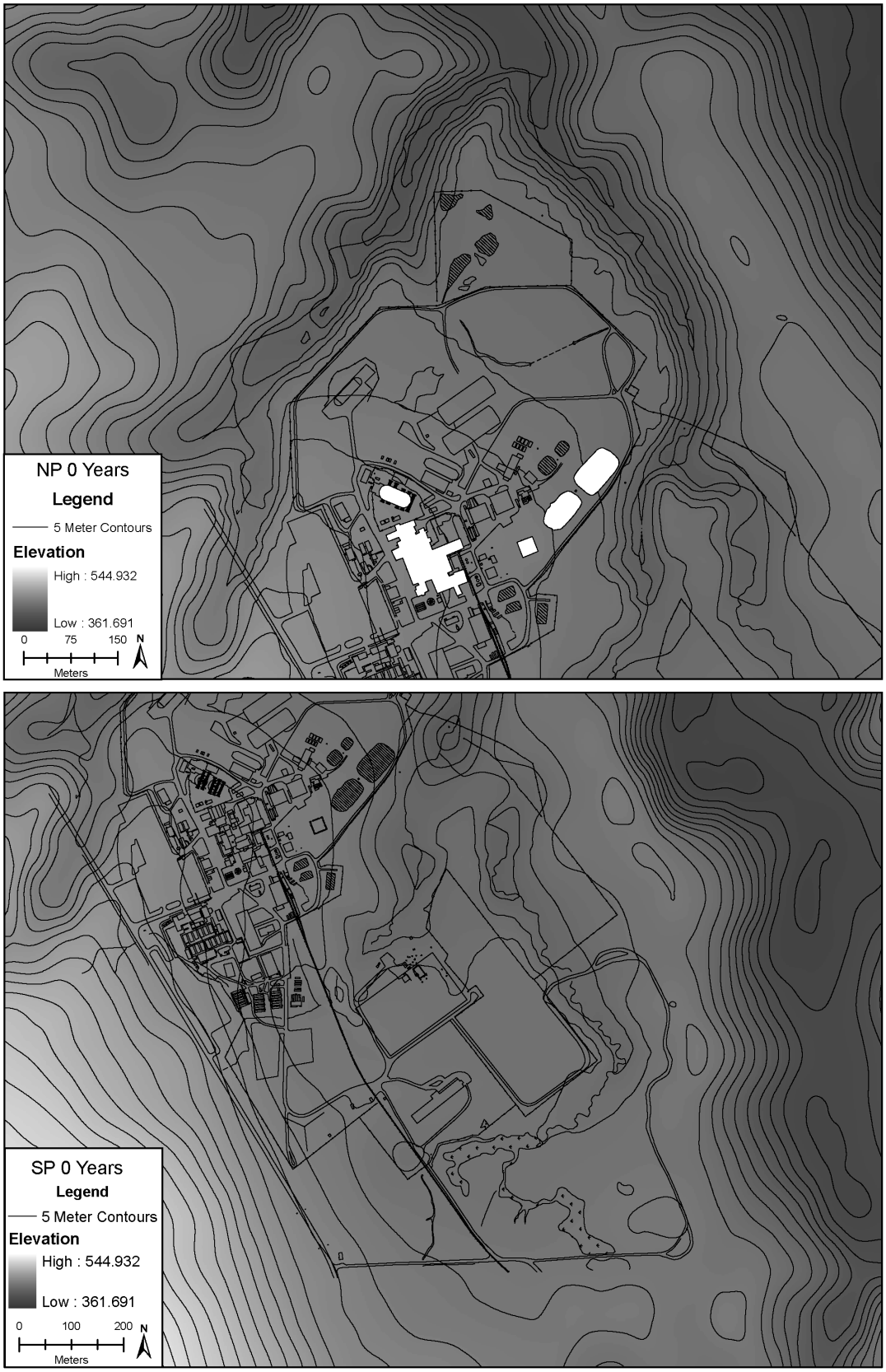

Figure F–14 Modern Topography of Buttermilk Creek Watershed

Figure F–15 Initial In-Place-Closure Topography North and South Plateaus

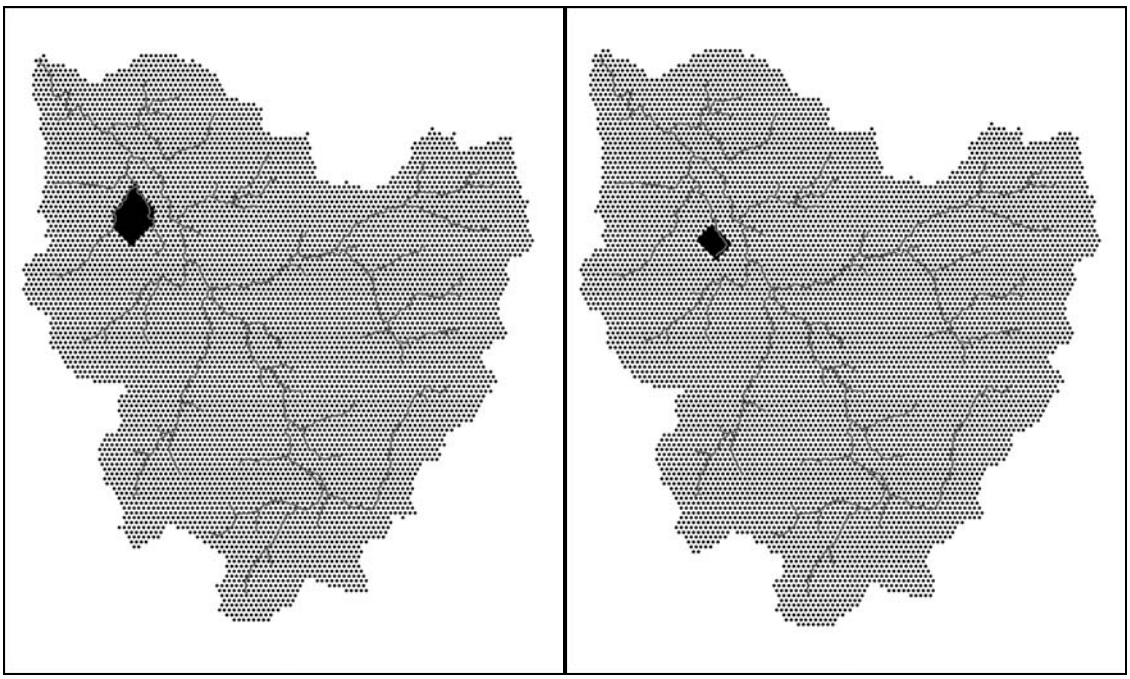

Figure F–16 CHILD Meshes with North Plateau at a 2.8-meter Resolution (left) and South Plateau at a 2.8-meter Resolution (right)

F.3.1.6.3 Mathematical Representation of Proposed Burial Structures

The burial structures (tumuli) proposed under the Sitewide Close-In-Place Alternative (see Appendix C) are designed to withstand direct water erosion, and to be geomechanically stable. However, few engineered structures without deep pilings can withstand being undermined by erosion of the ground that supports them. Thus, the greatest erosional threats to these structures are considered to be undermining by mass movement as valley rims widen in response to stream incision and undermining by adjacent gully incision. It was assumed that, with regard to hillslope mass movement, the materials composing the tumuli would not differ substantially from the natural soils and sediments on which they are built. With regard to water erosion, the material was assigned the same erodibility coefficient as the glacial sediments. This is a conservative assumption, as coarse mound material is likely to be more resistant to entrainment and transport by running water than typical till material.

F.3.1.6.4 "Wet" and "Fast-Creep" Scenarios

A future shift to a wetter climate, and/or a reduction in the infiltration capacity of soils, represents a potential threats to the erosional integrity of the burial areas. In order to assess the potential for accelerated erosion under altered climate and land use conditions, a "Wet" scenario was developed. The Wet scenario was designed to represent conditions in which (1) the mean precipitation intensity is twice the modern value estimated from West Valley rainfall data (2.9 millimeters [0.11 inches] per hour), and (2) the soil infiltration capacity takes on the minimum value in the calibration parameter range (0.436 millimeters [0.02 inches] per hour). The former represents a climatic shift in which both storminess and mean annual precipitation increase (that is, it doesn't rain more often than it does in the present, but when the rain comes it is twice as heavy). The latter a degraded land use condition in which runoff is amplified. In addition to the Wet scenario, a Wet + Fast Creep scenario was developed for the South Plateau only. This scenario was motivated by the possibility that the relatively low creep coefficients identified in the best-fit calibration runs may not be representative of the current or future creep rates. Because the calibration procedure relied heavily on features formed by water erosion (such as the main stream profile, the width function, the drainage-area distribution

function, and most of the slope-area curve), the creep coefficients associated with the best fitting runs are not necessarily the best parameters for the site. Accordingly, the Fast Creep scenario uses the highest of the plausible range of values identified in the parameter selection phase (0.036 square meters [0.39 square feet] per year) in addition to the Wet parameters. Because of computing-time limitations, it was only possible to run the Wet + Fast Creep scenario on the South Plateau. It is considered more significant at that location, because its considerably smaller drainage area makes it relatively more susceptible to creep- and landslide-erosion than the North Plateau, where the primary erosional hazard appears to be gullying.

F.3.1.6.5 Summary of Forward-Run Scenarios

Altogether, 26 forward runs were computed (**Table F–12)**. Of these, one—the Wet scenario for the North Plateau under the No Action Alternative—failed with numerical errors, which reflects a combination of high sediment flux and small grid spacing. The remainder ran to completion (Table F–12). The table also indicates the computationally intensive nature of these model calculations, with run times ranging from 5 to over 1,000 hours.

Table F–12 Summary of Forward Runs

Run	*Parameter Set*	*High-resolution Mesh Area*	*Scenario*	*Computation Time (hours)*
NPstd	Standard	North Plateau	No action	54
NPa1	Alternate 1	North Plateau	No action	54
NPa2	Alternate 2	North Plateau	No action	104
NPa3	Alternate 3	North Plateau	No action	459
NPa4	Alternate 4	North Plateau	No action	34
NPwet	Wet	North Plateau	No action	(run failed)
NPTstd	Standard	North Plateau	Sitewide Close-in-place	49
NPTa1	Alternate 1	North Plateau	Sitewide Close-in-place	50
NPTa2	Alternate 2	North Plateau	Sitewide Close-in-place	93
NPTa3	Alternate 3	North Plateau	Sitewide Close-in-place	558
NPTa4	Alternate 4	North Plateau	Sitewide Close-in-place	33
NPTwet	Wet	North Plateau	Sitewide Close-in-place	1,049
SPstd	Standard	South Plateau	No action	8
SPa1	Alternate 1	South Plateau	No action	13
SPa2	Alternate 2	South Plateau	No action	6
SPa3	Alternate 3	South Plateau	No action	15
SPa4	Alternate 4	South Plateau	No action	5
SPwet	Wet	South Plateau	No action	63
SPwc	Wet + Fast Creep	South Plateau	No action	76
SPTstd	Standard	South Plateau	Sitewide Close-in-place	8
SPTa1	Alternate 1	South Plateau	Sitewide Close-in-place	14
SPTa2	Alternate 2	South Plateau	Sitewide Close-in-place	7
SPTa3	Alternate 3	South Plateau	Sitewide Close-in-place	37
SPTa4	Alternate 4	South Plateau	Sitewide Close-in-place	6
SPTwet	Wet	South Plateau	Sitewide Close-in-place	69
SPwc	Wet + Fast Creep	South Plateau	Sitewide Close-in-place	82

F.3.1.6.6 Results: No Action Scenario, North Plateau

The standard, no action case (NPstd; **Figure F–17**) shows incision along Quarry Creek, which drives hillslope erosion on the northwest edge of the plateau. This prediction is consistent with the observed morphology of this stretch of Quarry Creek, which appears to be actively incising and has cut to bedrock along part of the reach. The simulation shows an upstream transition from net incision to (minor) net deposition along the stretch of Franks Creek between the Quarry Creek confluence and the Franks Creek–Erdman Brook junction. Incision along the lower portion of this reach is consistent with onsite observations. Sedimentation or net stability in the vicinity of the Franks Creek–Erdman Brook junction appears to be at odds with present-day observations of active incision, as discussed in the following text.

The simulation shows the formation of an approximately 100-meter (328-foot)-long gully on the northeast plateau rim, north of the present-day NP-2. Erosion is also concentrated along the rim of the plateau. Both of these features are generally consistent with erosion patterns observed at the site, though the position of the modeled gully does not correspond to either of the existing gullies (NP-2 and NP-3) along that portion of the rim. However, there is some concentration of erosion around the present-day NP-3 gully.

The NPa1 case (**Figure F–18**) is similar on the whole to the standard case. By contrast, NPa2 shows considerably more erosion (**Figure F–19**). As in the standard case, the greatest incision occurs along Quarry Creek, and particularly in the stretch northwest of the Process Building. The simulation also shows incision along the full stretch of Franks Creek between Quarry Creek and Erdman Brook. The NP-3 gully deepens and extends headward across the boundary road, while the NP-2 gully extends beyond the boundary fence. The largest gully in the simulation forms north of NP-2, with over 15 meters (49.21 feet) of vertical incision at its deepest point. The NP-1 gully also extends headward and deepens, generating a side branch that advances within the boundary fence. Additional gullies form along the northwestern plateau edge, north-northwest of the Main Plant Process Building.

Scenario NPa3 (**Figure F–20**) shows incision of up to 27 meters (88.58 feet) depth along Quarry Creek. In contrast, the behavior of Franks Creek resembles that of scenarios NPstd. The simulation shows a mixture of net incision and net aggradation around and above the Franks Creek–Erdman Brook confluence, with absolute height changes generally less than 10 meters (32.81 feet). Net incision occurs on the downstream reach of Franks Creek. Deep incision along Quarry Creek drives rim retreat, such that the plateau edge advances several tens of meters beyond the boundary road along the northwest plateau edge. The NP-1 gully lengthens and deepens somewhat. The largest gully to form in this scenario appears on the northeast edge, north of NP-2. This gully pushes the plateau rim some tens of meters beyond the perimeter fence, and shows a maximum deepening between 20 and 25 meters (65.62 and 82.02 feet). Erosion along the eastern plateau edge is much more muted, rarely exceeding 5 meters (16.40 feet). Scenario NPa4 (**Figure F–21**) is generally quite similar to NPa3.

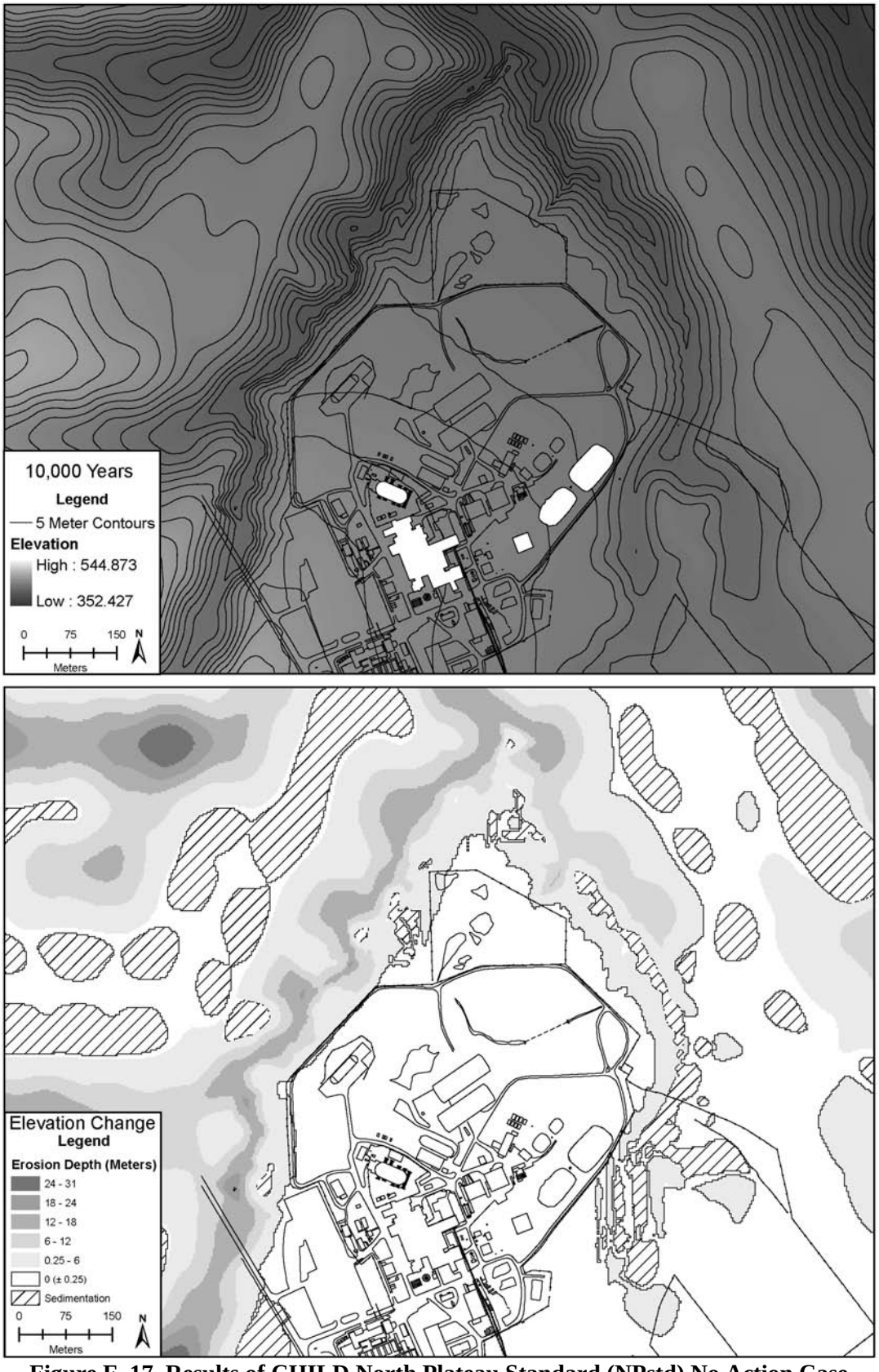

Figure F–17 Results of CHILD North Plateau Standard (NPstd) No Action Case

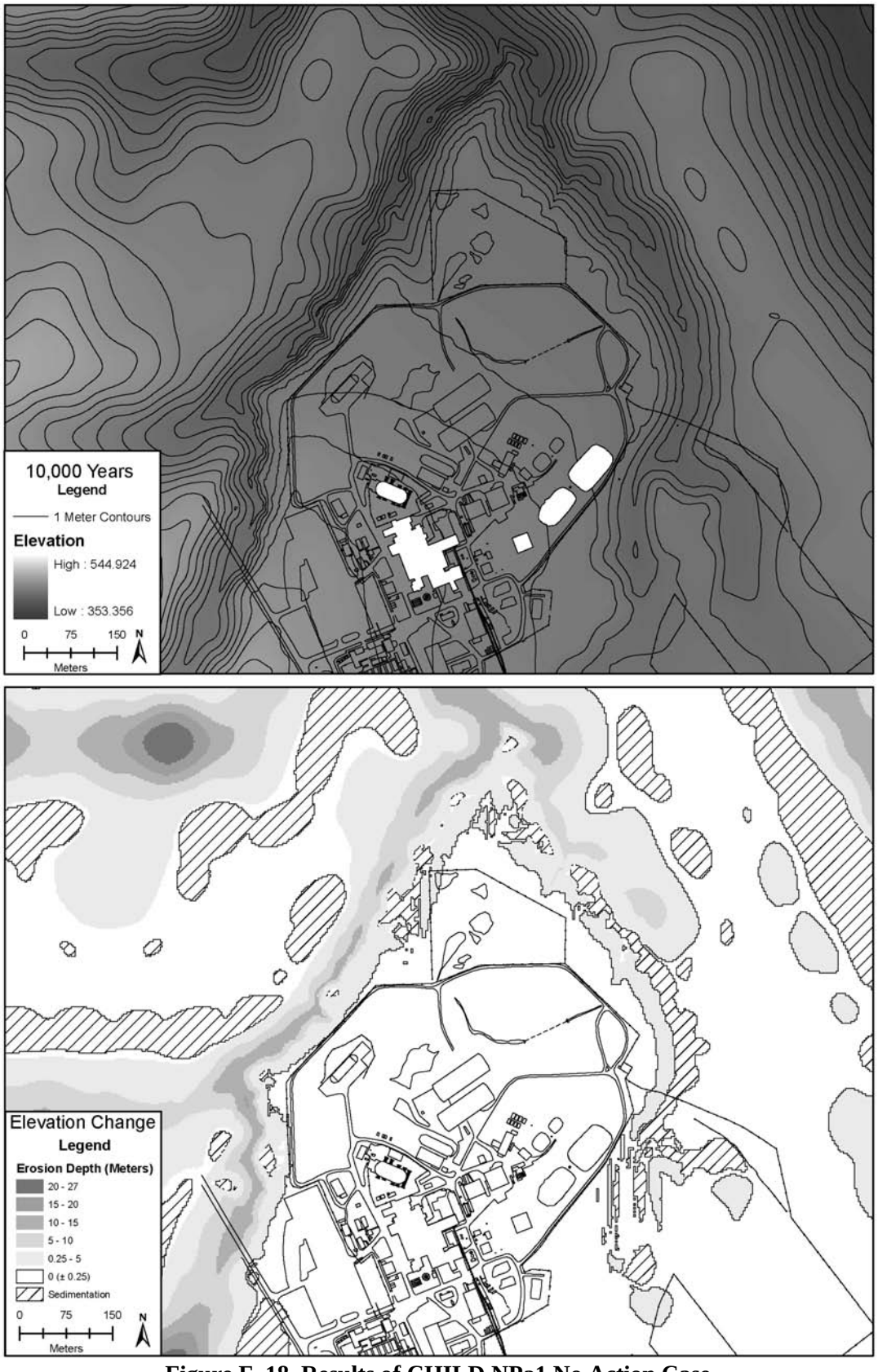

Figure F–18 Results of CHILD NPa1 No Action Case

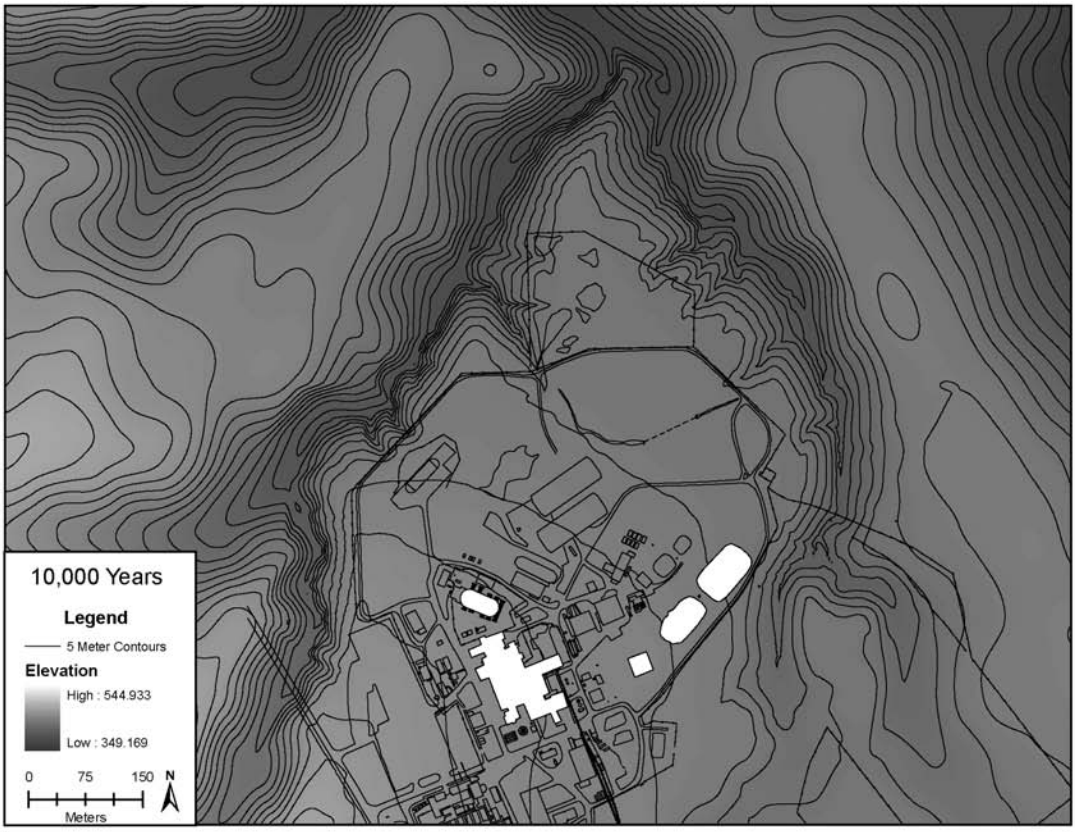

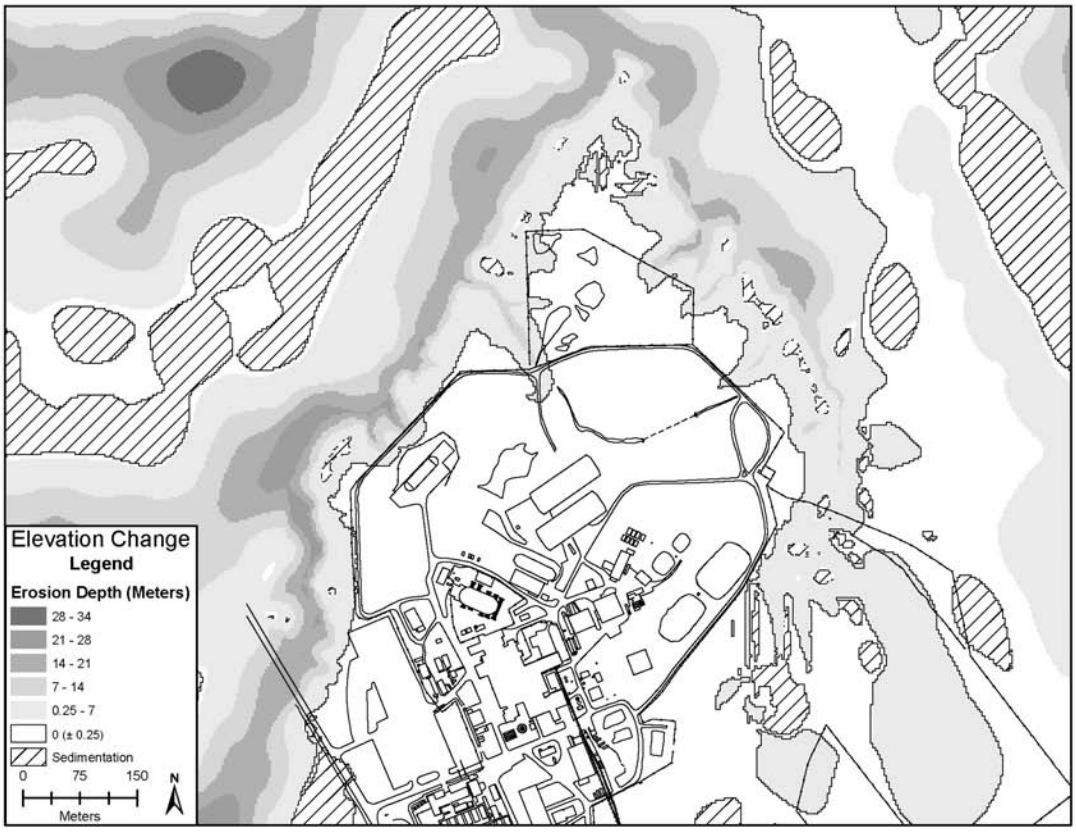

Figure F–19 Results of CHILD NPa2 No Action Case

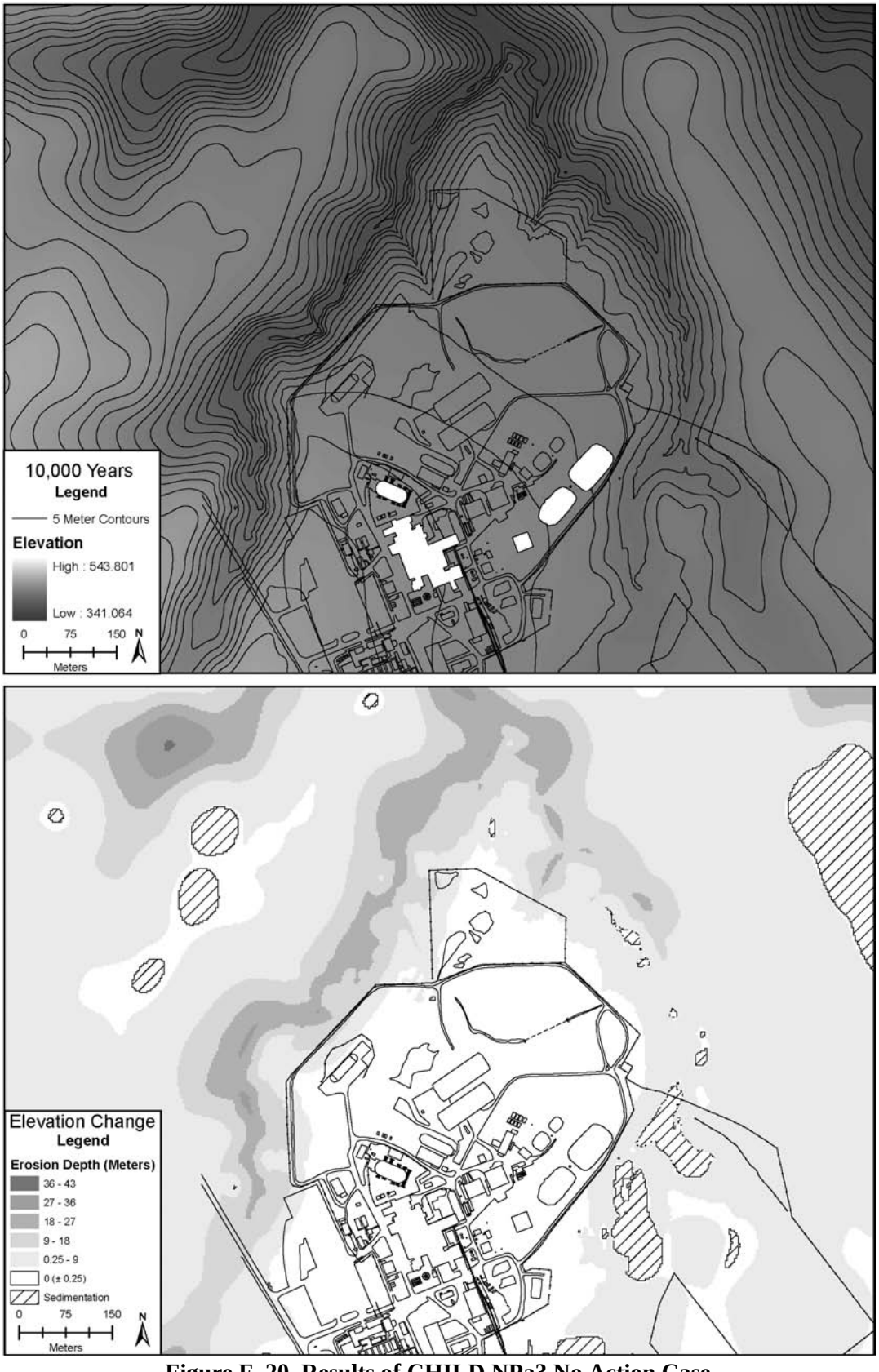

Figure F–20 Results of CHILD NPa3 No Action Case

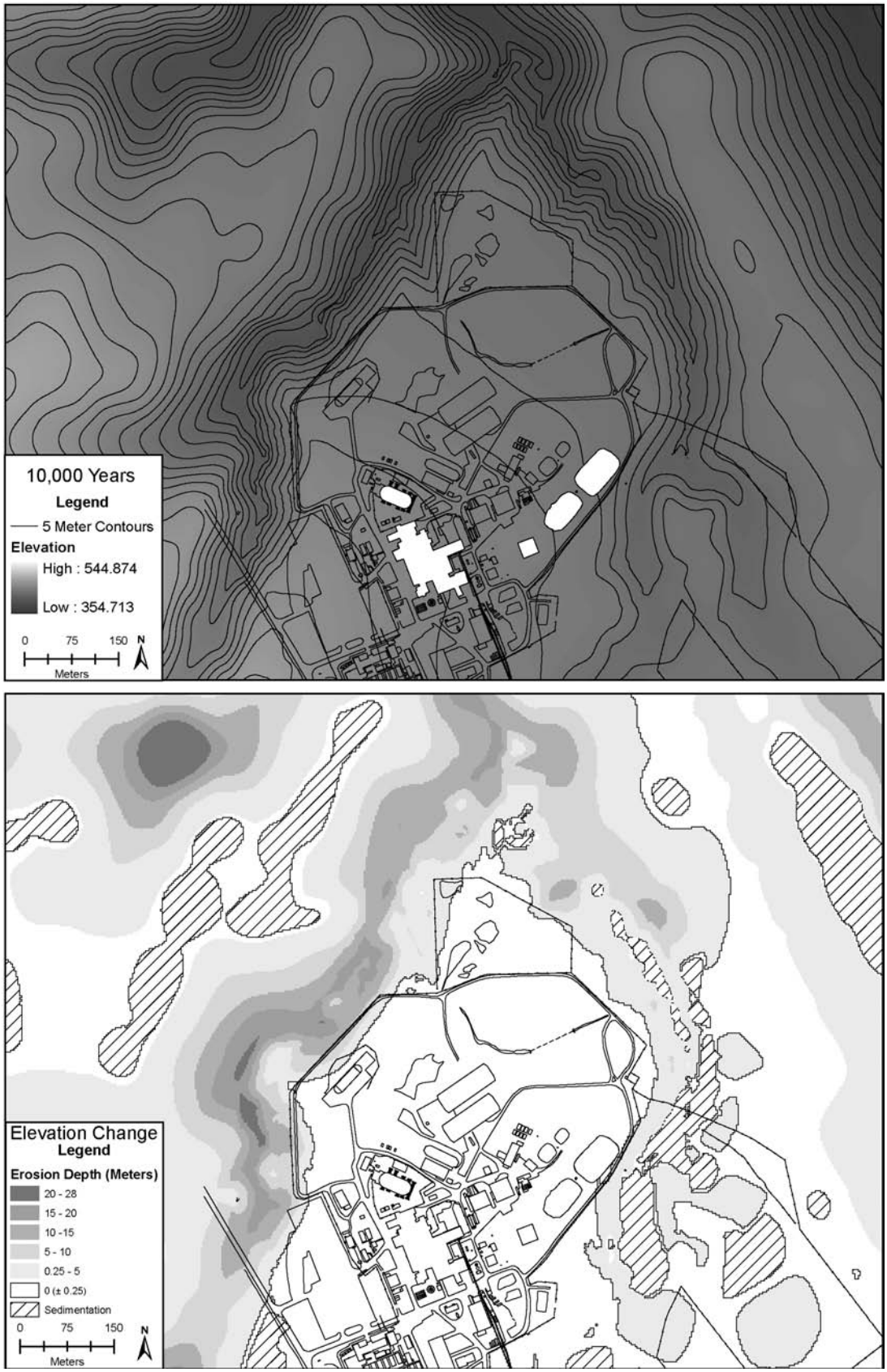

Figure F–21 Results of CHILD NPa4 No Action Case

F.3.1.6.7 Results: No Action Scenario, South Plateau

In general, the simulations using a dense mesh on the South Plateau show considerably less erosion than those for the North Plateau. Scenario SPstd (**Figure F–22**) shows less than 1 meter (3.28 feet) of net erosion along the east edge of the SDA, plus a small localized area of approximately 2 meters (6.56 feet) of erosion at the west corner of the NDA where Erdman Brook makes a right-hand turn. Upper Franks Creek shows stability.

Scenarios SPa1 (**Figure F–23**) and SPa2 (**Figure F–24**) show essentially no significant erosion or deposition. Scenario SPa3 (**Figure F–25**) shows erosion of up to 1 meter (3.28 feet) along the east rim of the SDA, locally higher, and the formation of a shallow (less than 1 meter [3.28 feet] deep) gully in the depression between the SDA and NDA. Upper Franks Creek shows minor incision in runs SPa2 and SPa3. Scenario SPa4 is generally similar to SPa3, but with overall stability in the Erdman Brook and upper Franks Creek drainages.

As expected, the SPwet scenario (**Figure F–26**) shows more-extensive erosion in the South Plateau. The existing shallow trough between the SDA and NDA deepens by up to 6.8 meters (22.31 feet), forming an approximately 200-meter (656.17-foot)-long gully that extends to the road that runs along the southeast side of the NDA. Erdman Brook and upper Franks Creek undergo incision on the order of 10 to 20 meters (32.81 to 65.62 feet), tapering upstream.

In the Wet + Fast Creep scenario (**Figure F–27**), the NDA gully forms but does not grow or deepen nearly as far as in SPwet. This reflects the suppression of incision by enhanced flux of sediment from the surrounding slopes. The east flank of the SDA experiences erosion depths locally approaching 4 meters (13.12 feet), while the north and west sides of the NDA show relatively minor erosion (less than 2 meters [6.56 feet]. Incision along Erdman Brook and upper Franks Creek is similar to the behavior of the SPwet scenario.

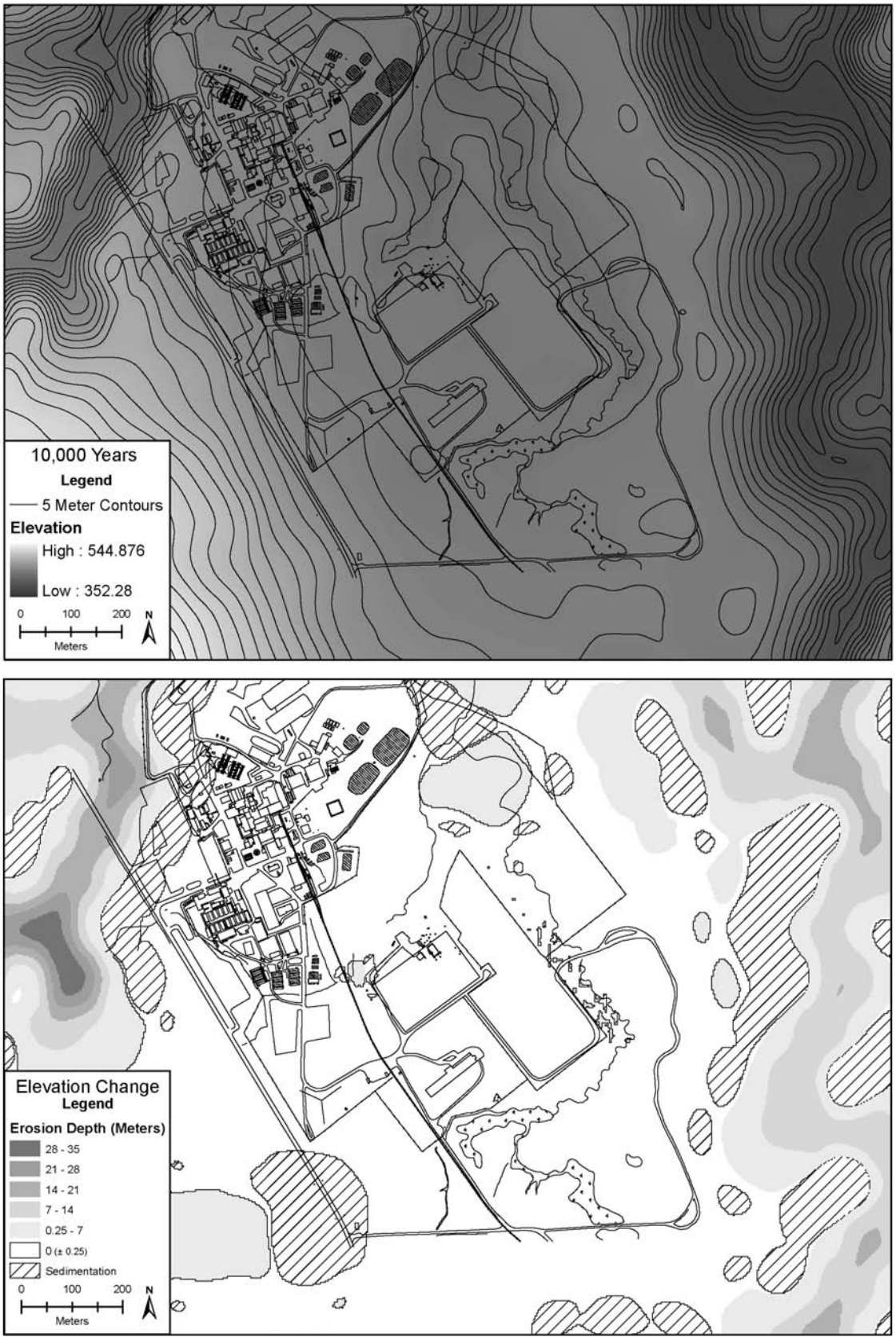

Figure F–22 Results of CHILD South Plateau Standard (SPstd) No Action Case

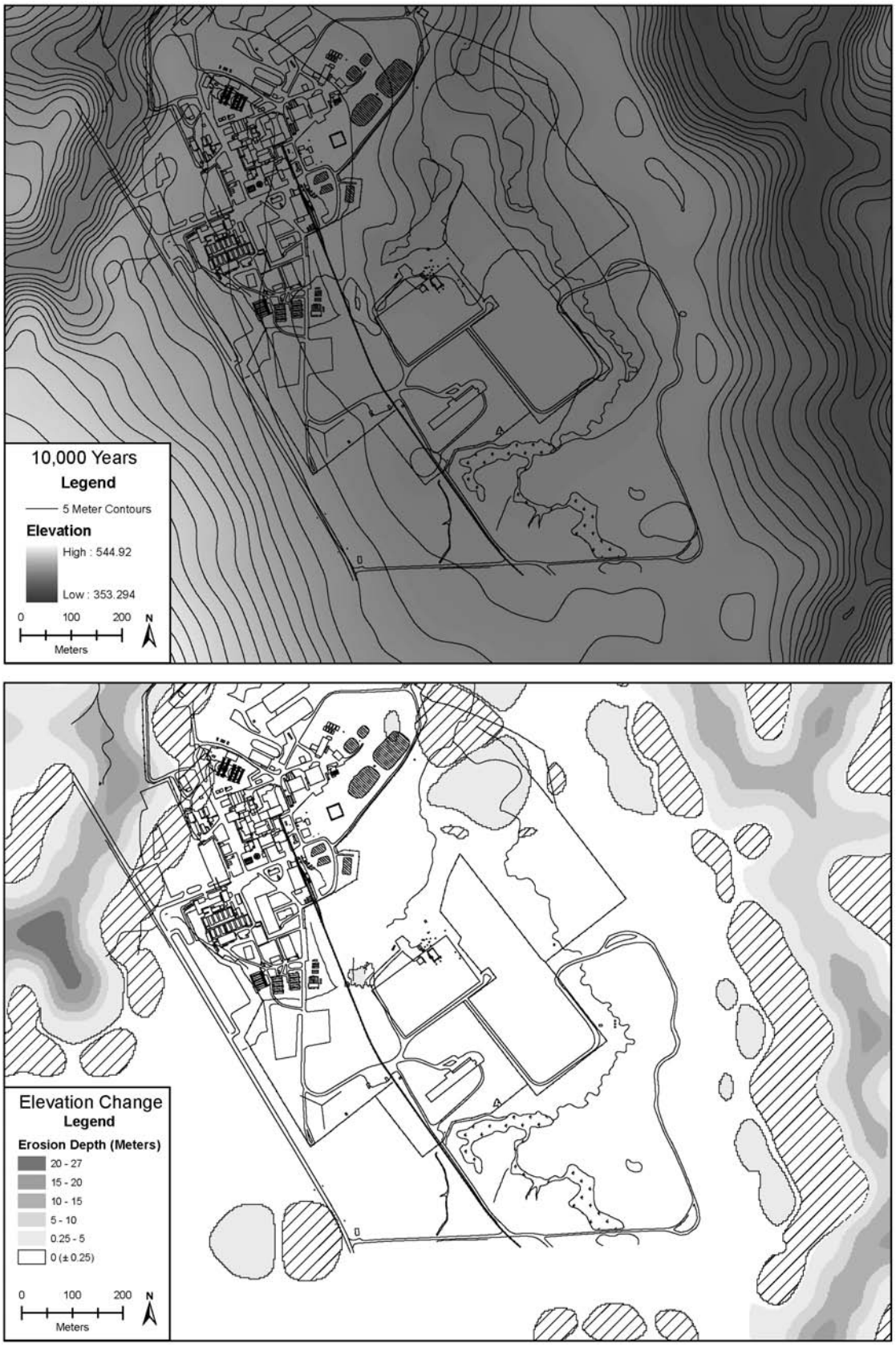

Figure F–23 Results of CHILD SPa1 No Action Case

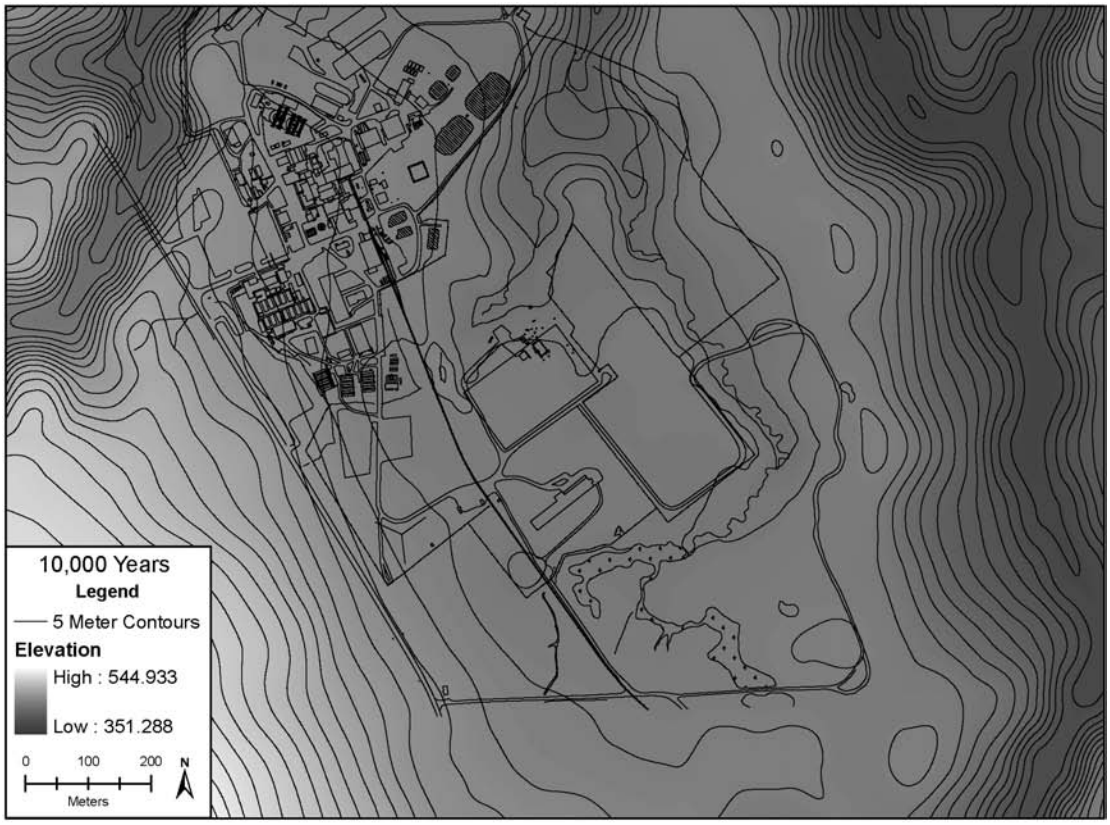

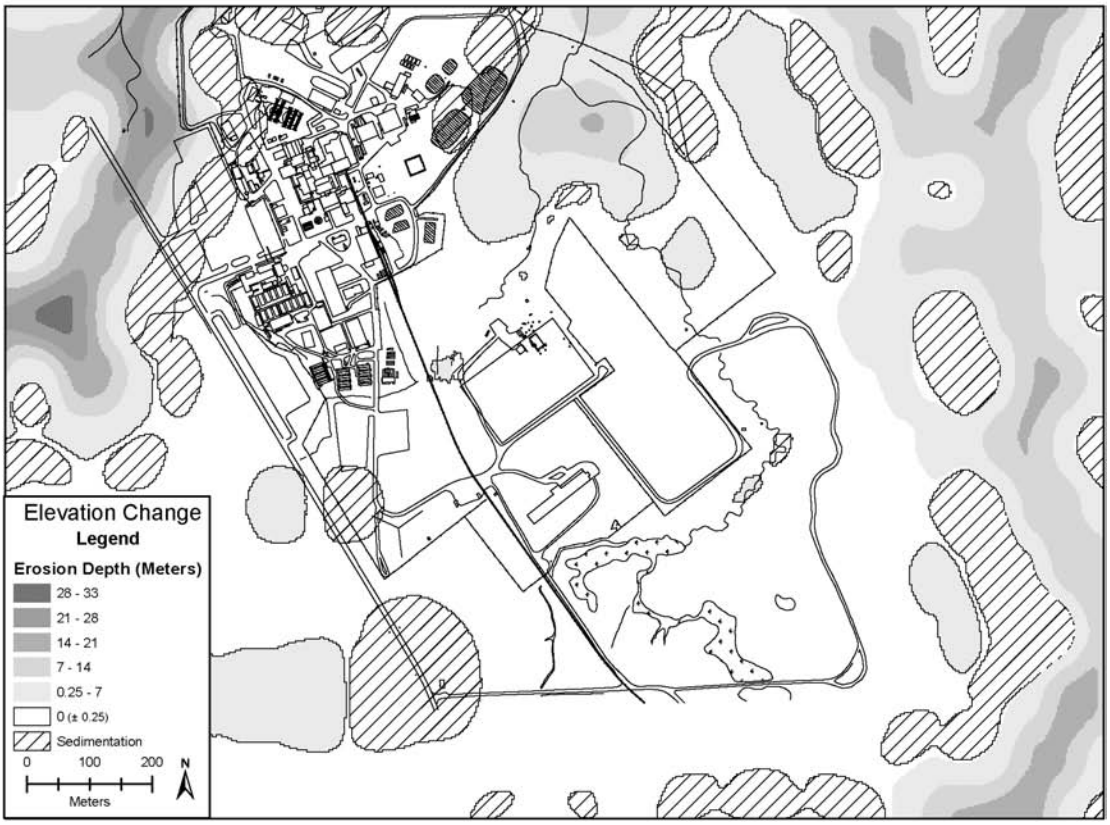

Figure F–24 Results of CHILD SPa2 No Action Case

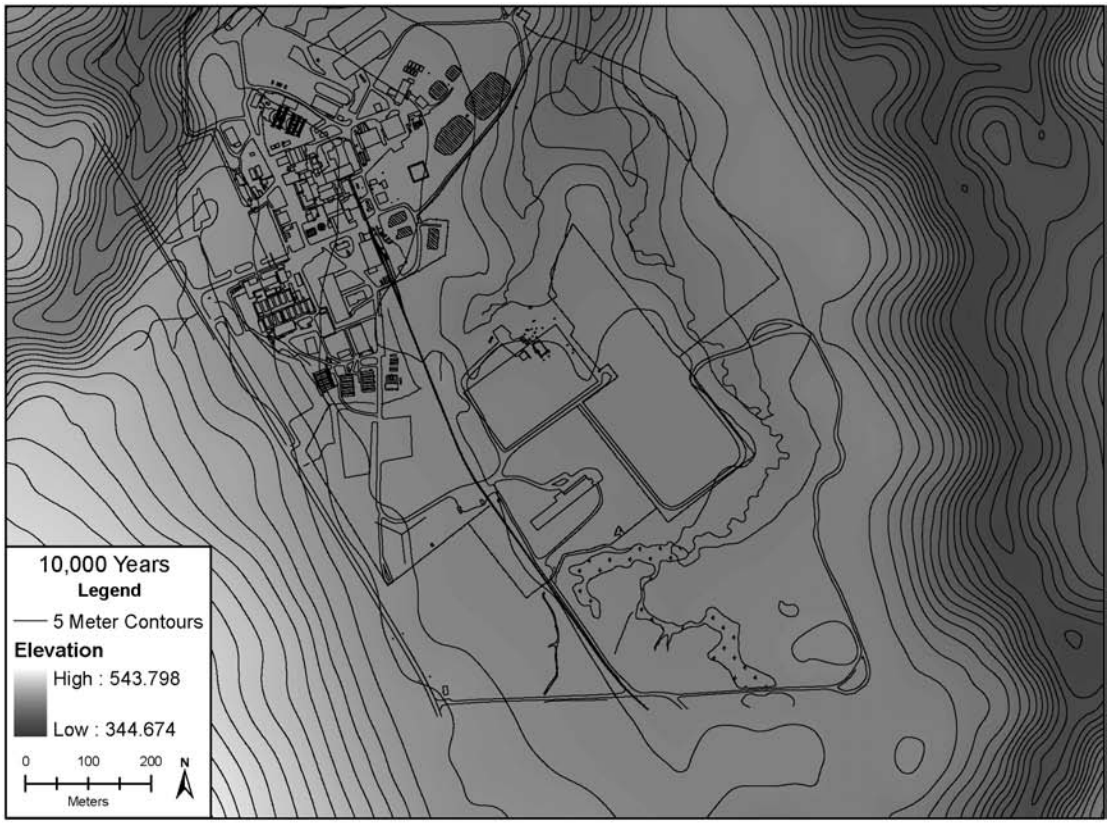

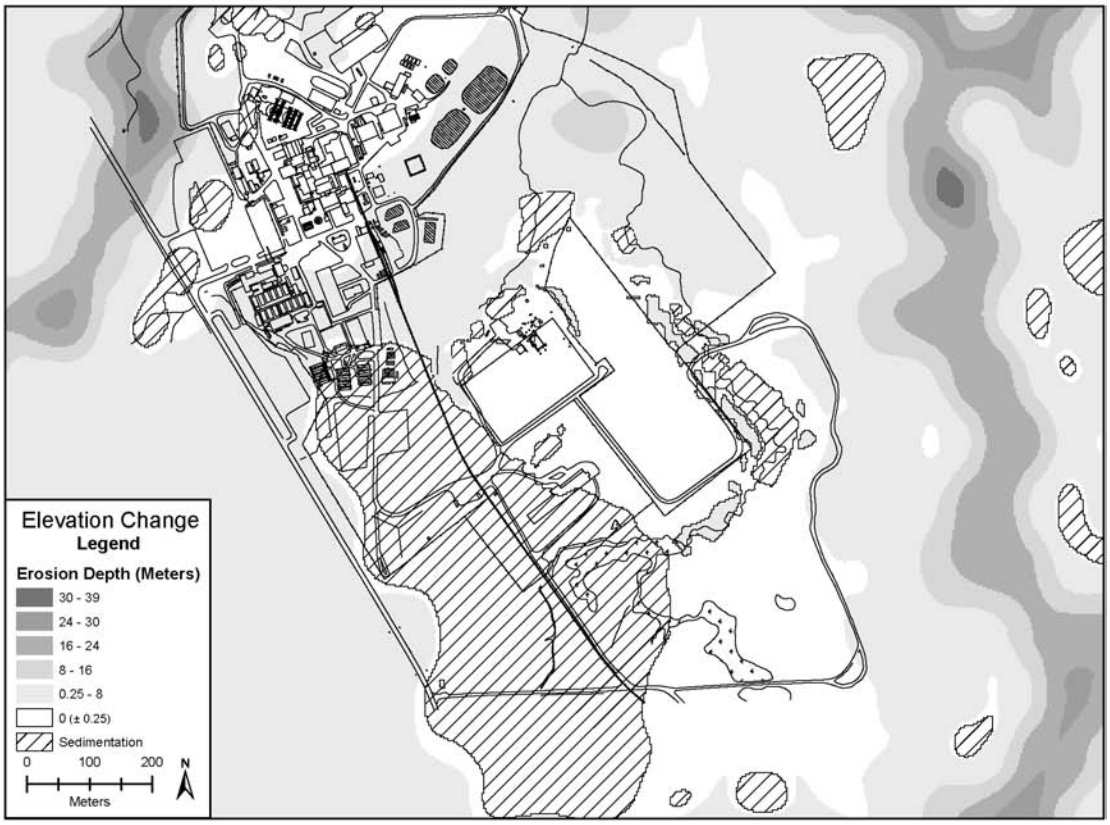

Figure F–25 Results of CHILD SPa3 No Action Case

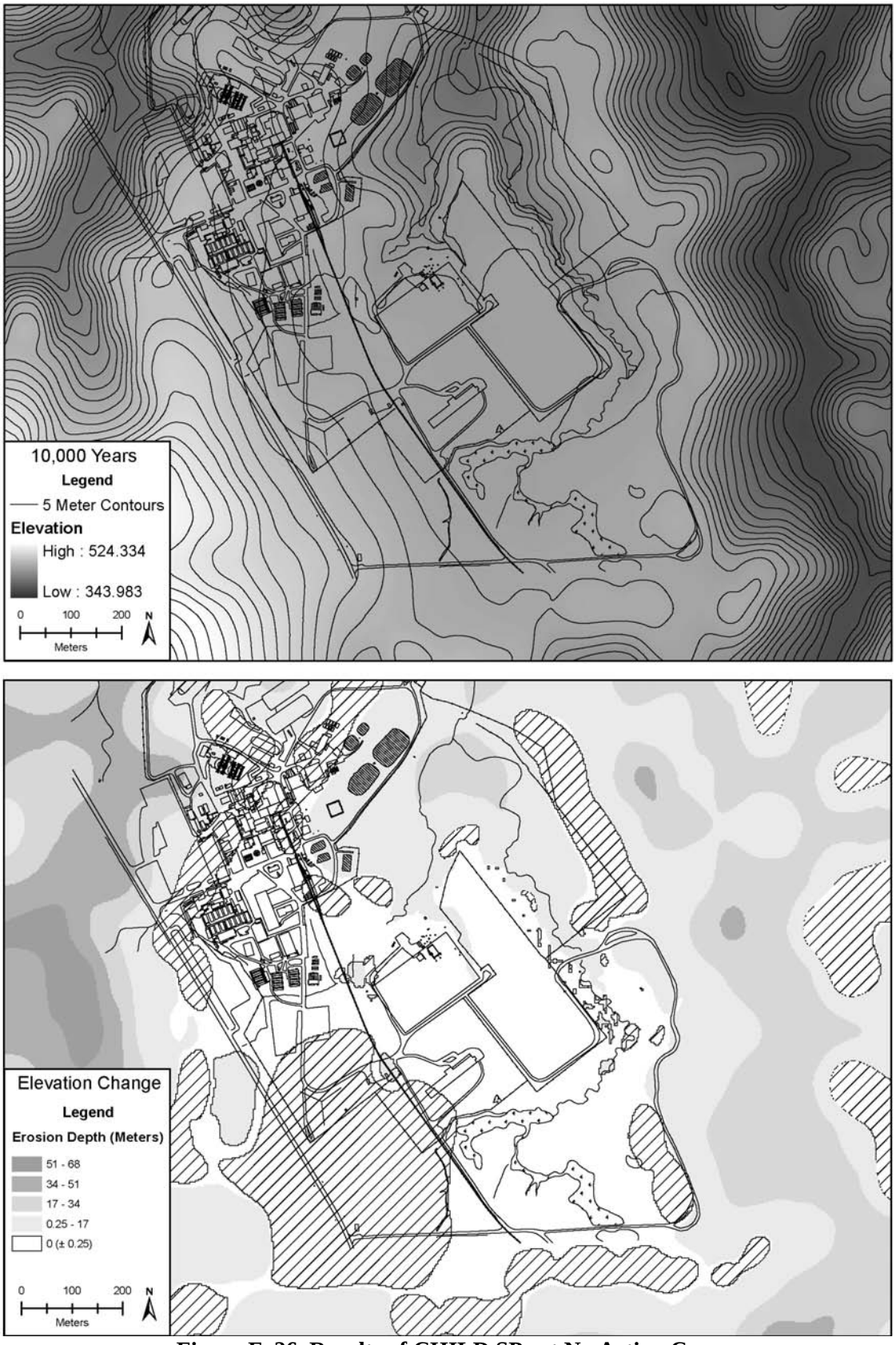

Figure F–26 Results of CHILD SPwet No Action Case

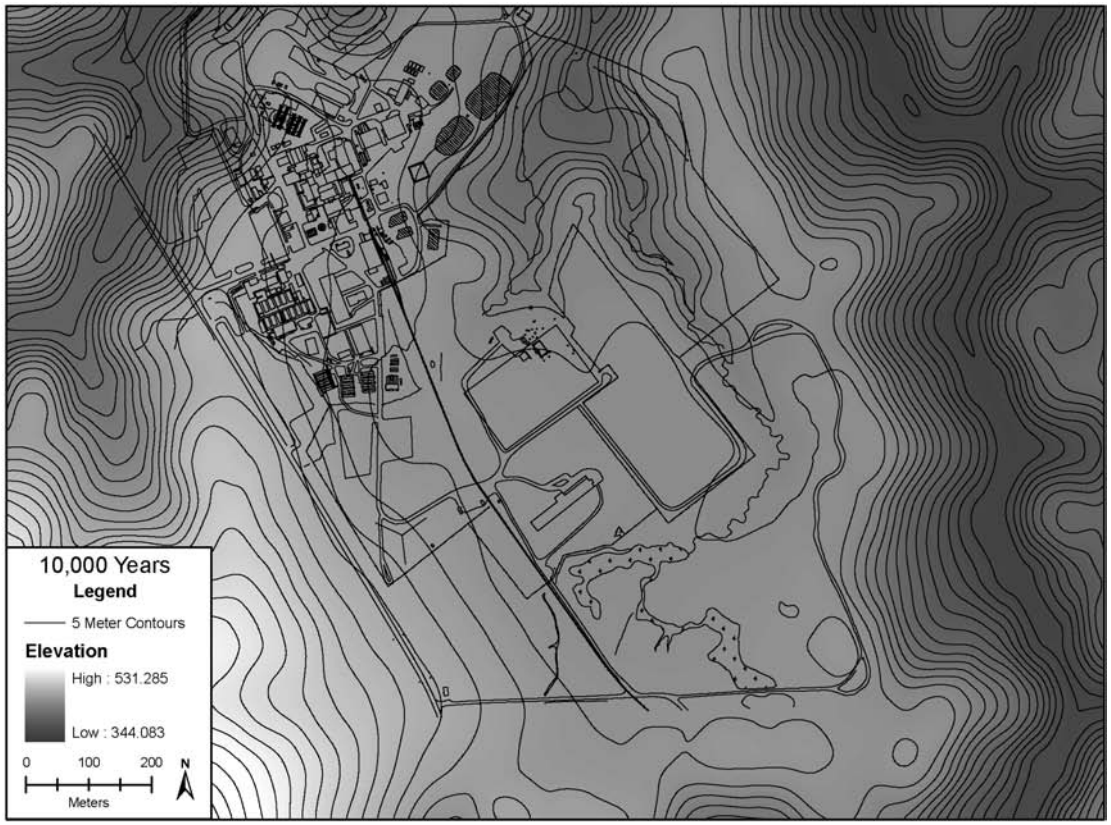

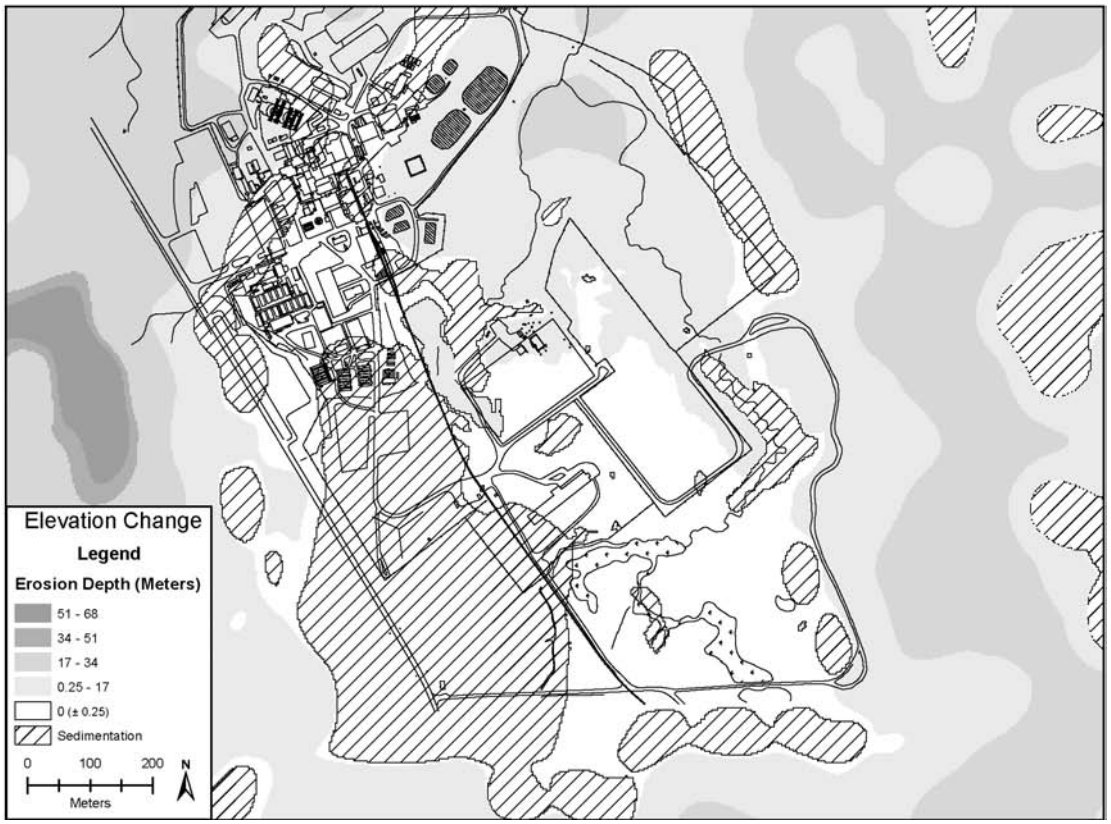

Figure F–27 Results of CHILD SP Wet + Fast Creep No Action Case

F.3.1.6.8 Results: Sitewide Close-In-Place Scenario, North Plateau

There are subtle but meaningful differences between the sitewide close-in-place runs and their no action counterparts. These differences result solely from the effect of the burial-mound structure on the runoff flow paths, and they serve to illustrate the sensitivity of gully networks to upstream topography. In NPTstd (**Figure F–28**), the behavior of the valley bottoms is quite similar to NPstd. However, where NPstd produced one large gully in the northeast, NPTstd generates two: one an approximately 200-meter (656.17-foot) extension of the present NP-2 gully, and the other to the north. The first of these is the longest, and it reaches well beyond the perimeter fence. Both gullies show maximum erosion depths between 8 and 12 meters (26.25 and 39.37 feet). A third small gully forms north of the Main Plant Process Building extending a few tens of meters beyond the site perimeter road.

Scenario NPTa1 (**Figure F–29**) shows patterns similar to NPTstd, with gullies to the northeast and north of the Main Plant Process Building, but with generally less overall erosion. Notably, the NP-1 gully is not active in this scenario, and its lower reach becomes a site of net deposition.

The NPTa2 simulation (**Figure F–30**) shows net incision along most of Franks Creek and lower Erdman Brook. The existing NP-2 gully deepens and extends approximately 200 meters (656.17 feet) into the plateau. The NP-1 gully deepens somewhat but does not significantly extend. A gully on the northwest rim, south of NP-1, advances about 130 meters (426.51 feet) toward the high-level radioactive waste tanks and the Main Plant Process Building. Several other gullies form or grow from existing gullies along the northeast and northwest rims.

The NPTa3 scenario (**Figure F–31**) is broadly similar to NPTa2, but with more extensive erosion. The NP-2 gully broadens and extends to the perimeter road. The NP-1 gully also extends headward to the perimeter road. A second gully on the western side extends toward, but falls about 100 meters (328.08 feet) short of the high-level radioactive waste tank area.

Scenario NPTa4 (**Figure F–32**), like several of the others, shows incision along Quarry Creek and lower Franks Creek, but general stability around upper Franks Creek, with height changes (both erosion and deposition) under 10 meters (32.81 feet). The largest gully (over 12 meters (39.37 feet) of erosion) forms at the northeast end of the plateau, while NP-1 deepens between 4 and 8 meters (13.12 and 26.25 feet). Rim widening along the northwest edge undermines the perimeter road.

Not surprisingly, the NPTwet scenario (**Figure F–33**) shows much more intense erosion in and around the North Plateau. Incision occurs along all of the stream valleys bounding the plateau. The plateau is bisected by the growth of a very large gully that begins near the site of present-day NP-2 and extends several hundred meters into the plateau, reaching to roughly 120 meters (393.70 feet) from the process plant. At the same time, a shorter but deeper gully along the western edge comes very close to the foot of the burial structure, between 100 and 150 meters (328.08 and 492.13 feet) from the Main Plant Process Building. This gully appears to be fed by flow diverted around the burial mound to the west. Overall, the plateau rim undergoes considerable retreat, with additional large gullies forming along both the northeast and southeast margins.

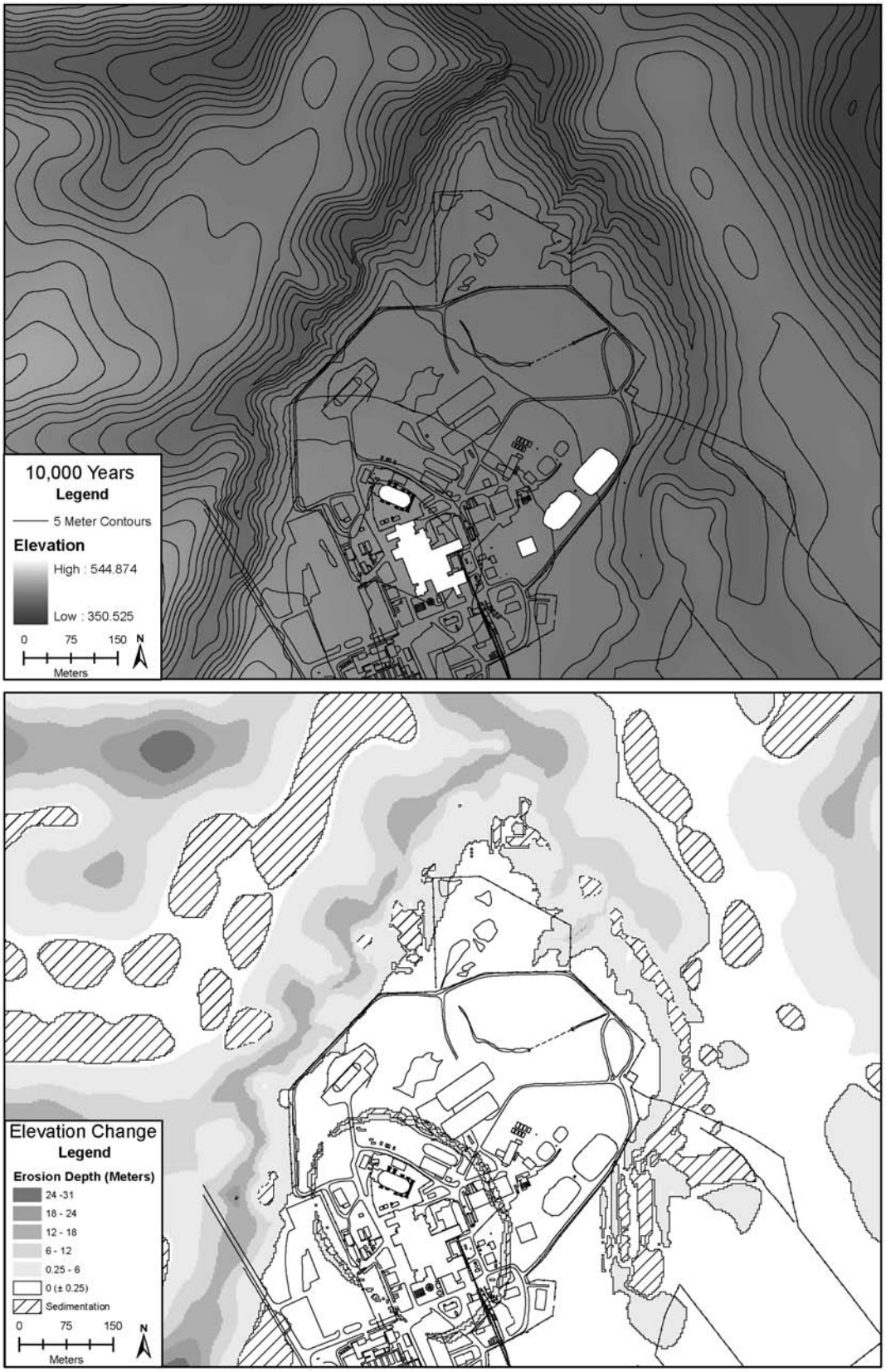

Figure F–28 Results of CHILD North Plateau Tumulus Standard (NPTstd) Sitewide Close-In-Place Case

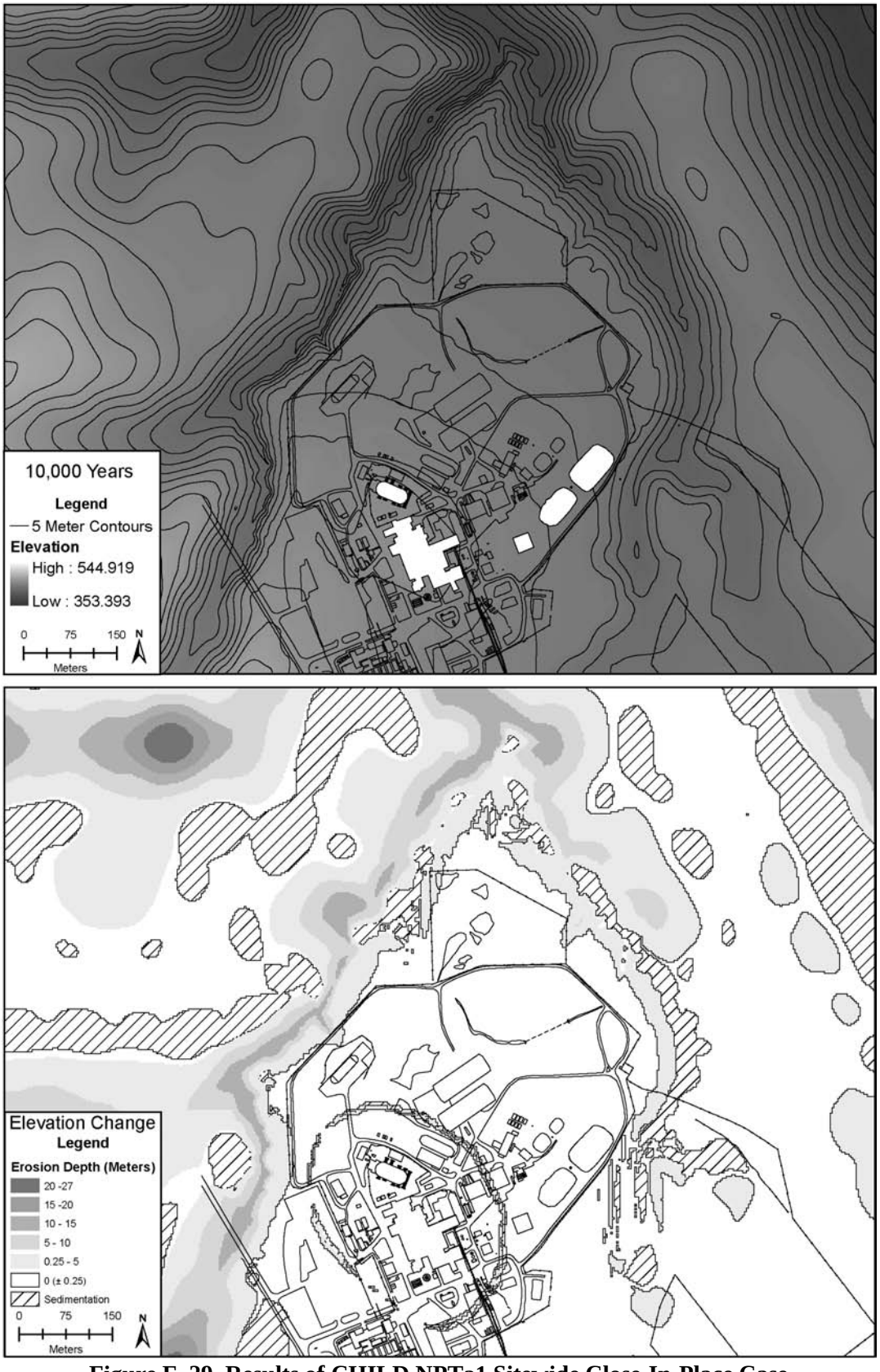

Figure F–29 Results of CHILD NPTa1 Sitewide Close-In-Place Case

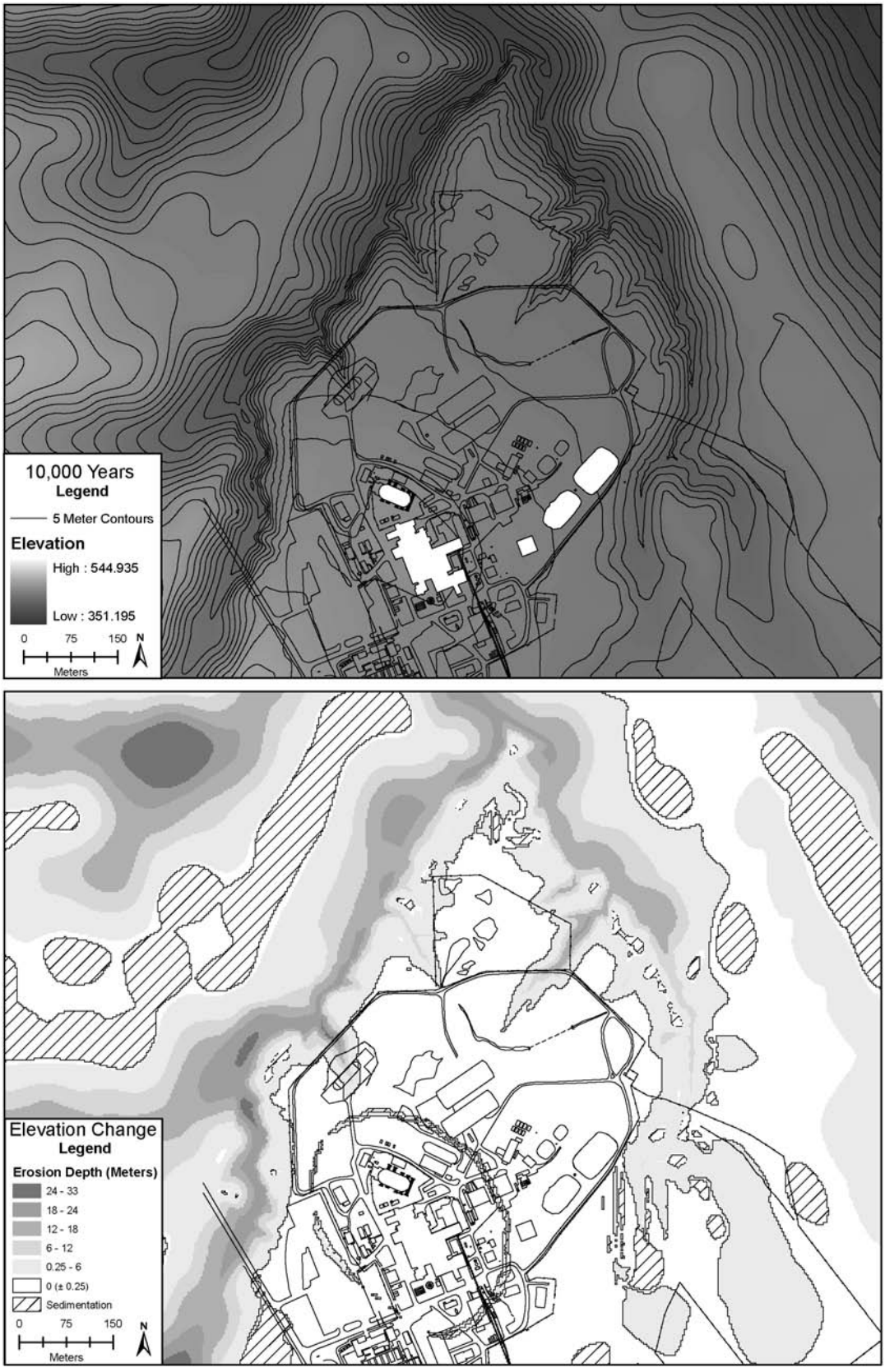

Figure F–30 Results of CHILD NPTa2 Sitewide Close-In-Place Case

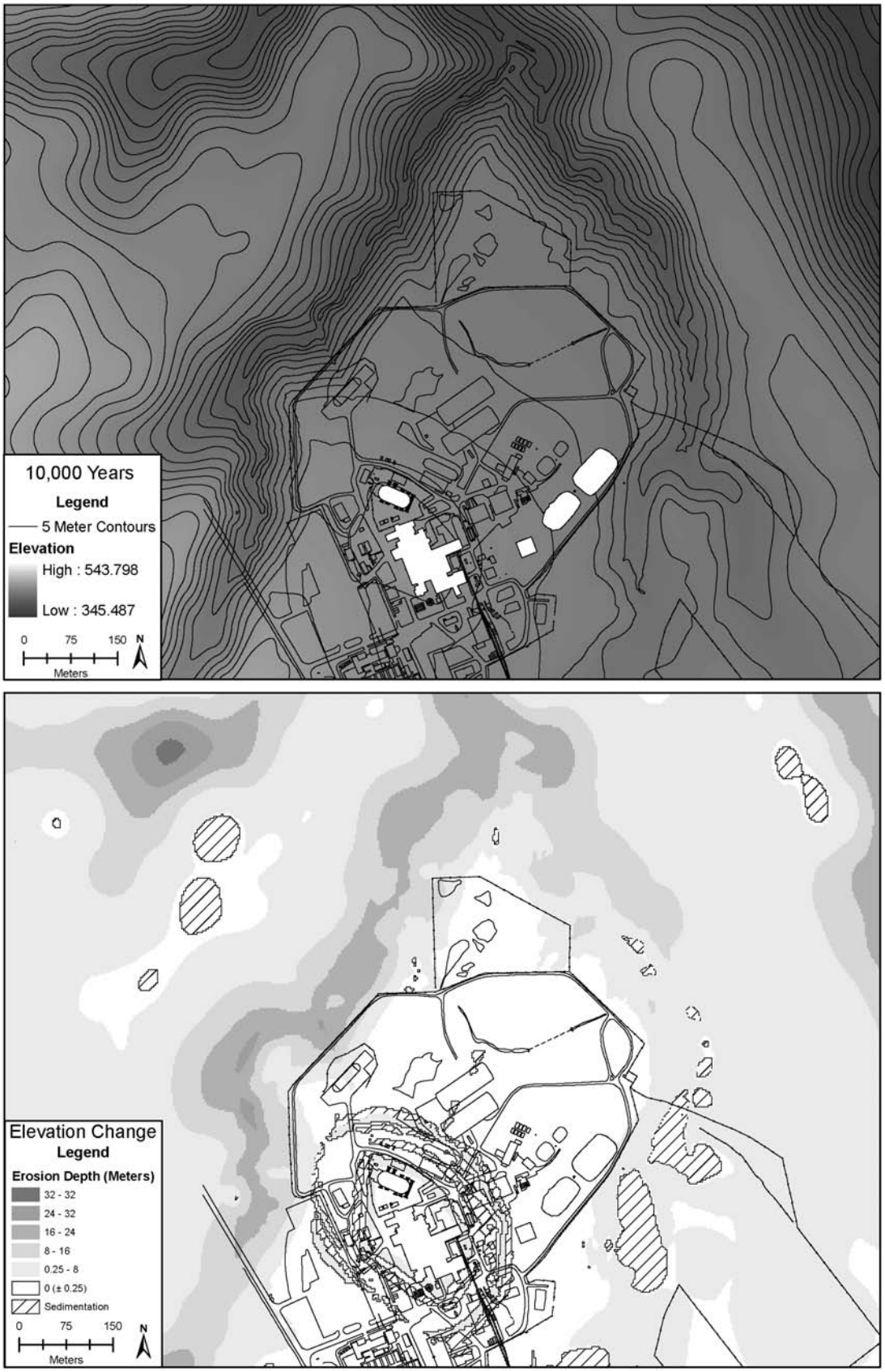

Figure F–31 Results of CHILD NPTa3 Sitewide Close-In-Place Case

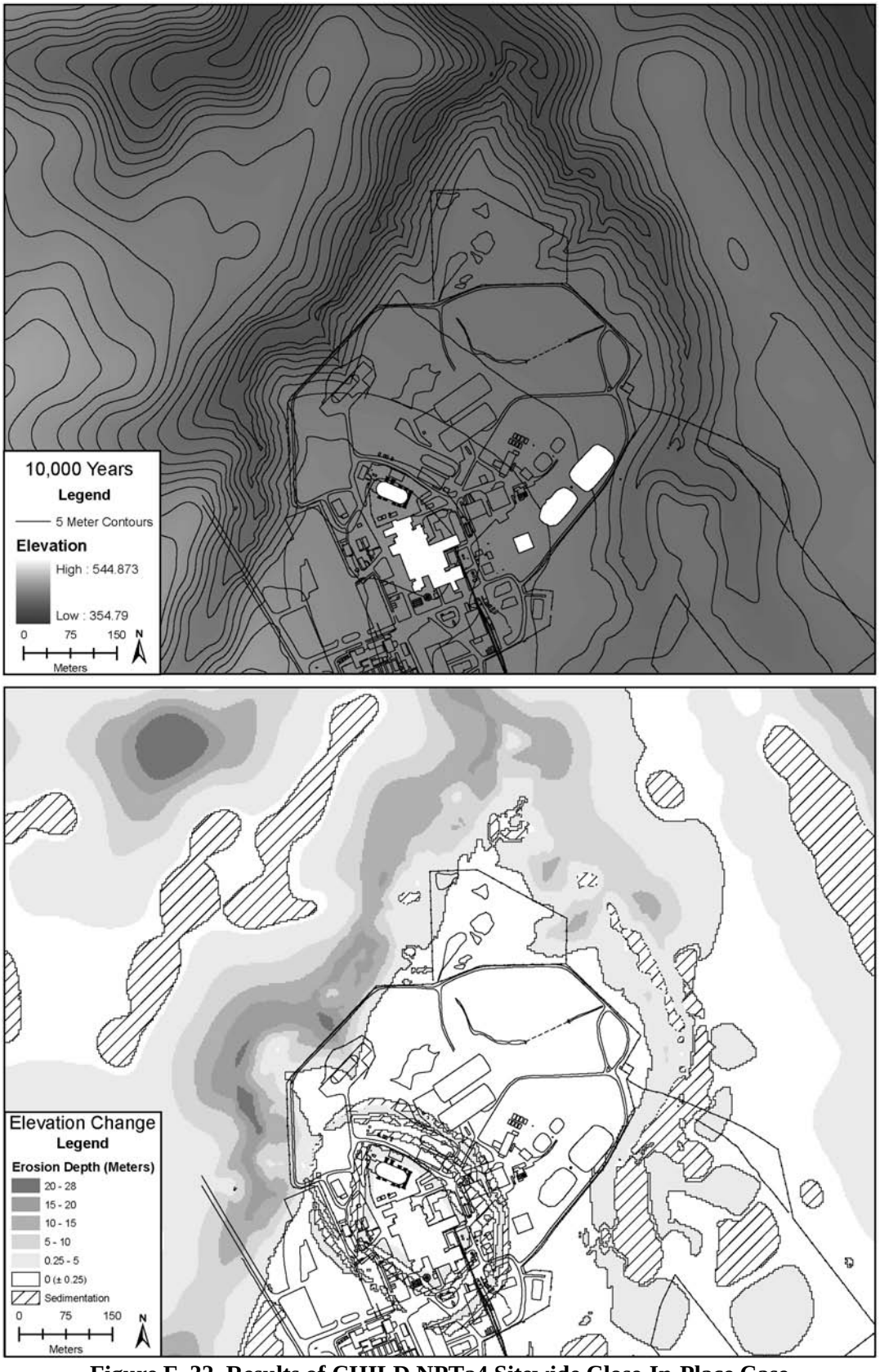

Figure F–32 Results of CHILD NPTa4 Sitewide Close-In-Place Case

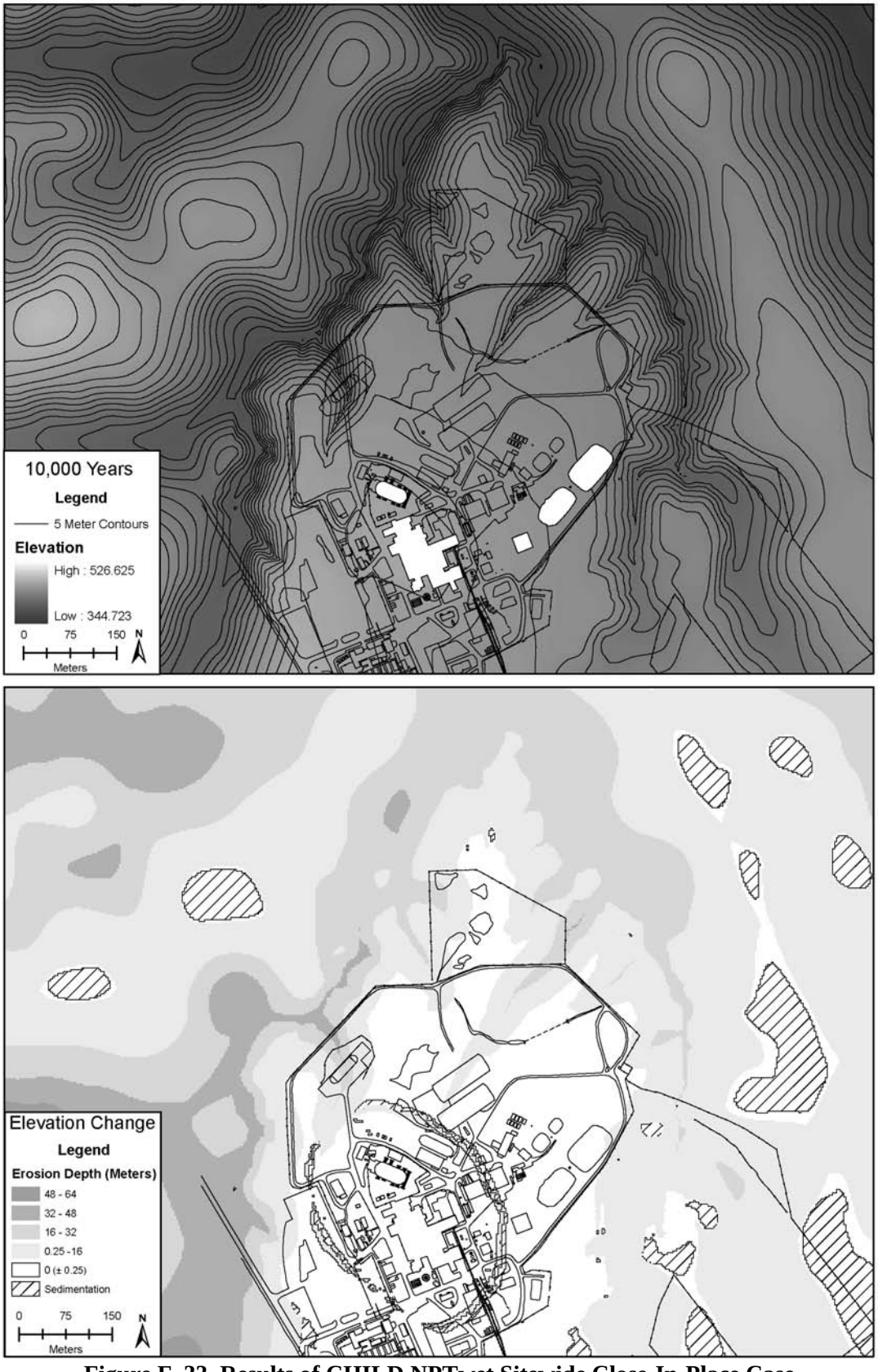

Figure F–33 Results of CHILD NPTwet Sitewide Close-In-Place Case

F.3.1.6.9 Results: Sitewide Close-In-Place Scenario, South Plateau

South Plateau erosion depths tend to be slightly higher under the sitewide close-in-place scenario, simply because the burial mounds add relief to the landscape. The SPTstd run (**Figure F–34**) shows erosion of less than half a meter around the edges of the two mounds, while the NDA gully undergoes aggradation as a result from sediment derived from the mounds. Upper Franks Creek remains essentially stable in this scenario. The pattern is similar but with reduced magnitudes in SPTa1 (**Figure F–35**). Hillslope erosion in SPTa2 (**Figure F–36**) is similar to SPTstd and SPTa1, while net valley incision occurs around the Erdman Brook–Franks Creek confluence depths on the order of 5 meters (16.40 feet), locally up to approximately 13 meters (42.65 feet). Net valley incision extends about halfway up the east flank of the SDA. Scenarios SPTa3 (**Figure F–37**) and SPTa4 (**Figure F–38**) show slightly higher levels of erosion around the mound rims, but overall erosion depths remain low (less than 1 meter [3.28 feet]).

The SPTwet scenario (**Figure F–39**) shows incision along upper Franks Creek in a pattern similar to SPwet, but the burial mounds remain quite stable. The SPTwc (Wet + Fast Creep) scenario (**Figure F–40**), by contrast, shows erosion depths of up to 4 meters (13.12 feet) at the north end of the SDA. The NDA gully undergoes aggradation.

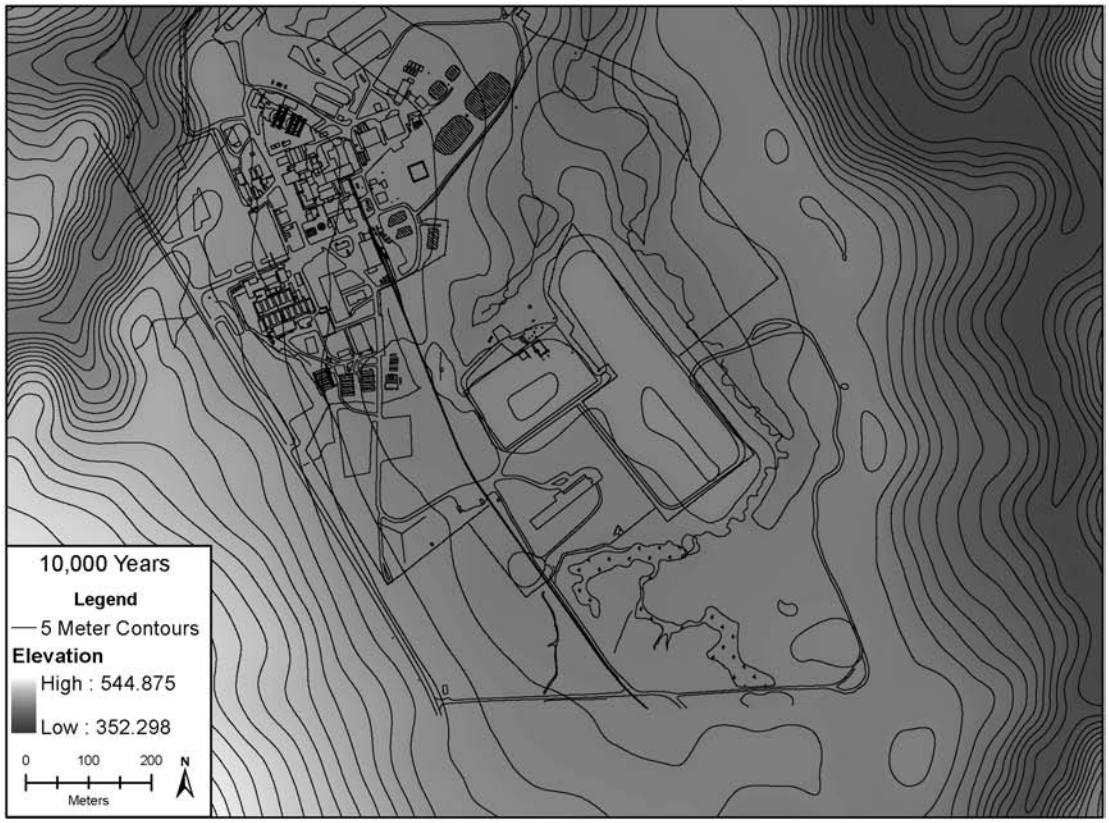

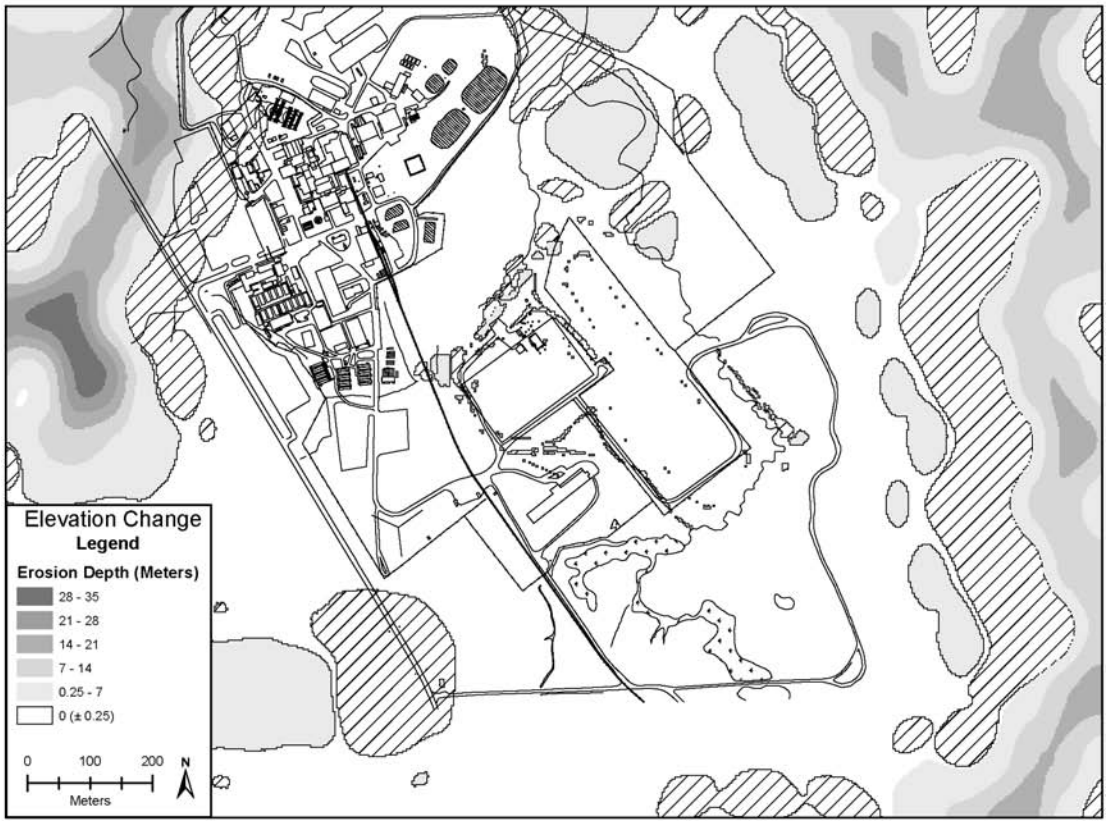

Figure F–34 Results of CHILD South Plateau Tumulus Standard (SPTstd) Sitewide Close-In-Place Case

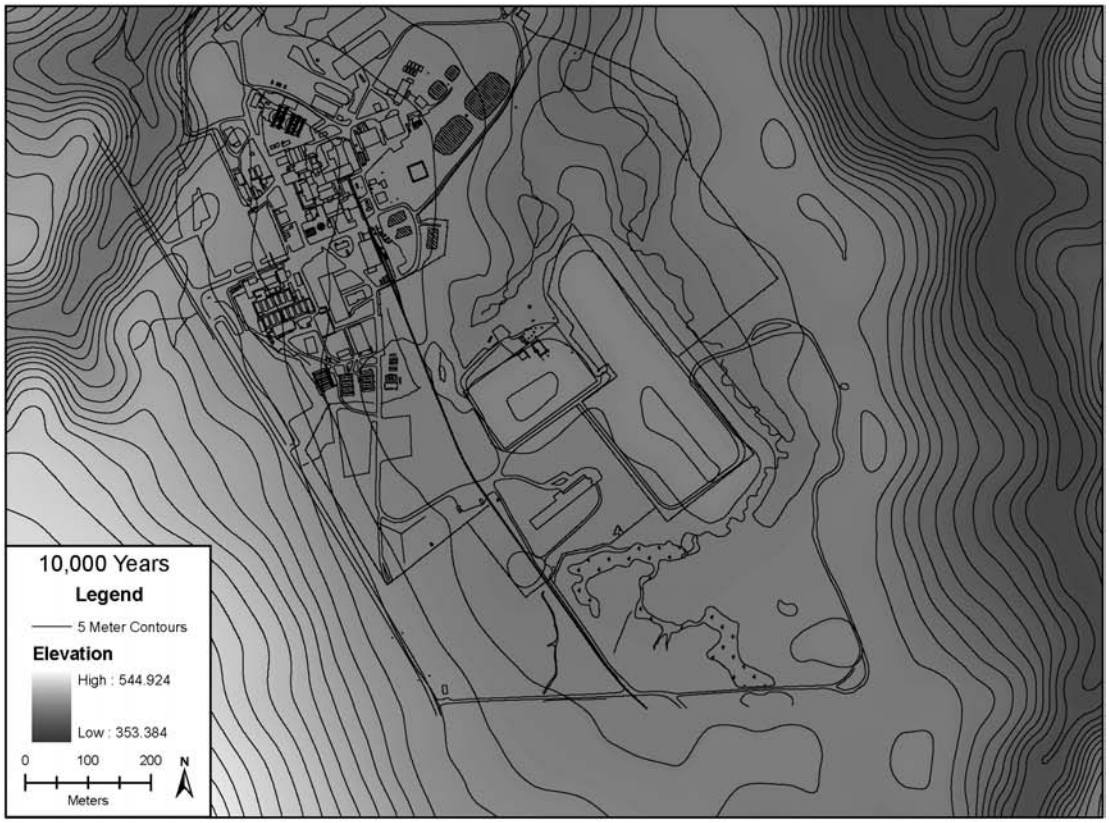

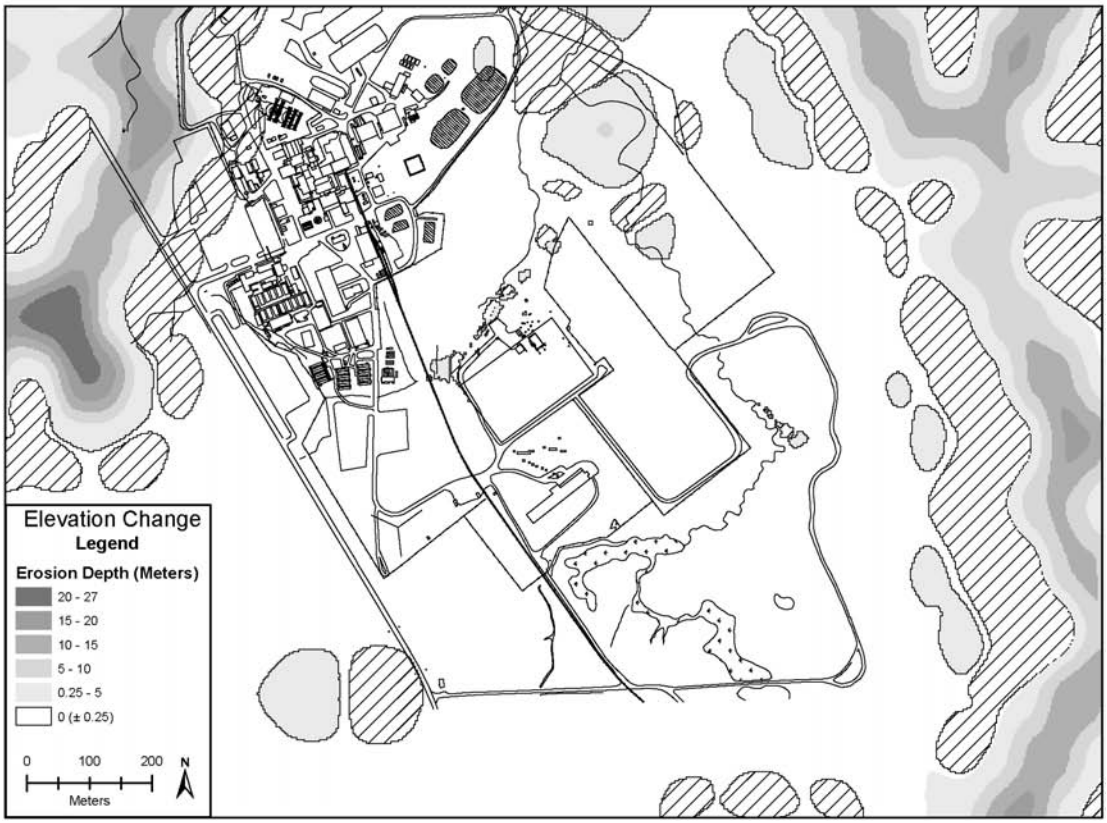

Figure F–35 Results of CHILD SPTa1 Sitewide Close-In-Place Case

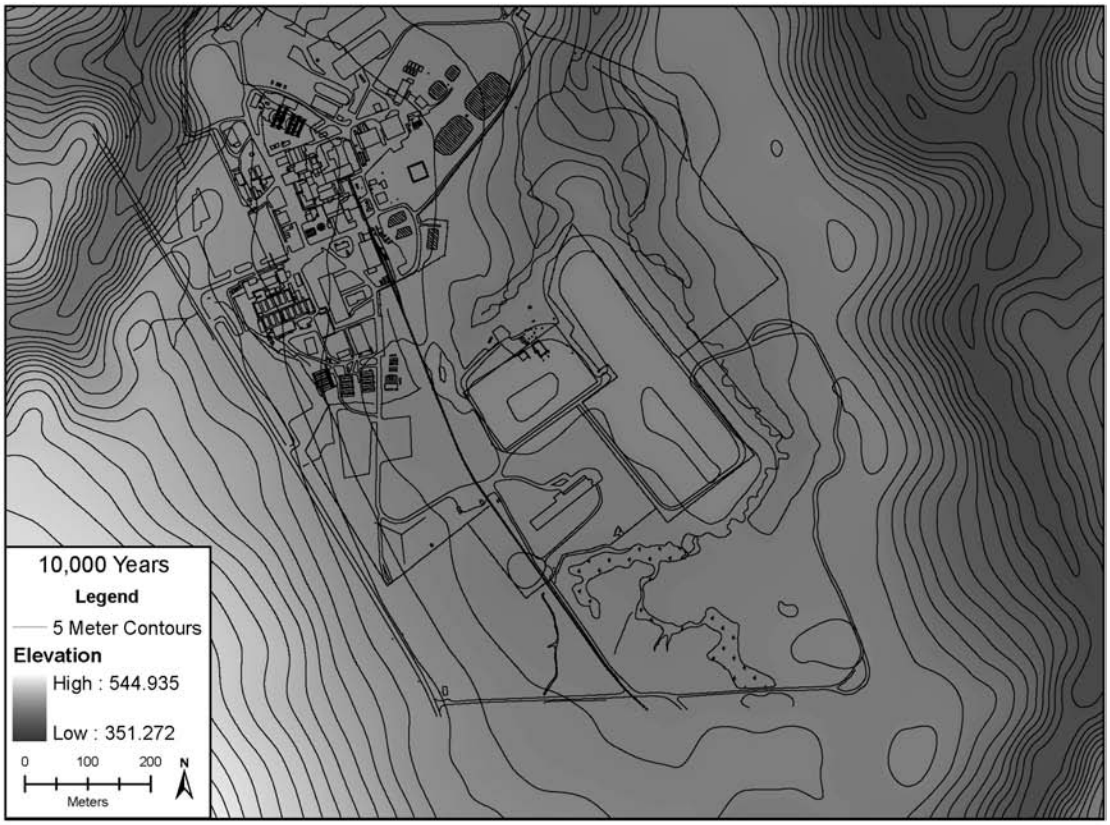

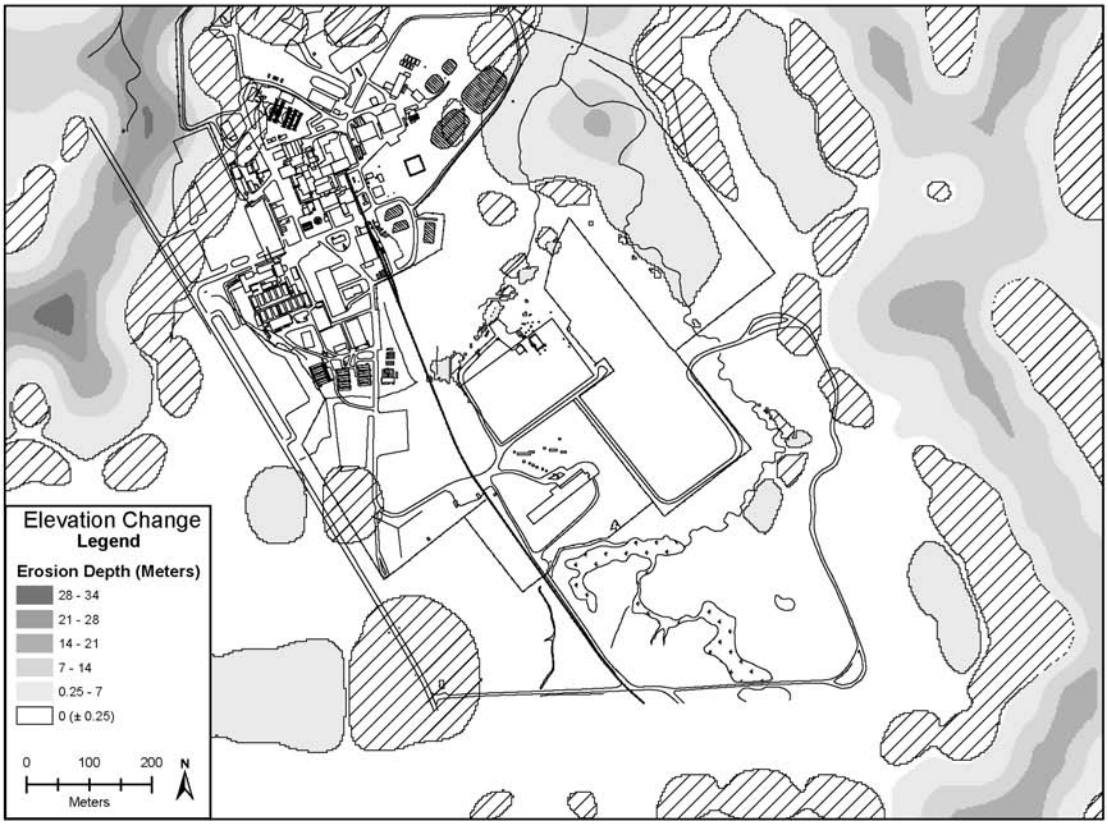

Figure F–36 Results of CHILD SPTa2 Sitewide Close-In-Place Case

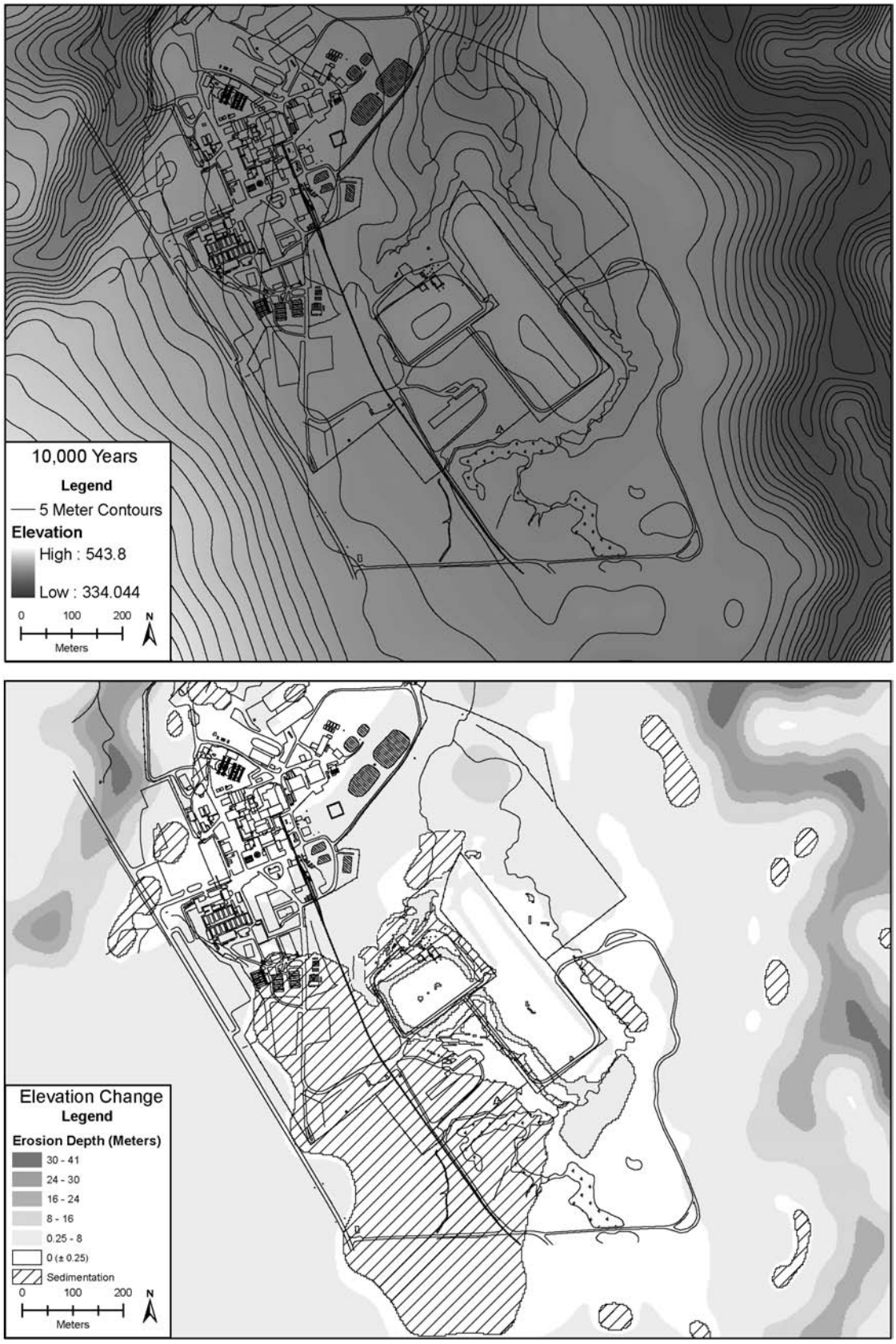

Figure F–37 Results of CHILD SPTa3 Sitewide Close-In-Place Case

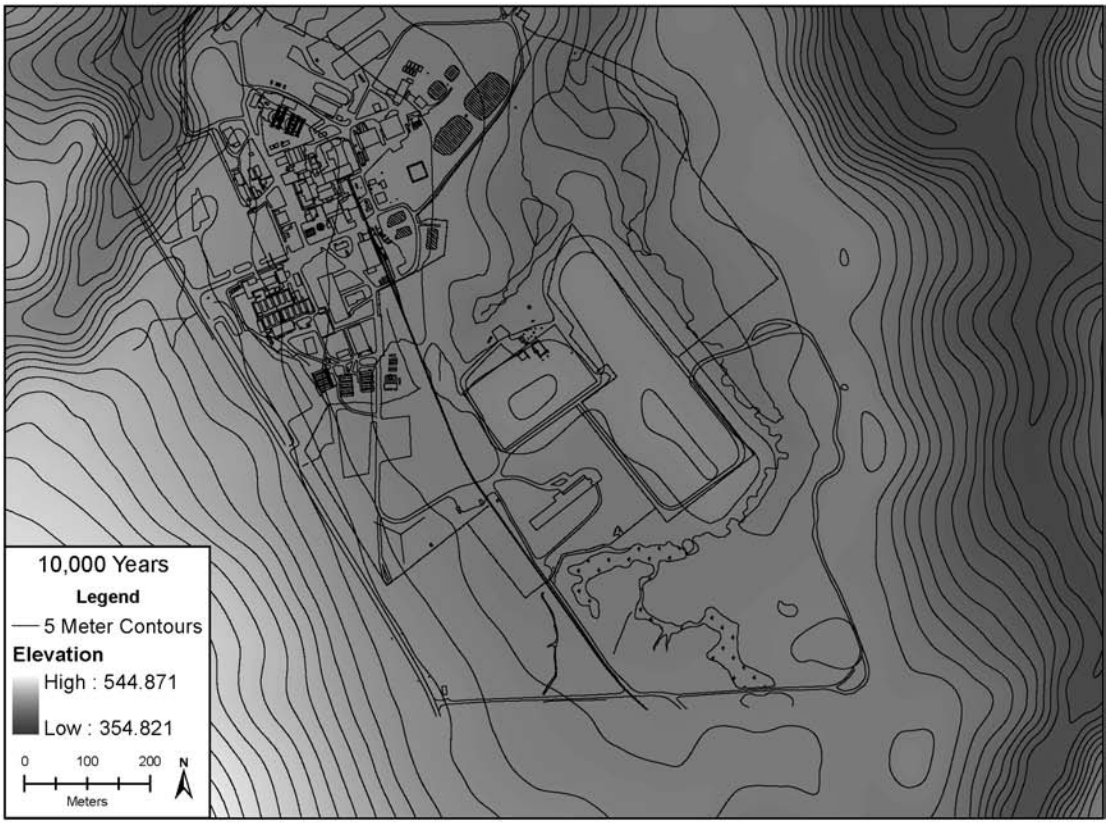

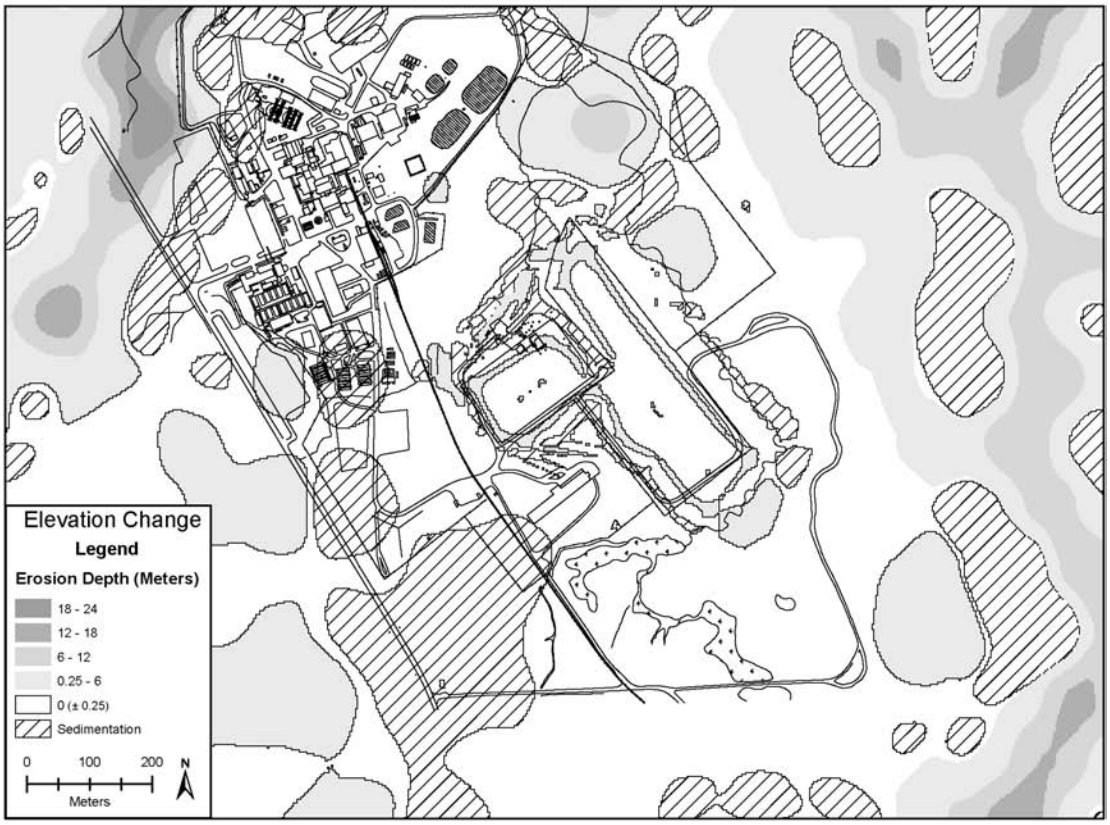

Figure F–38 Results of CHILD SPTa4 Sitewide Close-In-Place Case

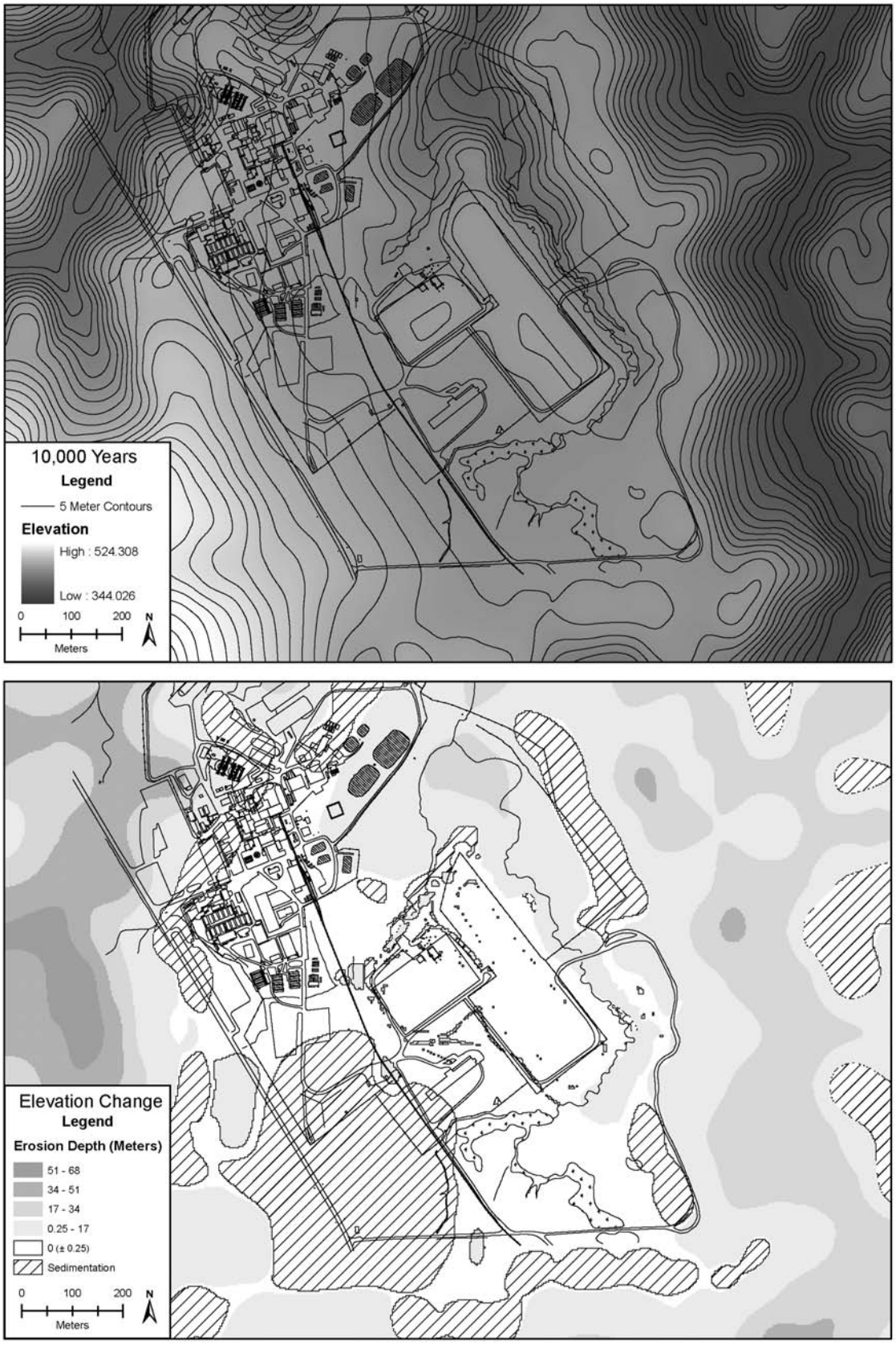

Figure F–39 Results of CHILD SPTwet Sitewide Close-In-Place Case

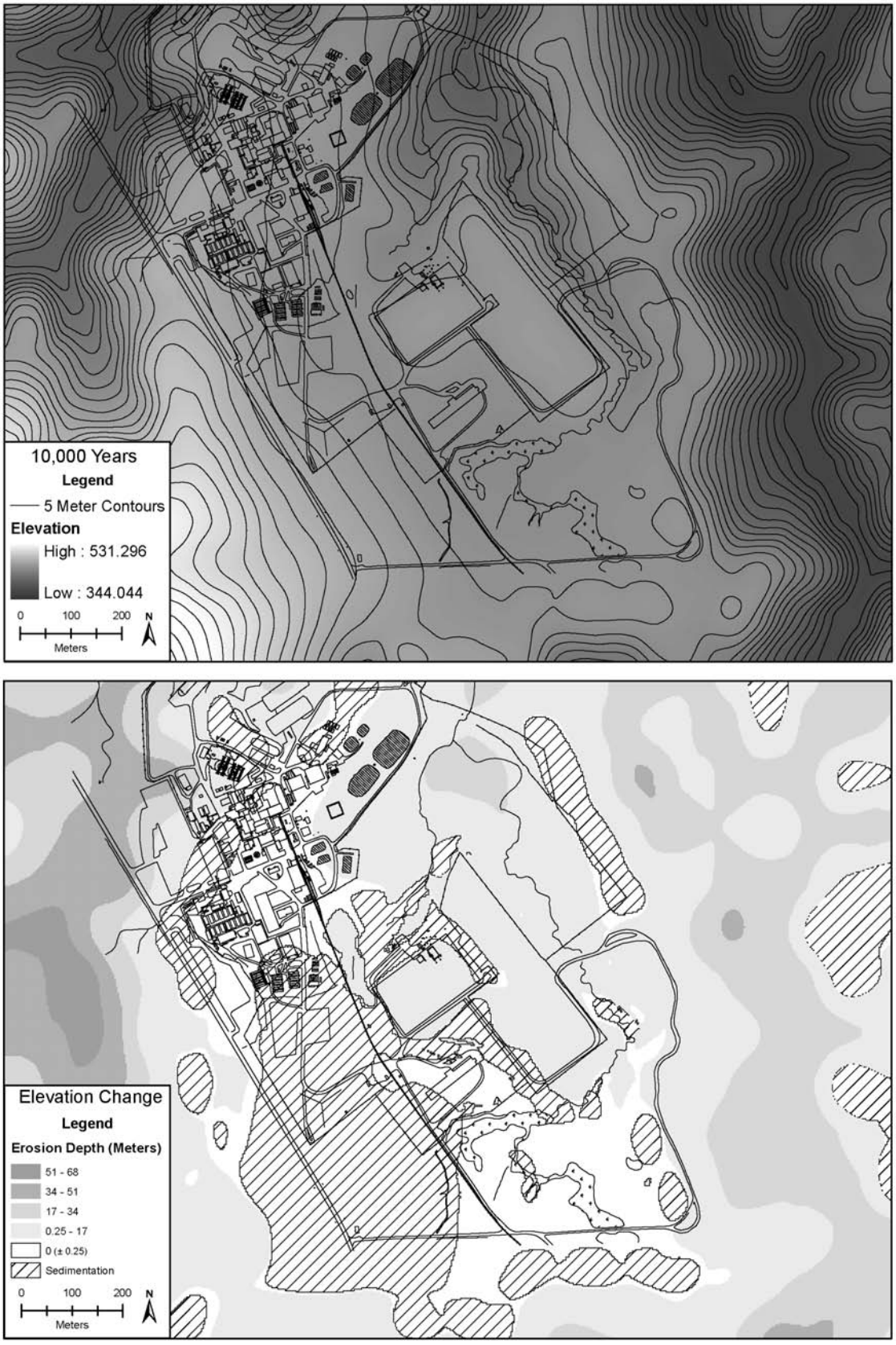

Figure F–40 Results of CHILD SPTwet + Fast Creep Sitewide Close-In-Place Case

F.3.1.6.10 Comparison with Present-Day Features and Processes

The simulations replicate many of the erosional processes and patterns observed in the present-day landscape. All simulations show some degree of gully growth around the North Plateau. The results therefore support the view that the propagation of gullies from the plateau rims represents a potential erosional threat to the site. Rates of modeled gully propagation appear to be consistent with onsite observations. During the first 100 simulation years, typical propagation rates for the largest or fastest simulated gullies are on the order of tens of centimeters per year (averaged over 100 years). This agrees with documented modern gully growth rates discussed in Section F.2.3.3. The simulations are also consistent with observed erosion along rim edges by mass movement processes driven by stream incision. The simulated rapid incision along Quarry Creek is also consistent with present-day behavior. For middle Quarry Creek, the incision rates in the area mapped as till in the model may be considered maxima, because the model does not account for the exposure of bedrock along the middle portion of Quarry Creek. The model is also consistent in predicting significant incision along the reach of Franks Creek between the junctions with Quarry Creek and Erdman Brook.

The biggest discrepancy between the model calculations and observations of present-day erosional activities concerns stream incision in the area around and upstream of the confluence of Erdman Brook and Franks Creek. Onsite observations and previous geomorphic studies (WVNS 1993a) indicate that the reach of Franks Creek between the Quarry Creek confluence and the security fence (just below the Erdman Brook–Franks Creek junction) is actively incising. Above the Erdman Brook confluence, a knickpoint divides an actively incising reach from a flat, marshy stretch with a U-shaped profile. Thus, to be consistent with present-day morphology, a simulation should produce net incision along the reach of Franks Creek downstream of the knickpoint east of the SDA. Model calculations in the A2 scenario are consistent with this pattern, showing a transition from net incision near and above the Franks Creek–Erdman Brook confluence to a generally stable profile upstream. Scenario A3 is similar to A2 in this regard. The Wet scenario predicts the greatest depth and extent and incision in the Franks Creek–Erdman Brook confluence area, with net incision depths along the northeast and northwest sides of the SDA/NDA on the order of 10 to 20 meters (32.81 to 65.62 feet) and locally reaching approximately 25 meters (82.02 feet). Other scenarios, however, show stability of the valley network in the Franks Creek–Erdman Brook confluence area, with some reaches undergoing net deposition and others net incision, all generally less than 10 meters (32.81 feet). Thus, scenarios A2, A3, and Wet are the most consistent with present-day stream incision/deposition patterns.

F.3.1.6.11 Discussion of Forward Modeling Results

There are three general categories of potential outcome that might arise from a study like this. First, one might find that under virtually all sets of scenarios and assumptions, the burial areas are prone to rapid erosional exhumation. Alternatively, one might find that nearly all scenarios point toward long-term future stability against erosion. Finally, one might obtain a more ambiguous result in which some scenarios show a significant erosional threat, and others do not. The results from this study contain elements of both the second and third outcomes. None of the scenarios showed large-scale erosional exhumation of the Main Plant Process Building, NDA, or SDA. However, the Wet scenario and its variations suggest a potential for exposure under certain conditions.

Under the No Action Alternative for the South Plateau, simulations of the Wet scenario show formation of a north-trending gully, approximately 200 meters (656.17 feet) long and up to 6.8-meters (22.31-feet) deep, along the margin between the SDA and NDA. This feature also appears under the "Wet + Fast Creep" scenario; in this case, it is shallower thanks to accelerated sediment contributions from the side slopes. This South Plateau gully disappears under the Sitewide Close-In-Place Alternative because (1) its source of water (i.e., catchment area) is reduced as runoff is diverted southward by the burial mounds, and (2) the NDA–SDA boundary strip receives considerable sediment input from the mounds. This calculation should be analyzed

with some caution, however, because it assumes that the mound material is equivalent to typical soil in terms of susceptibility to slope transport. With mound material that is more resistant to erosion and transport, as intended, one would expect less infilling, and possibly net incision, along the NDA–SDA boundary in the sitewide close-in-place scenario.

Apart from gully incision along the NDA–SDA boundary, all scenarios produced relatively little erosion on the South Plateau. The relative lack of computed erosion on the South Plateau may seem surprising, but it appears to be a robust outcome of the modeling. The absence of significant gully erosion along the SDA rim in the simulations, even under the Wet scenario, reflects the restricted surface drainage area available to feed gullies. All of the scenarios, to varying degrees, point toward continued incision of the North Plateau by gullies growing inward from the rim. Not surprisingly, the most extreme gully incision occurs under the Wet sitewide close-in-place scenario. In this scenario, the North Plateau is heavily dissected by several very large gullies extending from the north and west (Figure F–30). While none of these breach the proposed containment mound over the Main Plant Process Building, two of them come close: the tip of the western gully approaches within about 80 meters (262.46 feet) of the high-level radioactive waste tanks, while the tip of the northern gully comes within about 120 meters (393.70 feet).

How realistic is the Wet scenario? Its likelihood as a future-climate scenario is very difficult to quantify, simply because a great deal of uncertainty surrounds future-climate projections (particularly concerning rainfall). Yet one can ask first how representative it may be of modern conditions. The fact that this scenario is consistent with observed erosion around the Franks Creek–Erdman Brook confluence (more so than some of the other cases) suggests that it may be a closer representation of onsite conditions than the unrealistically high rainfall intensity might suggest. One weakness of the model in general is that it treats all soils as hydrologically uniform. Thus, the estimates of effective infiltration capacity discussed previously essentially lump together soils from across the catchment. Evidence from runoff records (Table F–9) suggest that the effective runoff coefficient in the Franks Creek watershed may be higher than that for Buttermilk Creek as a whole, presumably due to a higher proportion of low-permeability, till-derived soils. For this reason, the low infiltration capacity used in the Wet scenario may be a better match for the Franks Creek drainage, particularly in the South Plateau area, than the higher values obtained in the calibration process (with the exception of A1, shown in Table F–11 as Run 321). Thus, while the Wet scenario may be unlikely, it should not be considered implausible.

Another important finding from the forward simulations is variability in the positions and rates of gully growth. Although the overall rates of simulated erosion are robust, the locations of particular gullies are highly sensitive to small variations in parameter values and initial topography. For example, some of the North Plateau scenarios show the NP-2 gully growing substantially, while in other cases the NP-1 gully is more active. These differences reflect variations in the small-scale drainage patterns across the plateau surface. They are consistent with previous studies of drainage-network simulation models, which indicate that the details of a drainage-network pattern forming on a low-relief surface are sensitive to small variations in topography (Ijjasz-Vasquez et al. 1992). This implies that gully positions should be seen as subject to uncertainty. The model simulations indicate which locations along the rim have a high potential to seed large gullies (clearly, the three existing NP gullies have this potential), but they cannot tell us which of these sites will actually develop into a major geomorphic feature.

Finally, the simulation results should be interpreted with caution, for at least two reasons. First, the use of the constant climate assumption in the calibration process adds an unknown degree of uncertainty to the forward projections. It is possible that the postglacial climate was, on average, less erosive than the present-day climate (involving, for example, less total rainfall, less-intense rainfall, or vegetation conditions that would tend to inhibit runoff). If this were the case, then the calibrated model would tend to underestimate erosion rates under the present climate. On the other hand, it is also possible that the past climate was effectively more erosive

than the present climate (involving, for example, more-sparse vegetation cover and greater runoff rates in the early postglacial period). If this were true, then the calibrated model would tend to overestimate actual erosion rates. Second, uncertainty is introduced by the use of spatially homogeneous parameters, and in particular the soil infiltration capacity. Use of a homogeneous infiltration capacity means that the model may tend to underestimate runoff in relatively impermeable soils, such as those on the South Plateau, and overestimate runoff on relatively permeable areas, such as the upper headwaters of Franks and Quarry Creeks. These considerations form part of the rationale for introducing the Wet scenarios, which use quite a low value for infiltration capacity (as discussed in Section F.3.1.4.5). In effect, these scenarios can be seen as addressing not only the possibility of a future shift toward a more-erosive climate, but also the risk that the present climate/soil conditions at the site *are already* effectively more erosive (by a factor of more than two) than the calibrated model would suggest, because of possibly inaccurate assumptions in the calibration. In particular, while the Standard and Alternate scenarios are considered to be the most likely projections, the Wet scenario is considered a plausible representation of *either* an erosive future-climate state *or* an effectively more-erosive present-day environment due to a potential climate drift over the late-glacial to Holocene period and/or a potential overestimation of soil permeability in the calibration procedure.

F.3.1.6.12 Potential for Stream Capture

Stream capture occurs when headward or lateral growth drives one stream to intersect another, higher elevation stream, whose flow is then diverted (captured) into the lower elevation stream. Because the bed of Franks Creek lies at a higher altitude than the adjacent Buttermilk Creek Valley, there is a potential for capture either by gullies growing along the western edge of the Buttermilk Creek Valley, or by lateral erosion on Buttermilk Creek. The altitude of Franks Creek at the eastern corner of the SDA is approximately 414 meters (1,358.27 feet). The altitude of the closest reach of Buttermilk Creek, about 400 meters (1,312.34 feet) to the east, ranges from 375 to 381 meters (1,230.31 to 1,250.00 feet). Thus, there is a height difference between the two drainages of up to 40 meters (131.23 feet). Given the distance, capture would require either westward extension of a gully 400 meters (1,312.34 feet) from the Buttermilk Creek Valley, or lateral erosion over that distance, or a combination of the two. The likelihood of capture is difficult to assess definitively with a model like CHILD because the forward simulations did not account for lateral channel erosion. Nonetheless, the model results shed some light on the feasibility of capture. The large gully in the NPTwet scenario is long enough that, were it to have grown from the Buttermilk Creek Valley in the right place, capture might have occurred. However, that particular feature grew as far as it did because it was able to capture a substantial fraction of the drainage area on the North Plateau early in its evolution. The available drainage area for gullies feeding the Buttermilk Creek Valley southeast of the site appears to be far smaller. There may be a potential threat from the unnamed drainage that crosses Rock Springs Road just south of the intersection with Thornwood Drive. Currently, that drainage is diverted southward by the rail embankment into a pond. If the drainage were diverted northward, there is the possibility that it could either join with and accelerate one of the east-draining gullies, or join upper Franks Creek and accelerate incision. However, neither diversion toward Franks Creek, nor capture of Franks Creek by Buttermilk Creek, was observed in any of the 25 forward model runs. Furthermore, there is no obvious evidence for similar capture events elsewhere along Buttermilk Creek Valley. It is concluded therefore, that while capture cannot be ruled out, it is unlikely to occur over the performance-critical period unless climate or other factors change significantly.

F.3.2 Verification of Landscape Evolution Modeling Results – Short-term Modeling Studies

This section presents available, relevant, short-term erosion predictions that were made before the current long-term erosion modeling effort was initiated. The models were used to predict individual erosion processes, such as channel downcutting and sheet and rill erosion. They are included in this section to provide perspective by which to judge the reasonableness of the CHILD landscape evolution modeling results.

F.3.2.1 Short-term Sheet and Rill Erosion Prediction

Four methods were used to predict the sheet and rill erosion rate at WNYNSC. First, the Universal Soil Loss Equation (USLE) was used to predict the average annual soil loss from individual subwatershed areas that collectively represent the Franks Creek, Erdman Brook, and Quarry Creek watershed (referred to as the "Franks Creek watershed"). Second, the SEDMOT [Sedimentology by Distributed Model Treatment] II model was run to account for soil loss that occurs during major storm events within the same subwatershed areas. Third, the CREAMS [Chemicals, Runoff, and Erosion from Agricultural Management Systems] model was used to predict the average annual sediment yield from a small portion of the South Plateau. And fourth, the WEPP model was run to predict the sediment yield that occurs during major storm events as well as the average annual sediment yield from the hillslopes within the Franks Creek watershed.

Universal Soil Loss Equation

The USLE is an empirically derived relationship developed to predict soil loss rates for agricultural conditions. The empirical equation is the product of six major factors that utilize the quantity of rainfall, length and average gradient of the slopes, type of soil, and type of soil cover (e.g., forest, grass, bare soil). It predicts soil loss caused by overland flow from the point of origin to a channel (Weltz et al. 1992) and does not simulate soil deposition or gully and channel erosion (Foster 1982).

The USLE equation is:

$$A = R \times K \times LS \times C \times P$$

where:

A is the potential long-term average annual soil loss in metric tons per hectare per year.

R is the rainfall and runoff factor by geographic location. The greater the intensity and duration of the rainstorm, the higher the erosion potential. The runoff factor takes into account the variation in land use conditions.

K is the soil erodibility factor. It is the average soil loss per unit area (in metric tons per hectare) for a particular soil in cultivated, continuous fallow with an arbitrarily selected slope length of 72.6 feet and a slope steepness of 9 percent. K is a measure of the susceptibility of soil particles to detachment and transport by rainfall and runoff. Texture is the principal factor affecting K, but structure, organic matter, and permeability also contribute.

LS is the slope length–gradient factor. The LS factor represents a ratio of soil loss under given conditions to soil loss at a site with the "standard" slope steepness of 9 percent and slope length of 72.6 feet. The steeper and longer the slope, the higher the risk for erosion.

C is the crop/vegetation and management factor. It is used to determine the relative effectiveness of soil and crop management systems in preventing soil loss. The C factor is a ratio of soil loss from land under a specific crop and management system to soil loss from continuously fallow and tilled land.

P is the support practice factor. It reflects the effects of practices that will reduce the amount and rate of water runoff and thus reduce the amount of erosion. The P factor represents the ratio of soil loss by a support practice to soil loss attributable to straight-row farming up and down the slope.

The USLE method was used to predict the rate of soil loss from the hillslopes within the entire Franks Creek watershed. As shown on **Figure F–41**, the Project Premises and the SDA are near the downgradient end of the 440-hectare (1,040-acre) watershed. The watershed was divided into the same 22 subwatershed areas defined in the hydrologic modeling studies conducted by Dames and Moore (WVNS 1993c) to provide consistency in the analyses. Precipitation data were obtained from the site meteorological tower for the 1-year period of March 1, 1990, through February 28, 1991 (WVNS 1993a). Soil erodibility values were based on standard U.S. Department of Agriculture grain-size classifications of each soil unit, as defined in site-specific studies (WVNS 1993a). Vegetation cover values were based on a vegetation survey of the area (WVNS 1993d). Input values for cover management factors were obtained from source document tables (Wischmeier and Smith 1978). **Table F–13** summarizes input parameters used in the USLE for each of the 22 subwatershed areas and the results.

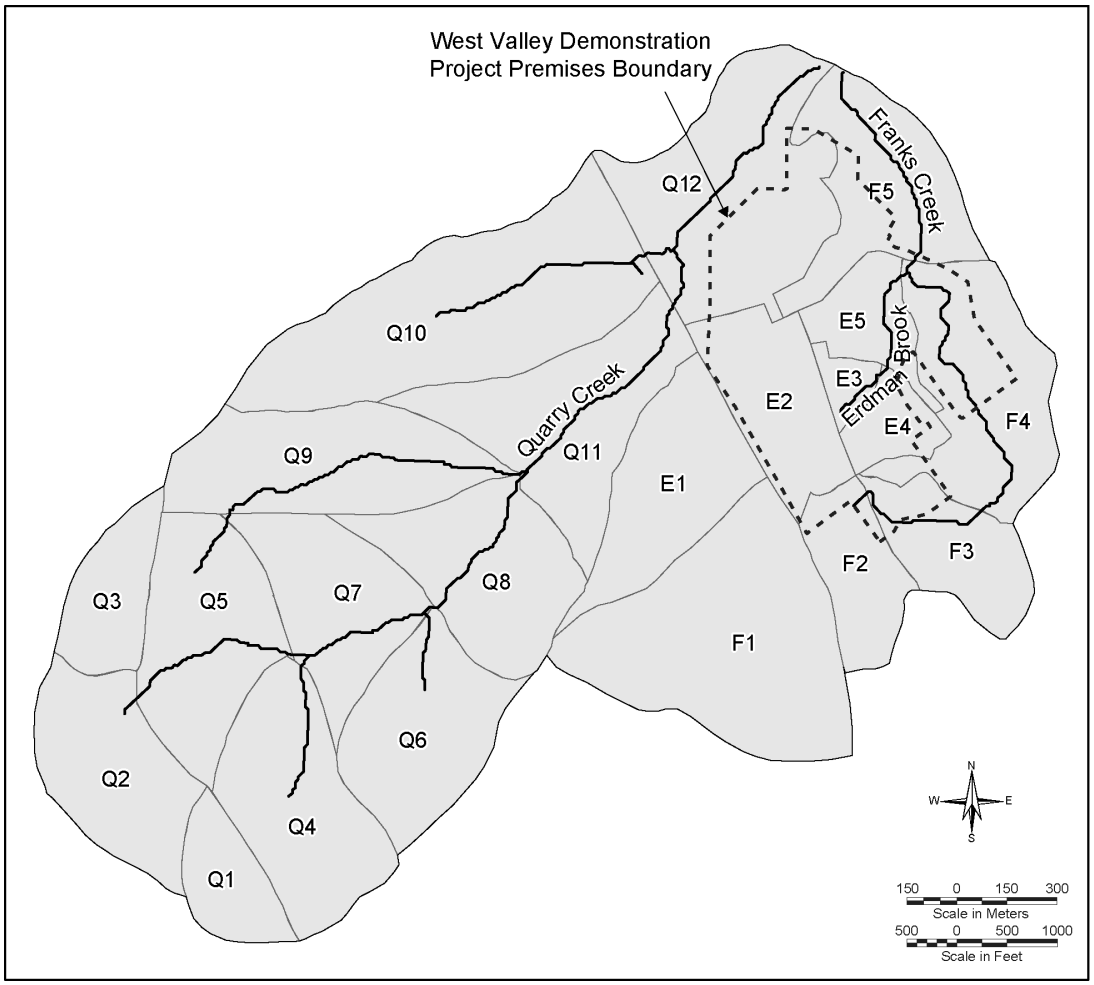

Figure F–41 USLE and SEDIMOT II Modeling Studies Subwatershed Areas

The results indicate that small quantities of soil are being removed from the hillslopes by the sheet and rill erosion process. The correlation indicates that the areas with the greatest soil loss were within the Quarry Creek drainage basin west and northwest of the Project Premises and within the Erdman Brook–Franks Creek drainage basin west and east of the Project Premises. The average soil loss for the watershed was estimated to be 0.19 metric tons per hectare (0.085 tons per acre) per year. This soil loss rate is equivalent to an average decrease in elevation of 12.8 millimeters (0.04 feet) per 1,000 years. These USLE estimates are based on only

1 year of site-specific precipitation data. USLE estimates are more accurate when applied over a period of at least 30 years, which dampens effects of isolated and unpredictable short-term fluctuations.

Table F–13 USLE Input Parameters and Results

Sub-area	*Area (hectares)*	*R (MJ × millimeters per hectare × hour × year)*	*LS*	*K (metric tons × hectares × hour / hectare × MJ × millimeter)*	*Soil Erodi-bility Factor Distr. Percent*	*C*	*P*	*Soil Loss (metric tons per hectare per year)*	*Soil Loss (metric tons per year)*
Q1	10.26	2067.33	3.2	0.0026	100	0.003	0.6	0.03	0.32
Q2	20.63	2067.33	4.3	0.0026	100	0.003	0.6	0.04	0.86
Q3	10.30	2067.33	1.8	0.0026	100	0.003	0.5	0.02	0.15
Q4	26.24	2067.33	11.0	0.0026	100	0.003	0.8	0.14	3.77
Q5	23.01	2067.33	5.0	0.0026	100	0.003	0.6	0.05	1.12
Q6	20.63	2067.33	9.1	0.0026	100	0.003	0.75	0.11	2.30
Q7	17.82	2067.33	5.8	0.0026	100	0.003	0.7	0.07	1.18
Q8	24.30	2067.33	19.2	0.0026	100	0.003	1.0	0.31	7.62
Q9	32.65	2067.33	23.4	0.0026	100	0.003	1.0	0.38	12.48
Q10	45.79	2067.33	16.9	0.0026 0.0020	90 10	0.003 0.003	0.8 0.8	0.20 0.02	9.14 0.76
Q11	26.35	2067.33	27.0	0.0026 0.0020	80 20	0.003 0.003	1.0 1.0	0.35 0.07	9.28 1.74
Q12	34.49	2067.33	3.6	0.0026 0.0020	60 40	0.003 0.003	0.55 0.55	0.02 0.01	0.66 0.34
E1	21.24	2067.33	22.5	0.0026	100	0.003	1.0	0.36	7.81
E2	12.13	2067.33	6.8	0.0026 0.0020	50 50	0.003 0.003	0.8 0.8	0.04 0.03	0.54 0.41
E3	2.99	2067.33	6.4	0.0026 0.0020	70 30	0.003 0.003	0.85 0.85	0.05 0.03	0.14 0.08
E4	6.41	2067.33	1.9	0.0026	100	0.003	0.55	0.02	0.11
E5	9.32	2067.33	1.9	0.0026 0.0020	60 40	0.003 0.003	0.55 0.55	0.01 0.01	0.07 0.06
F1	42.51	2067.33	15.1	0.0026	100	0.003	1.0	0.25	10.49
F2	12.24	2067.33	4.3	0.0026	100	0.003	0.7	0.05	0.60
F3	13.03	2067.33	1.9	0.0026	100	0.003	0.55	0.02	0.23
F4	27.58	2067.33	1.5	0.0026 0.0026	80 20	0.04 0.003	0.55 0.55	0.14 0.001	3.96 11.15
F5	23.47	2067.33	10.9	0.0026 0.0020	50 50	0.14 0	0.17 0.17	0.53 0.00	10.24 0.00

USLE = Universal Soil Loss Equation, R = rainfall and runoff factor, LS = slope length–gradient factor, C = crop/vegetation and management factor, P = support practice factor, MJ = megajoules.
Note: To convert millimeters to inches, multiply by 0.039; hectares to acres, multiply by 2.471; MJ to foot pounds, multiply by 737,562.18; metric tons to tons, multiply by 1.1.

Sedimentology by Distributed Model Treatment (SEDIMOT II)

The quantity of sheet and rill erosion during major storm events was estimated using the SEDIMOT II surface erosion model (WVNS 1993a), which simulates rainfall intensity and depth over a given time period, the resulting in surface-water runoff volume, and soil volume washed from the ground surface.

For WNYNSC, four 24-hour design storms were modeled: 2-, 10-, and 100-year, and the probable maximum precipitation event, which is the maximum rainfall that could conceivably occur. The hillslopes were modeled within the entire Franks Creek watershed. The watershed was divided into the same 22 subwatershed areas defined in the USLE hydrologic modeling study to provide consistency in the analyses. The rainfall amount anticipated from each of the design storm events was taken from standardized maps developed by the Soil Conservation Service (USDA 1986) using a Type II Soil Conservation Service storm designation and rainfall depths of 6.35 centimeters (2.5 inches) for the 2-year storm, 9.4 centimeters (3.7 inches) for the 10-year storm, 13.2 centimeters (5.2 inches) for the 100-year storm, and 63.2 centimeters (24.9 inches) for the probable maximum precipitation event. Hydrologic parameters for each of the subwatershed areas shown in **Table F–14** (WVNS 1993c). Soil properties for each of the subwatershed areas were based on the geotechnical evaluation of samples from the Lavery till, Kent till, and North Plateau surficial sand and gravel unit. The particle-size distribution used for each of these soil units is also shown in Table F–14 (WVNS 1996). The soil's cover condition within each subwatershed area was specified by a general land use condition designation of forest, agricultural, or disturbed.

Table F–14 SEDIMOT II Hydrologic and Soil Input Parameters

Hydrologic Parameters				*Soil Parameters – Particle-Size Distributions*				*Sediment Yield Results*			
Sub-area	*Area (hectares)*	*SCS Runoff Curve Number*	*Time of Concen-tration (hours)*	*Particle Size (mm)*	*Kent Till (%)*	*Surficial Sand and Gravel (%)*	*Lavery Till (%)*	*2-Year Storm Event (metric tons per hectare)*	*10-Year Storm Event (metric tons per hectare)*	*100-Year Storm Event (metric tons per hectare)*	*PMP Storm Event (metric tons per hectare)*
Q1	10.24	76	0.41	19	98	88	82	0.29	0.83	1.79	31.55
Q2	20.96	76	0.59	6.4	94	73	69	0.07	0.21	0.47	8.96
Q3	10.20	74	0.21	4.8	93	67	67	0.06	0.17	0.37	7.14
Q4	25.70	73	0.41	1.9	92	54	62	0.13	0.38	0.86	16.80
Q5	23.15	74	0.56	0.82	91	50	58	0.08	0.22	0.50	9.70
Q6	21.25	73	0.41	0.42	89	47	56	0.13	0.39	0.89	17.66
Q7	17.64	71	0.58	0.15	87	43	53	0.03	0.10	0.24	5.04
Q8	25.01	71	0.51	0.075	83	42	51	0.17	0.56	1.32	27.21
Q9	33.63	70	0.54	0.03	52	32	46	0.11	0.35	0.82	18.09
Q10	46.70	68	0.50	0.02	36	27	43	0.12	0.41	1.02	23.25
Q11	27.15	72	0.52	0.011	28	21	37	0.13	0.41	0.95	19.04
Q12	33.75	77	0.49	0.006	18	14	32	0.12	0.33	0.70	11.48
E1	20.88	72	0.40	0.003	11	9	24	0.08	0.25	0.58	11.89
E2	12.10	95	0.35	0.001	1	5	14	0.09	0.17	0.30	3.46
E3	2.79	80	0.34					0.13	0.34	0.71	12.66
E4	6.39	81	0.20					0.09	0.21	0.43	7.07
E5	11.90	81	0.42					0.17	0.38	0.72	9.79
F1	43.83	67	0.37					0.07	0.24	0.60	14.24
F2	12.18	77	0.48					0.03	0.09	0.20	3.85
F3	13.23	79	0.26					0.03	0.07	0.14	2.80
F4	27.96	70	0.76					1.84	3.77	6.60	92.06
F5	23.43	67	0.52					0.07	0.19	0.41	7.67

% = percent; mm = millimeters, PMP = probable maximum precipitation, SCS = Soil Conservation Service, SEDIMOT = Sedimentology by Distributed Model Treatment.
Note: To convert hectares to acres, multiply by 2.471; metric tons to tons, multiply by 1.1; millimeters to inches, multiply by 0.039.

To predict the average annual soil loss rate, it was assumed that 500 2-year storms, 100 10-year storms, 10 100-year storms, and one probable maximum precipitation event occurred over a 1,000-year period. Thus, the average soil loss for the watershed was estimated to be 0.16 metric tons per hectare (0.07 tons per acre) per year. This soil loss rate is equivalent to an average decrease in elevation of 11 millimeters (0.04 feet) per 1,000 years. The SEDIMOT II simulation results are consistent with the USLE analysis results. As in the USLE calculations, the predicted soil erosion rate was greatest in an area of the Franks Creek–Erdman Brook basin with disturbed or insufficient ground cover. The major determinant of the erosion rate was the large number of high-frequency storms (i.e., 2- and 10-year events), not the few low-frequency storms (i.e., 100-year and probable maximum precipitation events). This conclusion is consistent with other research findings reported in the literature (Wolman and Miller 1960).

Chemicals, Runoff, and Erosion from Agricultural Management Systems (CREAMS)

The CREAMS model was used to estimate erosion rates for a portion of the South Plateau over a 1-year period (Dames and Moore 1987). The purpose of the study was to evaluate the utility of the CREAMS model in predicting surface soil–water balances and erosion rates; therefore, only a small 2-hectare (5-acre) test area was used for the simulations instead of the entire Franks Creek watershed, as shown on **Figure F–42**. Unlike USLE and SEDIMOT II, CREAMS is a physically based, distributed-parameter, continuous-simulation erosion model capable of predicting sediment yield on a field-size area. The South Plateau portion selected for the study was a gently sloping open field covered with low-to-medium grasses.

Major input parameters used in the model are shown in **Table F–15**. The simulations involved the use of daily rainfall data for a single year as recorded at the West Valley Nuclear Services (WVNS) weather station in 1984. Soil properties for the weathered till were obtained from a New York State Geological Survey study conducted at WNYNSC (Hoffman et al. 1980). When site-specific data were not available, input parameter values were estimated from the data provided in the appendices of the Soil Conservation Service model manual (USDA 1984) for conditions similar to those at the site.

The CREAMS simulations produced an estimate of sediment yield for the study area that is greater than the soil loss estimates predicted by the USLE and SEDIMOT II models. According to those simulations, the average sediment yield for the watershed is 10.3 metric tons per hectare (4.6 tons per acre) per year. This rate is equivalent to an average decrease in elevation of 690 millimeters (2.3 feet) per 1,000 years. It should be noted that the CREAMS study is extremely limited in terms of areal extent and range of precipitation conditions. The small area used in the simulations has less protective ground cover and a more-limited range of slope conditions than the balance of WNYNSC, and thus is not considered representative of the watershed as a whole. Also, the 1-year simulation period is too short a time to account for long-term fluctuations in precipitation, and thus cannot be used reliably for long-term projections.

Water Erosion Prediction Project

The WEPP model was used to predict sediment yield based on consideration of the physical processes affecting the watershed for a set of seven storms with return periods ranging from 1 to 100 years. Like CREAMS, WEPP is a physically based, distributed-parameter, continuous-simulation erosion model capable of predicting sediment yield. Unlike CREAMS, WEPP can predict sediment yield on a small-watershed scale; it is not restricted to a field-size area.

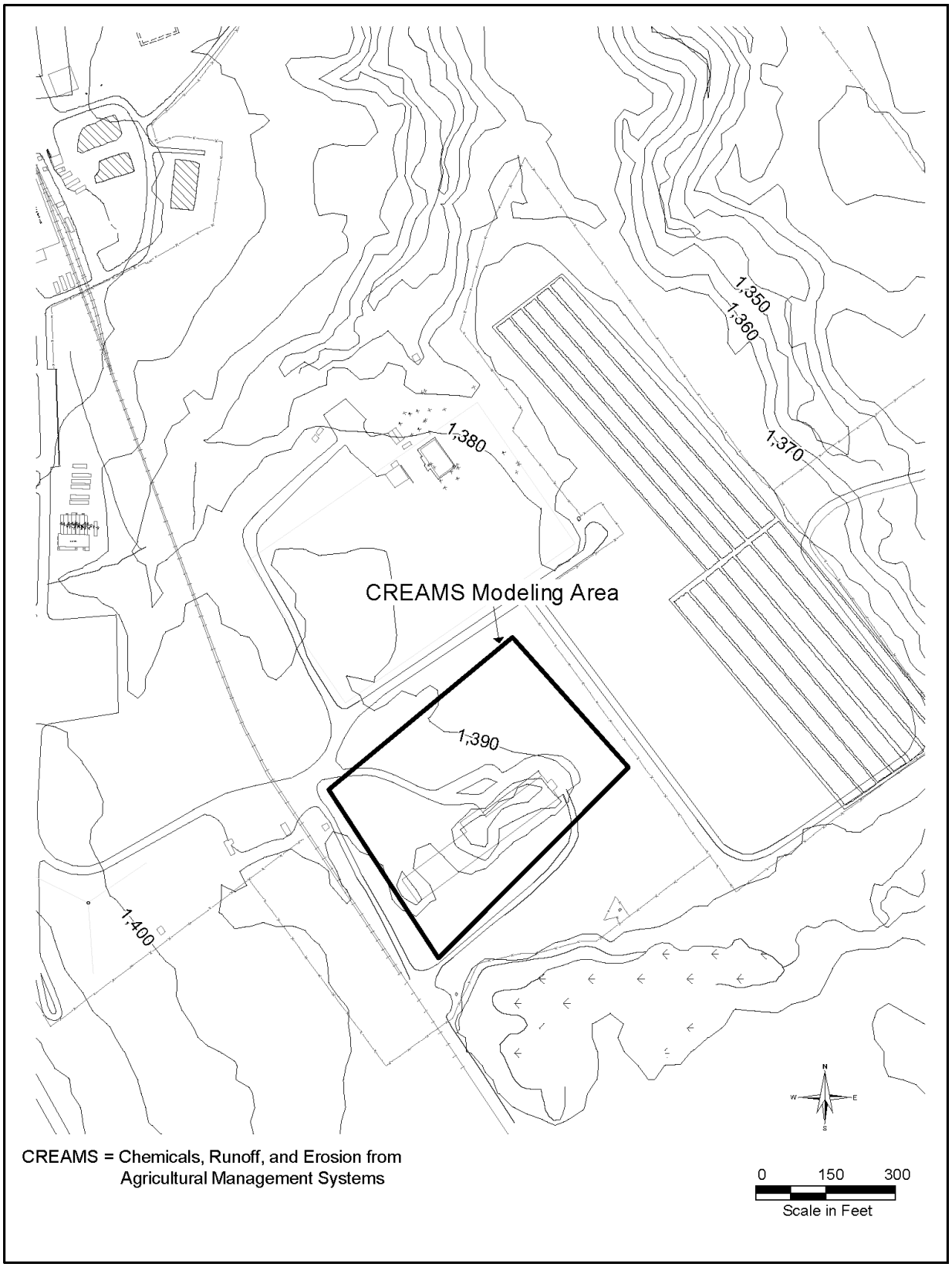

Figure F–42 Location of CREAMS Study Area

Table F–15 CREAMS Model Input Parameters and Results

Input Parameter Names	***Input Parameter Values***
Field Area Acreage	2.2 hectares
Slope of Field	0.02
Length of Field	152 meters
Annual Precipitation (1984)	113.8 centimeters
Soil Type/Hydrologic Soil Group	Silty clay/Hydrologic Soil Group D
Effective Hydraulic Conductivity	0.01 centimeters per year
Soil Conservation Service Curve Number	84
Soil Erodibility Factor	6.0
Soil Loss Ratio	0.26
Mannings '*n*' value for overland flow	0.046
Output Parameter Names	***Output Parameter Values***
Total Evapotranspiration	36.60 centimeters
Percolation	11.49 centimeters
Predicted Runoff	65.81 centimeters
Annual Soil Loss for Area	10.3 metric tons per hectares

CREAMS = Chemicals, Runoff, and Erosion from Agricultural Management Systems, Mannings '*n*' value = roughness coefficient that indicates the resistance to flow of the land surface, Soil Conservation Service Curve Number = a value that describes a catchment's runoff production behavior.
Note: To convert centimeters to inches, multiply by 0.393; hectares to acres, multiply by 2.471; metric tons to tons, multiply by 1.1.

In this study, the Quarry Creek and Franks Creek watersheds were modeled separately. As shown on **Figure F–43**, a network of 11 channel sections and 28 hillslope areas within the Quarry Creek watershed and 3 channels and 8 hillslope areas within the Franks Creek watershed were used to characterize the same study area as in the USLE and SEDIMOT II simulations. However, the subdrainage areas were defined in a slightly different manner than in those two simulations, because their size was dependent on the geometry of the branched-stream network in accordance with WEPP program constraints (USDA 1995). The subdrainage basin boundaries were delineated using the GeoWEPP ArcX 2004.3 version of the software package. Unlike the USLE and SEDIMOT II simulations, which modeled soil loss from individual hillslopes within the watershed assuming a constant gradient, this study modeled the soil movement down the hillslopes taking into account the variations in the slope gradients. This more-comprehensive modeling approach simulates both erosion and depositional processes on the hillslopes because it also takes into account the soil being deposited in the flatter slope areas and within depressions following initial movement.

Data were entered into the model to describe the climate, topography, soil properties, and cover conditions within the watersheds. WEPP used 24-hour design storms with return intervals of 1, 2, 5, 10, 50, and 100 years to determine single-storm event sediment yield rates. The rainfall amount anticipated from each of the design storms events was taken from standardized maps developed by the Soil Conservation Service (USDA 1986) using a Type II Soil Conservation Service storm designation and rainfall depths of 5.3 centimeters (2.1 inches) for the 1-year storm, 6.4 centimeters (2.5 inches) for the 2-year storm, 8.1 centimeters (3.2 inches) for the 5-year storm, 9.4 centimeters (3.7 inches) for the 10-year storm, 11.2 centimeters (4.4 inches) for the 25-year storm, 11.9 centimeters (4.7 inches) for the 50-year storm, and 13.2 centimeters (5.2 inches) for the 100-year storm. To determine average annual sediment yield rates, WEPP's climate simulator (CLIGEN) was used to stochastically project changes in the climatic conditions daily over a 100-year period based on records supplied from the Little Valley, New York, weather station (USDA 1995). Topographic profiles were entered for each hillslope area based on a high-resolution topographic map of the Project Premises as compiled by Erdman Anthony Consultants and

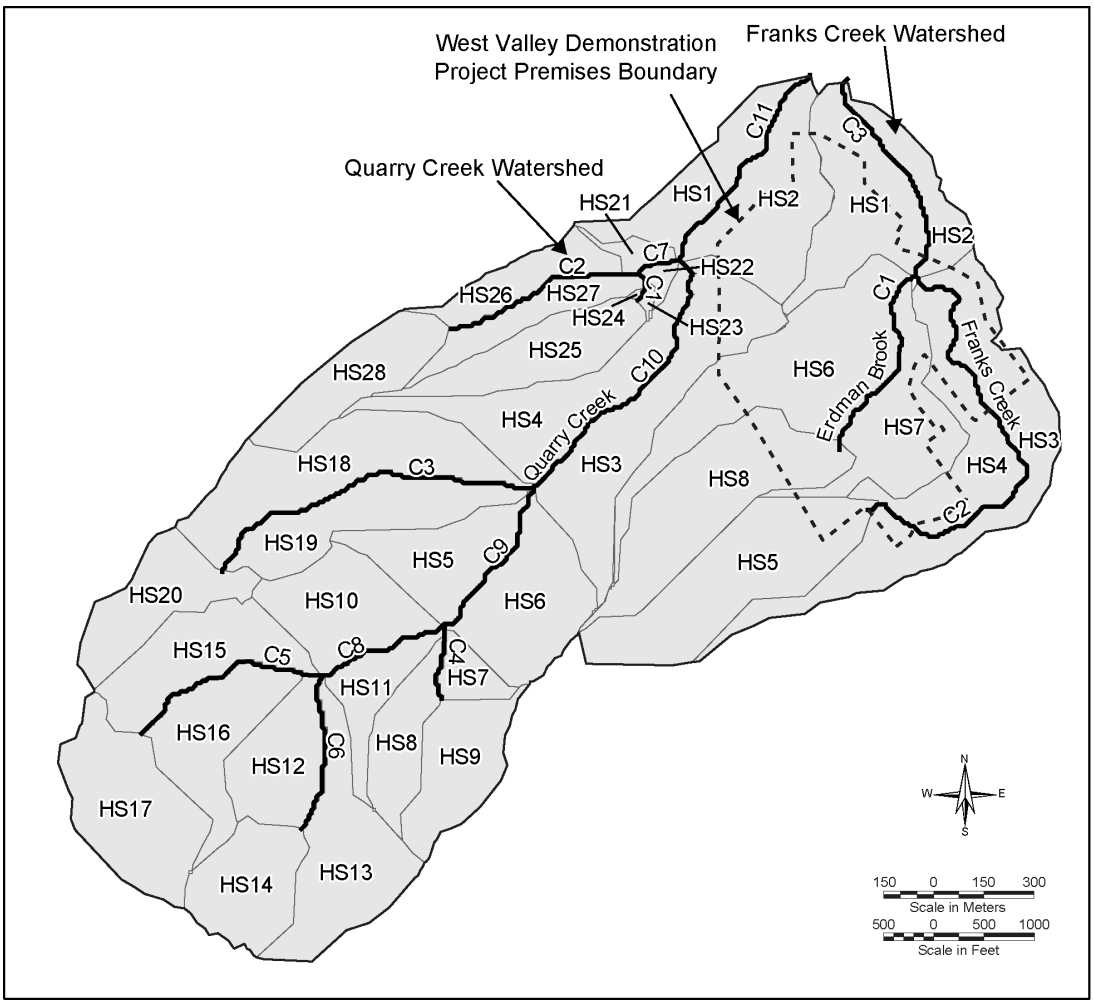

Figure F–43 Water Erosion Prediction Project Modeling Study Channel Network and Hillslope Areas

the 1:24,000 Ashford Hollow Quadrangle map compiled by the USGS. The soil unit distribution within the watershed area was determined from the Soil Conservation Service soil survey for Cattaraugus County (USDA 2006). Other soil parameters were established through review of site conditions and published values for similar conditions (Meyer and Gee 1999), as shown in **Table F–16**. Two cover conditions, 50-year-old forest and Old Field Recessional, were specified within the watershed area based on the site-specific vegetation survey (WVNS 1993a).

The WEPP simulation results are shown in **Table F–17**. The best-estimate value for the average annual sediment yield of the hillslope areas was determined to be 6.1 metric tons per hectare (2.7 tons per acre) per year from regression analysis of the single-storm events. This yield is equivalent to an average decrease in elevation of 408 millimeters (1.3 feet) per 1,000 years. During the 100-year storm event, the sediment yields of individual subwatershed areas vary from 0.0 to 4.9 metric tons per hectare (0.0 to 2.2 tons per acre), with an average value of 1.3 metric tons per hectare (0.60 tons per acre). This is equivalent to an average decrease in elevation of 91 millimeters (0.3 feet) per 1,000 years, indicating that, over a long-term period, the high frequency of smaller storm events has greater impact on erosion rates.

Table F–16 Water Erosion Prediction Project Model Soil Units and Properties

Site Location	*NRCS Soil Unit Number*	*NRCS Soil Unit Name*	*Soil Texture*	*Interrill Erodibility kg*s/mV*	*Rill Erodibility (seconds per meter)*	*Critical Shear (newtons per square meters)*	*Hydraulic Conductivity (millimeters per hour)*
North Plateau	81	Varysburg	Loamy sand	263762	0.00068	0.24	57.600
	135	Hudson	Clay	1083060	0.00206	3.292	0.154
	29	Chenango	Loamy sand	263762	0.00068	0.24	57.600
	32	Churchville	Clay	1083060	0.00206	3.292	0.154
	35	Rhinebeck	Clay	1083060	0.00206	3.292	0.154
South Plateau	32	Churchville	Clay	1083060	0.00206	3.292	0.154
	36	Canadice	Clay	1083060	0.00206	3.292	0.154
	75	Alden	Loam	945944	0.000788	2.508	3.427
	55	Darien	Clay loam	951524	0.001184	2.76	0.446
West hillslopes	51	Chadakoin	Loam	945944	0.000788	2.508	3.427
	55	Darien	Clay loam	951524	0.001184	2.76	0.446
	61	Schuyler	Loam	945944	0.000788	2.508	3.427
	80	Fremont	Loam	945944	0.000788	2.508	3.427
	56	Chautauqua	Loam	945944	0.000788	2.508	3.427
	63	Langford	Silt loam	928308	0.000704	2.62	1.094
	69	Erie	Loam	945944	0.000788	2.508	3.427
	72	Towerville	Loam	945944	0.000788	2.508	3.427
	78	Hornell	Clay	1083060	0.00206	3.292	0.154
	74	Ashville	Loam	945944	0.000788	2.508	3.427
	52	Valois	Loam	945944	0.000788	2.508	3.427
	76	Orpark	Loam	945944	0.000788	2.508	3.427

kg = kilograms; NRCS = ; s/mV = .
Note: To convert kilograms to pounds, multiply by 2.2; millimeters to inches, multiply by 0.03937; newtons to pound-force, multiply by 0.225; square meters to square feet, multiply by 10.764.
Sources: Soil Conservation Service Soil Survey for Cattaraugus County (USDA 2006) for soil unit and texture data and NUREG CR-6656 (Meyer and Gee 1999) for all other data.

Summary

A comparison of the USLE, SEDIMOT II, CREAMS, and WEPP short-term predictions is presented as **Table F–18**. The USLE and SEDIMOT II methods predict the lowest average annual soil loss rate from the hillslope areas, followed by WEPP and, lastly, CREAMS resulting in an erosion prediction range of 11 to 690 millimeters (0.04 to 2.3 feet) per 1,000 years. Although this range is relatively broad, these studies predict that the erosion from the hillslope areas will be relatively small compared to the dominant erosion processes (i.e., stream incision, gully migration, and soil creep/landsliding). This conclusion is in general agreement with the CHILD model's prediction of hillslope erosion. Typical local rates of modeled erosion on the low-gradient plateau surfaces in the CHILD scenarios range from approximately 10 to approximately 200 millimeters per 1,000 years, depending on the scenario. These simulations also predict areas of net deposition, depending on the microtopography, and are somewhat influenced by artifacts in the DEM. The Wet + Fast Creep scenario shows the highest rates of both erosion and deposition on plateau surfaces (typically 100-200 millimeters per 1,000 years), while the Standard, A1, and A2 scenarios show the lowest (typically 1 millimeter per 1,000 years). These rates are broadly consistent with short-term model estimates.

Table F–17 Water Erosion Prediction Project Modeling Hillslope Sediment Yield Results

Watersheds	*Hillslopes*	*Area (hectares)*	*Storm Event (metric tons per hectare)*						
			1-Year	*2-Year*	*5-Year*	*10-Year*	*25-Year*	*50-Year*	*100-Year*
Franks Creek hillslopes	HS1	14.27	0.00	0.00	0.00	0.00	0.00	0.00	0.00
	HS2	5.54	0.00	0.00	0.00	0.00	0.00	0.00	0.00
	HS3	20.70	0.11	0.18	0.09	0.16	0.20	0.27	0.15
	HS4	11.80	0.04	0.09	0.16	0.20	0.27	0.34	0.19
	HS5	20.62	0.20	0.47	1.26	1.93	2.76	3.50	2.19
	HS6	23.12	0.07	0.11	0.22	0.31	0.43	0.54	0.28
	HS7	12.40	0.00	0.00	0.00	0.00	0.00	0.00	0.00
	HS8	19.44	0.07	0.20	0.61	1.10	1.68	2.29	1.73
Quarry Creek hillslopes	HS1	9.07	0.00	0.00	0.00	0.00	0.00	0.00	0.00
	HS2	14.49	0.04	0.09	0.13	0.20	0.25	0.31	0.36
	HS3	19.24	0.00	0.00	0.09	0.20	0.63	0.99	1.28
	HS4	14.96	0.09	0.11	0.20	0.04	0.02	0.04	0.09
	HS5	9.99	0.04	0.04	0.09	0.18	0.40	0.61	0.96
	HS6	13.67	0.81	1.32	2.17	2.82	3.43	3.90	4.91
	HS7	2.89	0.00	0.00	0.00	0.02	0.09	0.18	0.31
	HS8	7.07	0.00	0.00	0.00	0.00	0.00	0.00	0.07
	HS9	10.14	0.07	0.09	0.18	0.25	0.38	0.61	1.23
	HS10	11.79	0.09	0.29	0.85	1.32	1.91	2.31	3.18
	HS11	5.69	0.00	0.00	0.00	0.00	0.00	0.00	0.18
	HS12	9.52	0.04	0.04	0.11	0.27	0.56	0.83	1.30
	HS13	15.32	0.09	0.13	0.25	0.36	0.47	0.58	0.69
	HS14	10.40	0.04	0.11	0.27	0.40	0.58	0.74	1.08
	HS15	12.24	0.02	0.04	0.07	0.11	0.16	0.20	0.27
	HS16	11.58	0.07	0.11	0.20	0.29	0.38	0.47	0.58
	HS17	16.10	0.07	0.13	0.25	0.34	0.45	0.58	0.69
	HS18	18.78	0.07	0.11	0.18	0.25	0.34	0.45	0.54
	HS19	11.97	0.11	0.16	0.29	0.43	0.58	0.74	0.96
	HS20	10.44	0.04	0.07	0.13	0.20	0.25	0.31	0.43
	HS21	1.48	0.16	0.22	0.02	0.02	0.02	0.02	0.04
	HS22	0.83	0.00	0.00	0.02	0.04	0.11	0.13	0.18
	HS23	0.30	0.02	0.04	0.07	0.11	0.13	0.18	0.20
	HS24	0.09	0.00	0.00	0.00	0.00	0.00	0.00	0.00
	HS25	10.38	0.09	0.13	0.25	0.13	0.52	1.12	2.04
	HS26	6.07	0.04	0.07	0.13	0.18	0.25	0.29	0.34
	HS27	5.90	0.04	0.07	0.11	0.02	0.00	0.00	0.02
	HS28	10.08	0.04	0.04	0.09	0.16	0.45	0.76	1.59

Note: To convert metric tons to tons, multiply by 1.1; hectares to acres, multiply by 2.471.

Table F–18 Short-term Modeling Soil Loss/Sediment Yield Results Comparison

Model Name	*Average Annual Soil Loss/Sediment Yield (metric tons per hectare per year)*	*Soil Loss/Sediment Yield During 100-Year Storm (metric tons per hectare)*	*Average Elevation Change (millimeters per 1,000 years)*
USLE	0.19	N/A	12.8
SEDIMOT II	0.16	1.1	11
CREAMS	10.3	N/A	690
WEPP	6.1	1.3	408

CREAMS = Chemicals, Runoff, and Erosion from Agricultural Management Systems, SEDIMOT = Sedimentology by Distributed Model Treatment, USLE = Universal Soil Loss Equation, WEPP = Water Erosion Prediction Project.
Note: To convert metric tons to tons, multiply by 1.1; hectares to acres, multiply by 2.471; millimeters to inches, multiply by 0.039.

F.3.2.2 Short-term Channel Downcutting and Valley Rim–Widening Prediction

An estimate of valley rim-widening was developed by modeling channel downcutting rates for individual storm events. The downcutting rates in both Franks Creek and Erdman Brook were estimated for six different storm events with return intervals of 2, 5, 10, 20, 100, and 500 years. The individual storm downcutting rates were predicted using the Hydrologic Engineering Center (HEC) HEC-6 code, a one-dimensional open-channel-flow numerical model designed to predict scour and/or deposition resulting from gradually changing sediment and hydraulic conditions over moderate time periods. Owing to its one-dimensional nature, HEC-6 is not capable of simulating the bank erosion or lateral-channel migration processes that are actively causing Franks Creek and Erdman Brook to widen and adjust their course. These processes slow the downcutting rate by adding large quantities of sediment that must also be removed from the streambed. In addition, the HEC-6 calculation assumes that no sediment enters at the head of the modeled reach. In a sense then, it represents what would happen if a sediment-retention dam were built just upstream of the modeled reach, leading to scour below. For these reasons, the model will overpredict the downcutting rate, which, will in turn, provide a conservative estimate of valley rim widening.

The model requires measurements of the stream cross-sectional geometry, flow rates, and elevations, as well as the selection of a sediment transport function. The stream cross sections, flow rates, and elevations for the current drainage system were taken from HEC-2 modeling runs performed by Dames and Moore (WVNS 1993c). Closely spaced cross sections (generally 30.5 to 46 meters [100 to 150 feet] apart) were used to approximate a steady, gradually varied flow condition despite stream irregularities. The *SAM Hydraulic Design Package for Channels*, developed by the Waterways Experiment Station (ACE 2002), identified the Laursen (Madden 1993) function as an appropriate sediment transport function based on site-specific measurements of the flow, sediment load, and geometry characteristics of Erdman Brook and Franks Creek (WVNS 1993c).

The calculated downcutting rate for the six reference storms is presented in **Table F–19**. These values represent the average downcutting that occurs along the stream profiles during the reference storms. The results show minimal change in downcutting for the storms with the higher frequency of occurrence, and there is little difference in the downcutting rates between Erdman Brook and Franks Creek. Table F–19 also shows the corresponding rim widening, which results from dividing the downcutting by the tangent of the 21-degree stable slope angle. In other words, these estimates assume that following channel downcutting, the adjacent slope fails at a constant 21-degree angle, resulting in rim widening. This rim-widening rate is the rate at which each of the streambanks moves in the horizontal direction. The rim-widening estimate is considered conservative because it assumes the slope will fail everywhere along the channel profile instead of being restricted to the most susceptible areas, such as the outside of meander loops.

Table F–19 Estimates of Channel Downcutting on Erdman Brook and Franks Creek from Single-Storm Events

Storm Event	*Frequency of Occurrence (1 per year)*	*Average Downcutting Distance from the Single Storm (meters)* [a]		*Average Rim-Widening Distance from the Single Storm (meters)*	
		Erdman Brook	*Franks Creek*	*Erdman Brook*	*Franks Creek*
2-year storm	0.50	0.20	0.14	0.52	0.36
5-year storm	0.20	0.21	0.19	0.55	0.49
10-year storm	0.10	0.22	0.20	0.57	0.52
20-year storm	0.05	0.30	0.23	0.78	0.60
100-year storm	0.01	0.32	0.23	0.83	0.60
500-year storm	0.002	4.10	3.50	10.68	9.12

[a] Positive numbers means degradation and the area is being scoured.
Note: To convert meters to feet, multiply by 3.281.

The storm frequency (return interval) estimates and rim-widening estimates were combined to develop probabilistic estimates for the long-term rim-widening rate from erosion. The probabilistic method estimated the probability of a specific storm combination (e.g., 20, 2-year storms and 5, 100-year storms) and combined it with the estimate for the total rim widening for all storms in the specific combination (e.g., 20 times the 2-year storm rim widening plus 5 times the 100-year storm rim widening). The summation of combinations considered storms of all magnitudes, equivalent to an averaging over an indefinite period of time. Nearly all (99.94 percent) possible storm combinations were considered. The sets of estimates for storm combination probability and total rim widening were arranged in order of increasing total rim widening. The ordered listing was used to estimate likelihood of a specific rim-widening rate. Selecting a rim-widening rate and summing probabilities for all rim-widening rates lower than the selected rate gives an estimated likelihood of the rate being the same as, or less than, the selected rate. The probability of a specific number of storms having the same recurrence interval over a given time was estimated using the Poisson distribution.

This method was used to estimate the long-term rim-widening rates for Erdman Brook and Franks Creek for the current drainage condition. **Table F–20** presents the probabilistic rim-widening rates. Results show that the 90 percent quantile for Erdman Brook is 0.158 meters (0.518 feet) per year, while the 90 percent quantile for Franks Creek is 0.153 meters (0.502 feet) per year, meaning that 90 percent of the erosion rates for the two streams are expected to be equal to or less than their 90 percent quantiles. A narrow distribution for the rim-widening rate is shown because the major determinant in the probabilistic rim-widening rate is the large number of high-frequency storms. This observation is consistent with the results presented in Table F–20.

Table F–20 Estimate of Long-term Rim-Widening for Erdman Brook and Franks Creek

Quantile (percent)	*Erdman Brook Average Rim Widening Rate (meters per year)*	*Franks Creek Average Rim Widening Rate (meters per year)*
10	0.138	0.134
20	0.140	0.137
30	0.143	0.139
40	0.145	0.141
50	0.147	0.143
60	0.149	0.145
70	0.151	0.147
80	0.154	0.149
90	0.158	0.153

Note: To convert meters to feet, multiply by 3.281.

As expected, the incision rates along the reach of Franks Creek between Erdman Brook and Quarry Creek computed in the CHILD scenarios are lower than those in the HEC-6 analysis, which are considered maxima. The CHILD rates range from 0.5 to 2.6 millimeters (1.02 to 0.10 inches) per year for the first 100 simulation years, depending on the scenario and the local grid resolution.

F.3.2.3 Short Term Infiltration Capacity Prediction

The Soil Water Assessment Tool (SWAT) model was used to simulate the Cattaraugus Creek watershed from its headwaters down to the Gowanda USGS gauging station near the town of Gowanda, New York. The model determined the quantity of precipitation, evapotranspiration, runoff, and lateral flow that occurred over the land surface and within the unsaturated soil layers of the watershed, as well as the quantity of flow that percolated to the shallow and deep groundwater aquifers. The simulation results were used to calculate the infiltration capacity at the confluence of Buttermilk and Cattaraugus Creeks, and thus, verify the range of values selected for the CHILD long-term erosion analysis.

SWAT is a physically based model that simulates the dominant processes in the hydrologic cycle on a watershed or basin scale. It operates on a daily time step and is capable of simulation periods of up to a few hundred years. The SWAT model was developed by the U.S. Department of Agriculture Agricultural Research Service to predict the impact of management on water, sediment, and agricultural chemical yields in ungauged watersheds as described in the theoretical documentation (Neitsch et al. 2005).

The SWAT model requires input parameters that describe the site-specific climate, soil properties, vegetation conditions, topographic properties (gradient, length, and width), point sources, and management conditions within the Cattaraugus Creek watershed area. The data input into the model are summarized in **Table F–21**. The SWAT model's automated watershed delineator was used to access the inputted DEM, soil, and land use files; create subbasin areas (see **Figure F–44**), and generate hydrologic response units (HRUs). Each HRU area is a unique combination of soil, slopes, and land use type within a subdrainage area. Slope intervals of 0 to 1 percent, 2 to 4 percent, and greater than 4 percent gradients were specified as break points, which resulted in the creation of 3,480 HRUs. Following the HRU creation step, the SWAT model was used to calculate the flow distribution within each of the HRU areas and the discharge at the outlets to the subdrainage areas.

Table F–21 Data Entered into the SWAT Model

Data Category	*Input Data*	*Data Source*
Daily precipitation Daily temperature	Little Valley (USGS COOP ID 304808) New Albion (USGS COOP ID 305673) Gowanda (USGS COOP ID 303354)	http://waterdata.usgs.gov/nwis/sw
Topography	DEM (10-meter grid spacing)	http://seamless.usgs.gov/index.php
Soil	STATSGO and Soils-5 databases	Databases built in to SWAT model
Land use	National Land Cover Database 2001 National Agricultural Statistics Service crop map 2002	http://datagateway.nrcs.usda.gov/GatewayHome.html) http://www.mric.gov/mrlc2k_nlcd.asp)
Point sources	Waste water treatment plant discharges (Cattaraugus, Otto, Arcade, and Springville) WNYNSC Lagoon 3 discharges	http://oaspub.epa.gov/enviro/ef_home2.water http://www.epa-echo.gov/echo/compliance_report_water.html Nuclear Fuel Services Inc. Quarterly Reports

DEM = Digital Elevation Model, STATSGO = State Soil Geographic Database, SWAT = Soil Water Assessment Tool, WNYNSC = Western New York Nuclear Service Center.
Note: To convert meters to feet, multiply by 3.281.

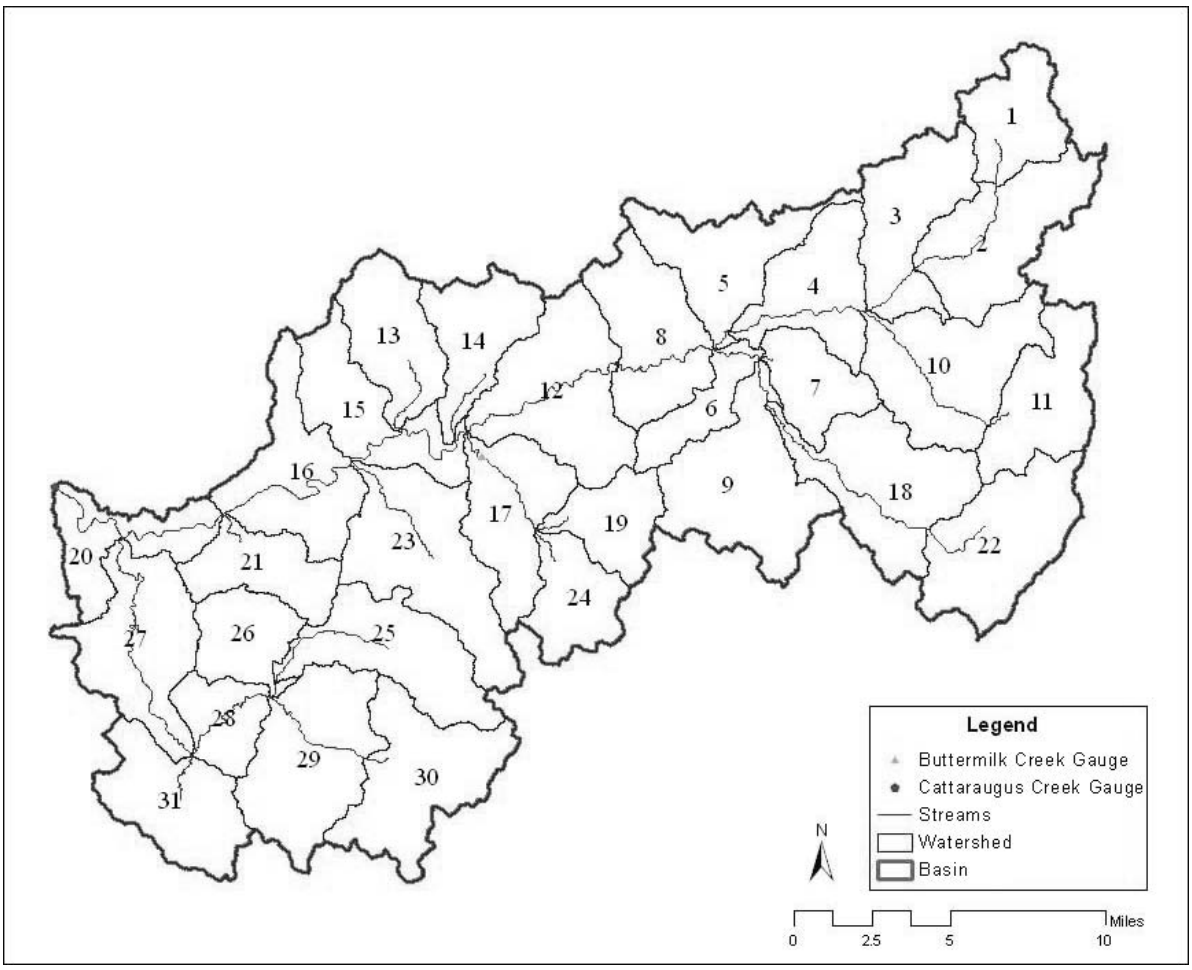

Figure F–44 SWAT Delineation of Subdrainage Basin Areas within Cattaraugus Creek Watershed

The SWAT model was calibrated and validated using available water quantity data to test its performance. Model calibration is the process of fine-tuning the SWAT simulation results to the observed results, whereas model validation is the process of repeating the SWAT simulation using a different time period for input data, without changing any parameter values that may have been adjusted during calibration. In this analysis, the SWAT-predicted daily stream flow data at the model outlet were compared to the daily stream flow data observed at the USGS Cattaraugus Creek gauge station at Gowanda, New York (USGS station number 04213500). The Gowanda gauge station recorded daily flow values from 1945 to 2008 with missing records from April 1998 through November 1999; therefore, a 63-year SWAT simulation was completed with the first 5 years (1945 to 1950) used to "warm up" the model (i.e., establish antecedent moisture conditions). The 1961 through 1965 time period was used for calibration with the remaining 58-year gauge record period (between 1950 and 2008) used for validation. The comparison of the simulated to observed data for the calibration period is shown on **Figure F–45**. The Nash-Sutcliffe efficiency (NSE) and RSR (RMS error–observations standard deviation ratio) goodness-of-fit measures were calculated to test the model's accuracy. The NSE measure can range from negative infinity to 1, with 1 denoting a perfect model with respect to data agreement and 0.5 and above denoting an acceptable model. The RSR measure varies from the optimal value of zero, which indicates perfect model simulation, to a large positive value. Model simulation can be judged as satisfactory if NSE is greater than 0.5 and RSR is less than or equal to 0.70 (Moriasi et al. 2007). In this analysis, NSE was determined to be 0.73 for the calibration period and 0.56 for the validation period, with RSR at 0.52 for the calibration period and 0.67 for the validation period.

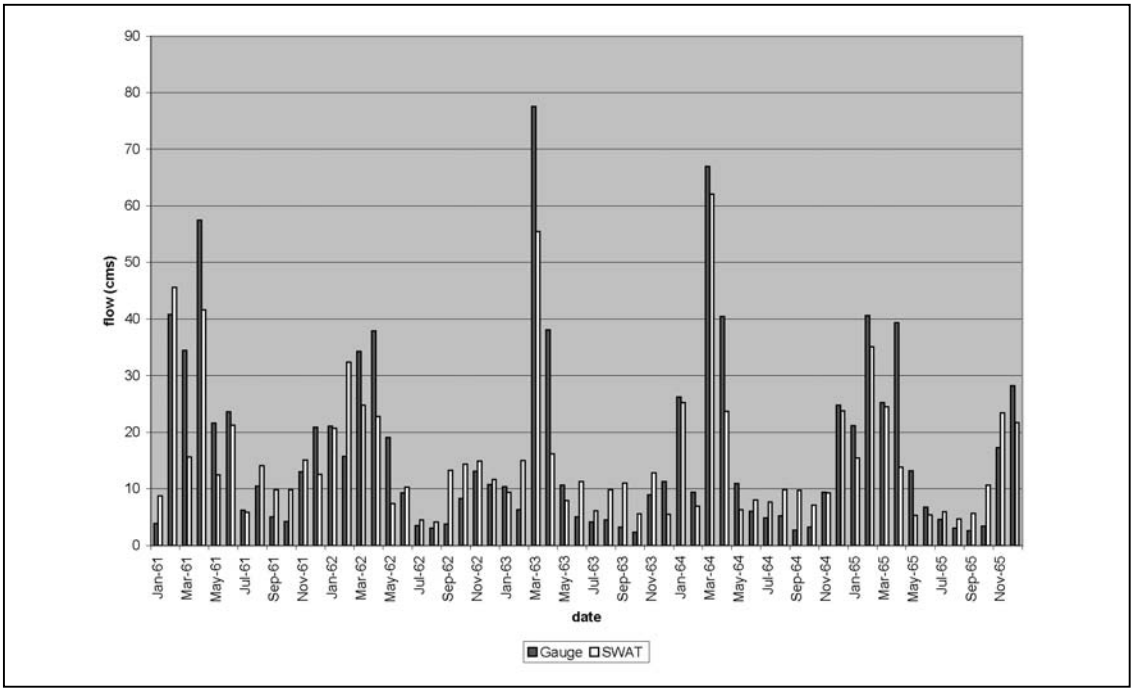

Figure F–45 Comparison of SWAT-simulated Streamflow to USGS Gowanda Gauge Observed Streamflow during Calibration Period 1961–1965.

Following calibration, the SWAT model was run for a 200-year period using climate data generated by SWAT's built-in climate generator. It uses monthly average values from the nearest weather station to stochastically generate daily climate values over the duration of the simulation. **Table F–22** presents the annual results averaged over the Buttermilk Creek watershed (subbasins 17, 19, and 24) for the 200-year period simulation and also for the 58-year calibration run. It shows the quantity of water entering the Buttermilk Creek subbasins as precipitation, as well as the quantity of water removed from the watershed to the atmosphere by evaporation and plant transpiration (evapotranspiration), and the quantity of water percolating past the root zone, which over a long time period is equal to the groundwater recharge (percolation).

Table F–22 Average Annual SWAT Modeling Results

Simulation	*Precipitation (millimeters)*	*Evapotranspiration (millimeters)*	*Percolation (millimeters)*
58-Year calibration run	1155.78	425.48	216.64
200-Year run	891.65	403.50	230.87

SWAT = Soil Water Assessment Tool.
Note: To convert millimeters to inches, multiply by 0.039.

The SWAT average annual values of precipitation, evapotranspiration, and percolation were entered into the infiltration capacity equation as described in Section F.3.1.4.5. The groundwater recharge (I_r) parameter in the infiltration capacity equation was assumed to be equal to the percolation due to the long duration of the simulations. Thus, the resulting infiltration capacity values were determined to be 10.33 meters (33.89 feet) per year and 15.83 meters (51.94 feet) per year for the 58-year calibration run and the 200-year run, respectively. These predictions fall within the expected range of 8.29 to 19.4 meters (27.20 to 63.65 feet) per year; and therefore, verify the appropriateness of the values used in the CHILD model.

F.4 Summary

Observations of modern geomorphic processes, together with results from OSL dating, support the conclusion from earlier studies that the WNYNSC has unusually high rates of erosion for a moderate-relief, humid-temperate setting. Long-term stream incision rates on the order of millimeters per year are more commonly associated with tectonically active landscapes than they are with tectonically quiet, moderate-relief continental interiors. These high rates reflect a combination of the site's postglacial legacy and the relatively soft glacial sediments that fill the main valley and mantle the uplands.

Analysis of landforms and present-day processes supports the view that gully erosion and mass wasting represent the greatest erosional threats to the burial areas. Observations, measurements, and calculations made with short-term erosion models suggest that hillslope erosion by processes such as overland-flow erosion, rill development, and raindrop impact are considerably less significant threats than gullying and landsliding.

The style of erosional development at the site places constraints on the type of geomorphic models that may be usefully applied for estimating long-term erosion. Gully erosion in particular involves substantial changes in topography and surface flow paths, such that there is a dynamic feedback between erosion and surface hydrology as the landscape evolves. Models of long-term potential future erosion at the site must be able to capture this feedback. Given the need to generate future-erosion scenarios that extend over millennia—a timeframe during which topography may be expected to change considerably—a landscape evolution model (which by definition accounts for changing topography) is the logical tool of choice. After review of several such models, the CHILD model was selected as offering the most appropriate range of capabilities and process laws for the site.

The most defensible approach to testing and calibrating such a model is to compare it with the reconstructed geomorphic history of the site over a timeframe comparable to that of the analysis period. At WNYNSC, such an approach is made possible by a fortuitous geological accident: the incised stream network of Buttermilk Creek and its tributaries formed during the period since the retreat of the Laurentide ice sheet about 17,000 years ago, and the nature of the pre-incision topography can be approximately reconstructed from the existing plateau remnants.

A probabilistic calibration process allowed the determination of five alternative sets of best-fit model parameters. The calibration models showed good agreement between observed and predicted present-day topography, both visually and in terms of a series of quantitative measurements of landscape and drainage network morphology. The agreement between modeled and observed topography increases confidence in the ability of the model to generate realistic future-erosion scenarios, though it is recognized that the enormous time span, limited data set, and imperfectly known process laws leave scope for uncertainty that must be acknowledged in interpreting any model results.

A group of 26 alternative forward-in-time simulations was designed. These generated a range of potential future-erosion scenarios. The computed patterns of landscape evolution were consistent with observations of present-day erosion processes in the sense that all predicted some degree of gully development along the North Plateau rim, and all predicted active erosion along steep valley sides. Among the scenarios, some were consistent with observed modern incision along upper Franks Creek and Erdman Brook, while others showed stability or minor sedimentation in these areas; the former scenarios are therefore considered to be more reliable than the latter. Collectively, the model results support the view that gully erosion, and to a lesser extent slope degradation and landsliding, represents the greatest erosional threat to the integrity of waste burial areas.

The model results highlighted several potential erosional "hot spots." These include the area around the present-day NP-2 and NP-3 gullies, the present-day NP-1 gully, and the plateau rim above Quarry Creek in the area north-northwest of the main plant. The low-lying area between the NDA and SDA is also a potential erosional hot spot.

While some degree of gully activity was common in the modeled scenarios, the location of the fastest-growing gullies is difficult to determine because the flow paths that feed the gullies are quite sensitive to small perturbations in topography. This sensitivity makes it essentially impossible to predict the exact positions of gullies, at least in a deterministic sense. The problem is somewhat analogous to the prediction of thunderstorm cells: numerical weather models give meteorologists a good idea of the conditions under which thunderstorms are likely to occur, but the exact position and timing of any particular storm are virtually impossible to predict.

The model scenarios are subject to several important sources of uncertainty. First, there is uncertainty associated with the structure of the model. Any model involves simplifications of nature, and these simplifications will inevitably distort the model's representation of natural phenomena. In some areas of the physical sciences, the resulting distortions are well known and may have a minimal effect on a set of phenomena under study (for example, Newtonian mechanics are known to be "wrong," yet their accuracy is so high that they are used to send spacecraft to Mars). With landscape evolution models, the underlying process theory is provisional (partly because the large time and space scales render direct experimentation impossible) and subject to ongoing research. Models like CHILD may be said to encapsulate the best present understanding of the processes involved over long time scales; their performance will undoubtedly continue to improve as the science evolves. Second, there is uncertainty associated with inputs. In this case, the largest source of uncertainty concerns the assumption of a constant climate state for purposes of model calibration. Errors in this assumption may lead either to overestimates or underestimates of future erosion. Other sources of uncertainty related to inputs are the representation of materials in the landscape, and the applied baselevel history at the outlet of Buttermilk Creek. Third, there is uncertainty in the initial conditions used in calibration. Fourth, there is (relatively minor) uncertainty in the topographic data and in other data sources (such as rainfall and streamflow). Fifth, there is uncertainty associated with possible future changes in climate, vegetation, and soil conditions, and with possible future human modifications to surface drainage patterns. Sixth, there is uncertainty associated with the degree of heterogeneity in soils, sediments, and rocks. The model has been calibrated using a representation that lumps materials into three types with regard to erosion and sediment transport, and one type with regard to runoff generation. Therefore, the model will tend to overpredict erosion for materials that are more resistant than average, and vice versa. Likewise, the model will tend to underpredict runoff from areas that are less permeable than average, and vice versa.

With these caveats in mind, it is notable that none of the scenarios produced stream capture in the headwaters of Franks Creek. Further, in no scenario were the initial steps toward such capture observed. In addition, inspection of topography data showed no obvious signs that similar capture events have occurred elsewhere along Buttermilk Creek in the past. It is concluded therefore that, as best as can be determined given the limits of present knowledge of quantitative landscape evolution, such capture is unlikely to occur during the performance period. However, this conclusion is offered with the caveat that the landscape evolution model used in this study did not account for lateral erosion and slope undercutting by Buttermilk Creek, which could increase the likelihood of stream capture.

None of the future-erosion scenarios showed large-scale erosional exhumation of waste burial areas. Two of the South Plateau scenarios showed partial gully penetration of the SDA (SPa3 and SPwet), while in the more-erosive North Plateau scenarios, gullies advanced to within about 100 to 200 meters (328 to 656 feet) of the Main Plant Process Building. Given (1) the close proximity of large gullies to waste burial areas in some model scenarios, (2) the various sources of uncertainty that influence predicted rates and patterns of erosion, and (3) the indeterminacy of gully positions, it is recommended that large-scale erosional exhumation of burial

areas in the next 1,000 to 10,000 years should be considered *unlikely but not implausible*. It is recommended that analyses of the potential radiological threat from erosion take account of the demonstrated uncertainty in the positions and growth rates of large active gullies.

The long-term erosion portion of Section H.2.2.1 discusses how the results from these erosion predictions were used to develop estimates of dose from unmitigated erosion predictions.

F.5 References

ACE (U.S. Army Corps of Engineers), 2002, *SAM Hydraulic Design Package for Channels*, Coastal and Hydraulics Laboratory, Vicksburg, Mississippi, September.

Albanese, J. R., S. L. Anderson, R. H. Fakundiny, S. M. Potter, W. B. Rogers, and L. F. Whitbeck, 1984, *Geologic and Hydrologic Research at the Western New York Nuclear Service Center, West Valley, New York*, NUREG/CR-3782, New York State Geological Survey/State Museum and New York State Education Department, Albany, New York, June.

Anderson, R. S. 1994, "Evolution of the Santa Cruz Mountains, California, through tectonic growth and geomorphic decay," *Journal of Geophysical Research*, Vol. 99, No. B10, p. 20,161–20,179, October 10.

Anderson, W. T., and H. T. Mullins, 1997, "Stable isotope record from Seneca Lake, New York: Evidence for a cold paleoclimate following the Younger Dryas," *Geology*; Vol. 25; No. 2, p. 135–138, February.

Arnold, J. G., P. M. Allen, R. Muttiah, and G. Bernhardt, 1995, "Automated base flow separation and recession analysis techniques," *Ground Water*, Vol. 33, Issue 6, p. 1010, November.

Arnold, L. J., R. G. Roberts, R. F. Galbraith and S. B. DeLong, 2009, "A revised burial dose estimation procedure for optical dating of young and modern-age sediments," *Quaternary Geochronology*, Vol. 4, p. 306–325.

Attal, M., G. E. Tucker, A. C. Whittaker, P. A. Cowie, and G. P. Roberts, 2008, "Modeling fluvial incision and transient landscape evolution: Influence of dynamic channel adjustment," *Journal of Geophysical Research*, Volume 113, p. F03013, August.

Bishop, P., 2007, "Long-term landscape evolution: linking tectonics and surface processes," *Earth Surface Processes and Landforms*, Vol. 32, p. 329–365.

Bogaart, P. W., G. E. Tucker, J. J. de Vries, 2003, "Channel network morphology and sediment dynamics under alternating periglacial and temperate regimes: a numerical simulation study," *Geomorphology*, Vol. 54, p. 257–277.

Boothroyd, J. C., B. S. Timson, and R. H. Dana, Jr., 1979, *Geomorphic and Erosion Studies at the Western New York Nuclear Service Center, West Valley, New York*, NUREG/CR-0795, December.

Boothroyd, J. C., B. S. Timson, and L. A. Dunne, 1982, *Geomorphic Processes and Evolution of Buttermilk Valley and Selected Tributaries, West Valley, New York*, Fluvial Systems and Erosion Study, Phase II, NUREG/CR-2862, July.

Buffington, J. M., and D. R. Montgomery, 1997, "A systematic analysis of eight decades of incipient motion studies, with special reference to gravel-bedded rivers," *Water Resources Research*, Vol. 33, No. 8, p. 1993–2029, August.

Chow, V. T., 1959, *Open-Channel Hydraulics*, McGraw-Hill, New York.

Clevis, Q., G. E. Tucker, S. T. Lancaster, A. Desitter, N. M. Gasparini, and G. Lock, 2006, "A simple algorithm for the mapping of TIN data onto a static grid: Applied to the stratigraphic simulation of river meander deposits," *Computers & Geosciences*, Vol. 32, p. 749–766.

Codilean, A. T., P. Bishop, and T. B. Hoey, 2006, "Surface process models and the links between tectonics and topography," *Progress in Physical Geography*, Vol. 30, 3, p. 307–333.

Collins, D. B. G., R. L. Bras, and G. E. Tucker, 2004, "Modeling the effects of vegetation-erosion coupling on landscape evolution," *Journal of Geophysical Research*, Vol. 109, F03004, August.

Crosby, B. T., K. X. Whipple, N. M. Gasparini, C. W. Wobus, 2007, "Formation of fluvial hanging valleys: Theory and simulation," *Journal of Geophysical Research*, Vol. 112, F03S10, August.

Dames and Moore, Inc., 1987, *Application of the CREAMS Computer Model to a Portion of the West Valley Demonstration Project Site*, CIN0193:SEA-69, July 29.

Delong, S. B., and L. J. Arnold, 2007, "Dating alluvial deposits with optically stimulated luminescence, AMS ^{14}C and cosmogenic techniques, western Transverse Ranges, California, USA, *Quaternary Geochronology*, Vol. 2, p. 129–136.

Dietrich, W. E., C. J. Wilson, D. R. Montgomery, and J. McKean, 1993, "Analysis of Erosion Thresholds, Channel Networks, and Landscape Morphology Using a Digital Terrain Model," *Journal of Geology*, Vol. 101, p. 259–278.

Dietrich, W. E., D. Bellugi, L. S. Sklar, J. D. Stock, D. G. Heimsath, and J. J. Roering, 2003, "Geomorphic Transport Laws for Predicting Landscape Form and Dynamics," *Prediction in Geomorphology*.

Dunn, I. S., 1959, "Tractive Resistance of Cohesive Channels," *Journal of the Soil Mechanics and Foundations Division*, SM3, June.

Dunne T., and R. Black, 1970, "Partial Area Contributions to Storm Runoff in a Small New England Watershed, *Water Resources Research*, Vol. 6, No. 5, p. 1297–1311.

Eagleson, P.S., 1978, "Climate, Soil, and Vegetation, The Distribution of Annual Precipitation Derived from Observed Storm Sequences," *Water Resources Research*, Vol. 14, No. 5, p. 713–721.

Elliot, W. J., A. M. Liebenow, J. M. Laflen, and K. D. Kohl, 1989, *A Compendium of Soil Erodibility Data from WEPP Cropland Soil Field Erodibility Experiments 1987 and 1988*, NSERL Report No. 3, The Ohio State University, and USDA Agricultural Research Service, August.

Ellis, K. G., H. T. Mullins, and W. P. Patterson, 2004, "Deglacial to middle Holocene (16,600 to 6000 calendar years BP) climate change in the northeastern United States inferred from multi-proxy stable isotope data, Seneca Lake, New York," *Journal of Paleolimnology*, Vol. 31, p. 343–361.

Fairbanks, R. G., R. A. Mortlock, T. C. Chiu, L. Cao, A. Kaplan, T. P. Guilderson, T. W. Fairbanks, A. L. Bloom, P. M. Grootes, and M. J. Nadeau, 2005, "Radiocarbon calibration curve spanning 0 to 50,000 years BP based on paired ^{230}Th/ ^{234}U/ ^{238}U and ^{14}C dates on pristine corals," *Quaternary Science Reviews*, Vol. 24, p. 1781–1796.

Fakundiny, R. H., 1985, "Practical Applications of Geological Methods at the West Valley Low-Level Radioactive Waste Burial Ground, Western New York," *Northeastern Environmental Science*, Vol. 4, Nos. 3/4, p. 116–148.

Fleurant, C., G. E. Tucker, and H. A. Viles, 2008, "Modelling cockpit karst landforms," *Geological Society, London, Special Publications*, Vol. 296, p. 47–62.

Flores-Cervantes, J. H., E. Istanbulluoglu, and R. L. Bras, 2006, "Development of gullies on the landscape: A model of headcut retreat resulting from plunge pool erosion," *Journal of Geophysical Research*, Vol. 111, F01010.

Foster, G. R., 1982, "Modeling the Erosion Process", *Hydrologic Modeling of Small Watersheds*, ASAE Monograph No. 5, American Society of Agricultural Engineers.

Galbraith R. F., and G. M. Laslett, 1993, "Statistical Models for Mixed Fission Track Ages," *Nuclear Tracks and Radiation Measurements*, Vol. 21, No. 4, p. 459–470.

Gasparini, N. M., K. X. Whipple, and R. L. Bras, 2007, "Predictions of steady state and transient landscape morphology using sediment-flux-dependent river incision models," *Journal of Geophysical Research*, Vol. 112, F03S09.

Goldenfeld, N., and L. P. Kadanoff, 1999, "Simple Lessons from Complexity," *Science*, Vol. 284, p. 87–89, April 2.

Hancock, G., and G. Willgoose, 2001a, "The Production of Digital Elevation Models for Experimental Model Landscapes," *Earth Surface Processes and Landforms*, Vol. 26, p. 475–490.

Hancock, G., and G. Willgoose, 2001b, "Use of a landscape simulator in the validation of the SIBERIA catchment evolution model: Declining equilibrium landforms," *Water Resources Research*, Vol. 37, No. 7, p. 1981–1992, July.

Hancock, G. R., G. R. Willgoose, and K. G. Evans, 2002, "Testing of the Siberia Landscape Evolution Model Using The Tin Camp Creek, Northern Territory, Australia, Field Catchment," *Earth Surface Processes and Landforms*, Vol. 27, p. 125–143.

Hanks, T. C., 2000, "The Age of Scarplike Landforms From Diffusion-Equation Analysis," from *Quaternary Geochronology: Methods and Applications*, p. 313–338.

Hawk, K. L., and P. S. Eagleson, 1992, *Climatology of Station Storm Rainfall in the Continental United States: Parameters of the Bartlett-Lewis and Poisson Rectangular Pulses Models*, Report No. 336, Ralph M. Parsons Laboratory, Hydrology and Water Resource Systems, May.

Hoffman, V. C., R. H. Fickies, R. H. Dana, V. Ragan, 1980, *Geotechnical Analysis of Soil Samples and Study of a Research Trench at the Western New York Nuclear Service Center, West Valley, New York*, NUREG/CR-1566, New York Geological Survey/State Museum and New York State Education Department, October.

Holcombe, T. L., L. A. Taylor, D. F. Reid, J. S. Warren, P. A. Vincent, and C. E. Herdendorf, 2003, "Revised Lake Erie Postglacial Lake Level History Based on New Detailed Bathymetry," *Journal of Great Lakes Research*, Vol. 29, p. 681–704.

Howard, A. D., 1980, "Thresholds in River Regimes," *Thresholds in Geomorphology*, p. 227–258.

Howard, A. D., 1994, "A detachment-limited model of drainage basin evolution," *Water Resources Research*, Vol. 30, No. 7, p. 2261–2285, July.

Howard, A. D., and G. Kerby, 1983, "Channel changes in badlands," *Geological Society of America Bulletin*, Vol. 94, p. 739–752, June.

Howard, A. D., W. E. Dietrich, and M. A. Seidl, 1994, "Modeling fluvial erosion on regional to continental scales," *Journal of Geophysical Research*, Vol. 99, No. B7, p. 13,971–13,986, July 10.

Ibbitt, R. P., G. R. Willgoose, and M. J. Duncan, 1999, "Channel network simulation models compared with data from the Ashley River, New Zealand," *Water Resources Research*, Vol. 35, No. 12, p. 3875–3890, December.

Ijjasz-Vasquez, E. J., R. L. Bras, and G. E. Moglen, 1992, "Sensitivity of a Basin Evolution Model to the Nature of Runoff Production and to Initial Conditions," *Water Resources Research*, Vol. 28, No. 10, p. 2733–2742, October.

Ijjasz-Vasquez, E. J., and R. L. Bras, 1995, "Scaling regimes of local slope versus contributing area in digital elevation models," *Geomorphology*, Vol. 12, p. 299–311.

Istanbulluoglu, E., and R. L. Bras, 2005, "Vegetation-modulated landscape evolution: Effects of vegetation on landscape processes, drainage density, and topography," *Journal of Geophysical Research*, Vol. 110, F02012.

Istanbulluoglu, E., R. L. Bras, H. Flores-Cervantes, and G. E. Tucker, 2005, "Implications of bank failures and fluvial erosion for gully development: Field observations and modeling," *Journal of Geophysical Research*, Vol. 110, F01014.

Julian, J. P., and R. Torres, 2006, "Hydraulic erosion of cohesive riverbanks," *Geomorphology*, Vol. 76, p. 193–206.

Julien, P. Y., 1995, *Erosion and sedimentation*, Cambridge University Press.

Kappel, W. M., and W. E. Harding, 1987, *Surface-Water Hydrology of the Western New York Nuclear Service Center, Cattaraugus County, New York*, U.S. Geological Survey, Water-Resources Investigations Report 85-4309, Ithaca, New York.

Kirkby, M. J., and L. J. Bull, 2000, "Some factors controlling gully growth in fine-grained sediments: a model applied in southeast Spain," *Catena*, Vol. 40, p. 127–146.

LaFleur, R. G., 1979, *Glacial Geology and Stratigraphy of Western New York Nuclear Service Center and Vicinity, Cattaraugus and Erie Counties, New York*, U.S. Geological Survey, Open File Report 79-989, Albany, New York.

Lancaster, S. T., S. K. Hayes, and G. E. Grant, 2003, "Effects of wood on debris flow runout in small mountain watersheds," *Water Resources Research*, Vol. 39, No 6.

Leopold, L. B., M. G. Wolman, and J. P. Miller, 1964, *Fluvial Processes in Geomorphology*, Part II, Chapter 7, May.

Madden, E. B., 1993, *Modified Laursen Method for Estimating Bed-Material Sediment Load*, Dallas, Texas, October.

Magee, J. W., G. H. Miller, N. A. Spooner, D. Questiaux, 2004, "Continuous 150 k.y. monsoon record from Lake Eyre, Australia: Insolation-forcing implications and unexpected Holocene failure," *Geology*, Vol. 32, No. 10, p. 885–888, October.

Mahan, S. A., 2007, Informal Memo from USGS Luminescence Dating Lab, U.S. Geologic Survey, March 15.

Martin, Y., 2003, "Evaluation of bed load transport formulae using field evidence from the Vedder River, British Columbia, *Geomorphology*, Vol. 53, p. 75–95.

Martin, Y., and M. Church, 2004, "Numerical modelling of landscape evolution: geomorphological perspectives," *Progress in Physical Geography*, Vol. 28, No. 3, p. 317–339.

McKean, J. A., W. E. Dietrich, R. C. Finkel, J. R. Southon, and M. W. Caffee, 1993, "Quantification of soil production and downslope creep rates from cosmogenic ^{10}Be accumulations on a hillslope profile," *Geology*, Vol. 21, p. 343–346, April.

Meyer, P. D., and G. W. Gee, 1999, *Information on Hydrologic Conceptual Models, Parameters, Uncertainty Analysis, and Data Sources for Dose Assessments at Decommissioning Sites*, NUREG/CR-6656, PNNL-13091, Pacific Northwest National Laboratory, Richland, Washington, November.

Millar, R. G., 2005, "Theoretical regime equations for mobile gravel-bed rivers with stable banks," *Geomorphology*, Vol. 64, p. 207–220.

Moriasi, D. N., J. G. Arnold, M. W. Van Liew, R. L. Bingner, R. D. Harmel, T. L. Veith, 2007, "Model Evaluation Guidelines for Systematic Quantification of Accuracy in Watershed Simulations, *Transactions of the ASABE*, ISSN0001-2351, Vol. 50(3), p. 885–900, March.

Muller, E. H., and P. E. Calkin, 1993, "Timing of Pleistocene glacial events in New York State," *Canadian Journal of Earth Sciences*, Vol. 30, p. 1829–1845.

Mullins, H. T., E. J. Hinchey, R. W. Wellner, D. B. Stephens, W. T. Anderson Jr., T. R. Dwyer, and A. C. Hine, 1996, "Seismic stratigraphy of the Finger Lakes: A continental record of Heinrich event H-1 and Laurentide ice sheet instability," *Geological Society of America*, Special Paper 311.

Mulvihill, C. I., A. G. Ernst, and B. P. Baldigo, 2005, *Regionalized Equations for Bankfull Discharge and Channel Characteristics of Streams in New York State: Hydrologic Region 6 in the Southern Tier of New York*, SIR 2005-5100, U.S. Geological Survey, Reston, Virginia.

Nash, D., 1980, "Forms of Bluffs Degraded for Different Lengths of Time in Emmet County, Michigan, USA," *Earth Surface Processes*, Vol. 5, p. 331–345.

Nash, D. B., 1984, "Morphologic dating of fluvial terrace scarps and fault scarps near West Yellowstone, Montana," *Geological Society of America Bulletin*, Vol. 95, p. 1413–1424, December.

Neitsch, S. L., J. G. Arnold, J. R. Kiniry, and J. R. Williams, 2005, *Soil and Water Assessment Tool Theoretical Documentation, Version 2005*, Temple, Texas.

Nivière, B., and G. Marquis, 2000, "Evolution of terrace risers along the upper Rhine graben inferred from morphologic dating methods: evidence of climatic and tectonic forcing," *Geophysical Journal International*, Vol. 141, p. 577–594.

Nivière, B., G. Marquis, and J.-C. Maurin, 1998, "Morphologic dating of slowly evolving scarps using a diffusive analogue," *Geophysical Research Letters*, Vol. 25, No. 13, p. 2325–2328, July 1.

Oehm, B., and B. Hallett, 2005, "Rates of soil creep, worldwide: weak climatic controls and potential feedback," Z. Geomorph. N. F., Vol. 49, No. 3, p. 353–372, September.

Prudic, D. E., 1986, *Ground-Water Hydrology and Subsurface Migration of Radionuclides at a Commercial Radioactive-Waste Burial Site, West Valley, Cattaraugus County, New York*, U.S. Geological Survey Professional Paper 1325.

Putkonen, J., and M. O'Neal, 2006, "Degradation of unconsolidated Quaternary landforms in the western North America," *Geomorphology*, Vol. 75, p. 408–419.

Rittenour, T. M., 2008, "Luminescence dating of fluvial deposits: applications to geomorphic palaeoseismic and archaeological research," *Boreas*, Vol. 37, pp. 613–635, November.

Rodriguez-Iturbe, I., and A. Rinaldo, 1997, *Fractal River Basins, Chance and Self-Organization*, College Station, Padova, March.

Roering, J. J., J. W. Kirchner, and W. E. Dietrich, 1999, "Evidence for nonlinear, diffusive sediment transport on hillslopes and implications for landscape morphology," *Water Resources Research*, Vol. 35, No. 3, p. 853–870.

Roering, J. J., K. M. Schmidt, J. D. Stock, W. E. Dietrich, and D. R. Montgomery, 2003, "Shallow landsliding, root reinforcement, and the spatial distribution of trees in the Oregon Coast Range," *Canadian Geotechnical Journal*, Vol. 40, p. 237–253.

Rosenbloom, N. A., and R. S. Anderson, 1994, "Hillslope and channel evolution in a marine terraced landscape, Santa Cruz, California," *Journal of Geophysical Research*, Vol. 99, No. B7, p. 14,013–14,029, July 10.

Simons, D. B., and F. Sentürk, 1992, "Sediment Transport Technology, Water and Sediment Dynamics," *Water Resources Publications*, Littleton, Colorado.

Sloan, J., J. R. Miller, and N. Lancaster, 2001, "Response and recovery of the Eel River, California, and its tributaries to floods in 1955, 1964, and 1997," *Geomorphology*, Vol. 36, p. 129–154.

Snyder, N. P., K. X. Whipple, G. E. Tucker, and D. J. Merritts, 2000, "Landscape response to tectonic forcing: Digital elevation model analysis of stream profiles in the Mendocino triple junction region, northern California," *Geological Society of America Bulletin*, Vol. 112, No. 8, p. 1250–1263.

Snyder, N. P., K. X. Whipple, G. E. Tucker, and D. J. Merritts, 2002, "Interactions between onshore bedrock-channel incision and nearshore wave-base erosion forced by eustasy and tectonics," *Basin Research*, Vol. 14, p. 105–127.

Sólyom, P. B., and G. E. Tucker, 2004, "Effect of limited storm duration on landscape evolution, drainage basin geometry, and hydrograph shapes," *Journal of Geophysical Research*, Vol. 109, F03012.

Stock, J. D., and D. R. Montgomery, 1999, "Geologic constraints on bedrock river incision using the stream power law," *Journal of Geophysical Research*, Vol. 104, No. B3, p. 4983–4993.

Summerfield, M. A., 1986, "Tectonic geomorphology: macroscale perspectives," Progress reports, *Progress in Physical Geography*, Vol. 10, No. 2, p. 227–238.

Tomkin, J. H., M. T. Brandon, F. J. Pazzaglia, J. R. Barbour, and S. D. Willett, 2003, "Quantitative testing of bedrock incision models for the Clearwater River, NW Washington State," *Journal of Geophysical Research*, Vol. 108, No. B6, 2308, p. ETG 10-1–10-19.

Tucker, G. E., 2004, "Drainage basin sensitivity to tectonic and climatic forcing: Implications of a stochastic model for the role of entrainment and erosion thresholds," *Earth Surface Processes and Landforms*, Vol. 29, p. 185–205.

Tucker, G. E., 2008, *CHILD Users Guide*, Version R8.11, Draft, University of Colorado, Boulder, Colorado, November 18.

Tucker, G. E., and K. X. Whipple, 2002, "Topographic outcomes predicted by stream erosion models: Sensitivity analysis and intermodel comparison," *Journal of Geophysical Research*, Vol. 107, No. B9.

Tucker, G. E., and R. L. Bras, 2000, "A stochastic approach to modeling the role of rainfall variability in drainage basin evolution," *Water Resources Research*, Vol. 36, No. 7, p. 1953–1964.

Tucker, G. E., S. T. Lancaster, N. M. Gasparini, and R. L. Bras, 2001a, "The Channel-Hillslope Integrated Landscape Development Model (CHILD)," *Landscape Erosion and Evolution Modeling*, p. 349–388.

Tucker, G. E., S. T. Lancaster, N. M. Gasparini, R. L. Bras, and S. M. Rybarczyk, 2001b, "An object-oriented framework for distributed hydrologic and geomorphic modeling using triangulated irregular networks," *Computers & Geosciences*, Vol. 27, p. 959–973.

USDA (U.S. Department of Agriculture), 1976, *Procedure for Determining Rates of Land Damage, Land Depreciation, and Volume of Sediment Produced by Gully Erosion*, Soil Conservation Service, Technical Release No. 32, July.

USDA (U.S. Department of Agriculture), 1984, *User's Guide for the CREAMS Computer Model*, Washington Computer Center Version, Technical Release No. 72, Soil Conservation Service, December.

USDA (U.S. Department of Agriculture), 1986, *Urban Hydrology for Small Watersheds*, Natural Resources Conservation Service, Technical Release No. 55, June.

USDA (U.S. Department of Agriculture), 1995, *USDA ¥Water Erosion Prediction Project (WEPP), Hillslope Profile and Watershed Model Documentation*, NSERL Report No. 10, USDA-ARS, National Soil Erosion Research Laboratory, West Lafayette, Indiana, July.

USDA (U.S. Department of Agriculture), 2006, "Cattaraugus County, New York soil survey" (available at http://soildatamart.nrcs.usda.gov/Survey.aspx?County=NY009), December 11.

USGS (U.S. Geological Survey), 1979, Ashford Hollow quadrangle, New York (map), 1:24,000, 7.5 Minute Series, Washington, DC.

van der Beek, P., and P. Bishop, 2003, "Cenozoic river profile development in the Upper Lachlan catchment (SE Australia) as a test of quantitative fluvial incision models," *Journal of Geophysical Research*, Vol. 108, No. B6, p. ETG 11-1–11-27.

Walker, M., 2005, *Quaternary Dating Methods*, University of Wales, Lampeter, UK.

Weltz, M. A., H. D. Fox, S. Amer, F. B. Pierson and L. J. Lane, 1992, "Erosion Prediction on Range and Grazing Lands: A Current Perspective," *Grazingland Hydrology Issues: Perspectives for the 21st Century*, p. 97–116.

Werner, B. T., 1999, "Complexity in Natural Landform Patterns," *Science*, Vol. 284, p. 102–104, April 2.

Whipple, K. X., N. P. Snyder, and K. Dollenmayer, 2000, "Rates and processes of bedrock incision by the Upper Ukak River since the 1912 Novarupta ash flow in the Valley of Ten Thousand Smokes, Alaska," *Geology*, Vol. 28, No. 9, p. 835–838, September.

Willgoose, G., 1994, "A physical explanation for an observed area-slope-elevation relationship for catchments with declining relief," *Water Resources Research*, Vol. 30, No. 2, p. 151–159, February.

Willgoose, G., 2005, "Mathematical Modeling of Whole Landscape Evolution," *Annual Review of Earth and Planetary Sciences*, Vol. 33, p. 443–459.

Willgoose G., R. L. Bras, and I. Rodriguez-Iturbe, 1991, "A Physical Explanation of an Observed Link Area-Slope Relationship," *Water Resources Research*, Vol. 27, No. 7, p. 1697–1702, July.

Wischmeier, W. H., and D. D. Smith, 1978, *Predicting Rainfall Erosion Losses, A Guide to Conservation Planning*, Agriculture Handbook No. 537, U.S. Department of Agriculture.

Wolman, M. G. and J. P. Miller, 1960, "Magnitude and Frequency of Forces in Geomorphic Processes," *Journal of Geology*, Vol. 68, pp. 54–74.

WVNS (West Valley Nuclear Services Company, Inc.), 1993a, *Environmental Information Document, Volume III, Hydrology: Part 3 of 5, Erosion and Mass Wasting Processes*, WVDP-EIS-009, Rev. 0, West Valley, New York, February 12.

WVNS (West Valley Nuclear Services Company, Inc.), 1993b, *Environmental Information Document, Volume III, Hydrology: Part 1, Geomorphology of Stream Valleys*, WVDP-EIS-009, Rev. 0, West Valley, New York, January.

WVNS (West Valley Nuclear Services Company, Inc.), 1993c, *Environmental Information Document, Volume III, Hydrology: Part 2, Surface Water Hydrology*, WVDP-EIS-009, Rev. 0, West Valley, New York, January.

WVNS (West Valley Nuclear Services Company, Inc.), 1993d, *Environmental Information Document, Volume III, Hydrology: Part 4 of 5, Groundwater Hydrology and Geochemistry*, WVDP-EIS-009, Rev. 0, West Valley, New York, February.

WVNS (West Valley Nuclear Services Company, Inc.), 1996, *Environmental Information Document, Volume XI, Ecological Resources of the Western New York Nuclear Service Center*, WVDP-EIS-010, Rev. 0, West Valley, New York, March.

Yager, R. M., 1987, *Simulation of Groundwater Flow near the Nuclear-Fuel Reprocessing Facility at the Western New York Nuclear Service Center, Cattaraugus County, New York*, Geological Survey, Water-Resources Investigations Report 85-4308, U.S. Nuclear Regulatory Commission, Ithaca, New York.